Methoden zur Bestimmung mikrophysikalischer Parameter mit einem Mehrkanal–Polarisations–LIDAR

Kennwort: MUSCLE

zum DFG–Schwerpunktprogramm
Physikalische Methoden der Fernerkundung von Atmosphäre und Hydrosphäre

Bericht des Mathematischen Instituts
der Ludwig–Maximilians–Universität München
von
M. Kerscher, M. Noormohammadian, U.G. Oppel

April 1995

Contents

Chapter 1

Summary and historical introduction

1.1 The classical LIDAR equation and multiple scattering

A **LIDAR** is not only used for **li**ght **d**etection **a**nd **r**anging, but nowadays it is one of the most powerful instruments for analyzing the atmosphere. A LIDAR consists of a transmitter and a receiver. The transmitter is sending a fairly collimated pulsed or modulated beam of monochromatic LASER light of a certain frequency into the atmosphere where this light is absorbed or scattered by the particles (molecules, water droplets, ice crystals, dust) of the atmosphere. The highly sensitive receiver registrates light which is reflected by the atmosphere from a certain field of view (FOV) and with or without a certain state of polarisation.

The transmitter and the receiver may be situated in the same place (then we call the LIDAR monostatic) or they may be situated in different places (then we call the LIDAR bistatic). Furthermore, the FOV may be directed in the same or in a different direction as the (FOV of the) transmitted beam. Very often the FOV of the transmitter and of the receiver are coaxial cones; sometimes the receiver has several FOVs (e.g. a narrow central FOV and a ringshaped outer FOV) and registers several states of polarisation (e.g. parallel and perpendicular to the direction of polarisation of the transmitted beam) for these FOVs even simultaneously. The Micro-LIDAR of the DLR is such a LIDAR (see Krichbaumer et al. [28]). Furthermore, some LIDARs have the possibility of transmitting and receiving several frequencies almost simultaneously. The DIAL-LIDAR of the DLR is such a LIDAR. In addition to that some LIDARs have the possibility of scanning the atmosphere; the LIDAR of the Meteorological Institute of the Ludwig–Maximilians University in Munich is such a LIDAR. LIDARs may be ground-based, airborne or space-based; they may be used preferably for remote sensing of the atmosphere, but also for in situ measurements.

In the early days the analysis of LIDAR signals was based on what we call the classical LIDAR equation which we present here in a very simple version for a monostatic LIDAR:

$$P_R \;=\; P_0 \, \frac{c\tau}{2} \frac{1}{r^2} \, \beta(r) \, A \, \exp\Big(-2 \int_0^r \sigma(s) ds \Big) \tag{LE1}$$

where

P_0	transmitted power at time t_0,
c	speed of light,
τ	duration of the transmitted LASER pulse,
β	backscatter coefficient,
σ	extinction coefficient,
r	range,
A	area of receiver, and
P_R	received signal.

This equation is nothing but the well–known RADAR equation. This classical LIDAR equation describes the part of the LIDAR signal which is produced by single scattering only. But here this equation is used for much higher frequencies (i.e. much shorter wavelenghts of 0.1 to 10 μm) and highly dispersed objects of smaler size in relation to the wavelength as this is done usually for RADAR signals. We shall see that in many environmental situations in which a LIDAR is used for remote sensing of the atmosphere there is considerable or even prevailing multiple scattering which forces us to use more precise models and equations to describe the LIDAR signal.

Besides of the parameters of the LIDAR only a few locally variable environmental parameters enter into the classical LIDAR equation. Knowing these parameters it is very simple to calculate the LIDAR signal. Therefore, based on the classical LIDAR equation it is possible at most to obtain these environmental parameters from the LIDAR signal. For example, for a monostatic LIDAR it should be possible to obtain the range resolved extinction and absorption coefficients and the range resolved backscattering coefficient.

The most primitive and very often (but not always) not very effective method of evaluating LIDAR signals is to compare them with an appropriate set of calculated signals.

A more sophisticated method of evaluating LIDAR signals is to invert the LIDAR equation mathematically. But even if we assume that there is no absorption, in this equation there are at least two local unknowns, the local extinction coefficient and the local backscattering coefficient. Hence, without additional assumptions it is not possible to resolve the classical LIDAR equation for these local parameters. Under such assumptions, however, it is very simple to solve the classical LIDAR equation for these parameters:

Assuming slabs of constant extinction coefficient and constant backscattering coefficient, it is easy to obtain the locally constant extinction coefficients from the LIDAR signal by the slope method; e.g. see Viezee et al. [46] and Collis et al. [11].

Assuming a functional relation between the local backscattering coefficient β and the local extinction coefficient σ (e.g. such as $\beta = \sigma^k$), it is possible to obtain σ as a (numerically stable) solution of a (Riccati) differential equation; see Klett [24] and [25]. Such functional relations, however, seem not to be realistic; see Evans [13].

Having several and properly chosen freqencies available, it is possible to solve the classical LIDAR equation for the extinction coefficient (e.g. with a DIAL–LIDAR) or for the size distribution (under certain assumptions on the presence of spherical particles and on the type of the size distribution; e.g. see Müller et al. [35], Herman et al. [17]), and Bend–David et al. [3], [4]. But especially the sophisticated methods for the determination of the size distribution are problematic for mathematical reasons, the corresponding inversion problems are ill-posed.

The dependence of the more elegant inversion procedures of the (classical and other) LIDAR equations on additional assumptions and their ill-posedness are the reason why the above mentioned primitive evaluation of LIDAR signals by primitive comparison may be superior to sophisticated inversion methods if they are properly designed, automatically done, and augmented by a sensitivity analysis (which may be obtained as a byproduct from the comparison method). We shall discuss this in more detail.

Using effects of polarisation, it is possible to draw conclusions from the depolarisation ratio on the ice-water relation of the atmosphere. This analysis is based on the fact that a spherical water droplet will not change the polarisation for single backscattering, but nonspherical ice particles will.

Very early phenomena like depolarisation by spherical particles, pulse broadening and lengthening, asphericity of LIDAR signals from dense clouds, from gaseous layers, and from far distant cirrus clouds where observed which were understandable only with the help of multiple scattering effects; e.g. see Liou et al. [32], Bucher [9], Ryan et al. [43], and Kunkel et al. [30]. Multiple scattering was regarded to be a nasty and disturbing effect. Krichbaumer has studied these effects on inversion formulas in detail for many examples (see Krichbaumer [26]).

Several attempts were made to overcome these problems by introducing correction terms for multiple scattering effects into the classical LIDAR equation; e.g. see Shipley [45]. According to our opinion these attempts failed to solve the problem of multiple scattering effects for sufficiently general situations.

Hence, it was necessary to cope with the problem of multiple scattering in a more efficient way. It was necessary to make a better physical and mathematical model including multiple scattering and, based on these models, to derive new LIDAR equations which describe the LIDAR signal more precisely by taking into account not only the part of the LIDAR signal which is due to single scattering, but also the part of the LIDAR signal which is due to some or all the orders of multiple scattering.

Different techniques of modeling the process of light propagation have been proposed and used to obtain formulas and algorithms to calculate the multiply scattered parts of the LIDAR signal. The modeling may be based on transport theory (integro-differential or integral transport equation; stationary or nonstationary), approximations of transport equations (e.g. small angle approximation), the physical Monte Carlo simulation, stochastic models (e.g. Rayleigh random walk, transport processes), and iterated applications of the Maxwell equations; for more details and comparisons of calculations see Bissonnette et al. [2]. Using any of these approaches, the multiple scattering process can be formulated with or without polarisation.

All these modeling techniques of multiple scattering are essentially based on the idea of iterating the single scattering process. Again, single scattering may be modeled using different techniques (e.g. linear optics, Maxwell equations, approximations of Maxwell equations). Single scattering is characterized by the scattering distribution, defined by the phase function or by the indicatrix in models without polarisation and by the scattering matrix (e.g. of the Stokes or the Mueller type) in models with polarisation.

In April 1991 a cooperation between the Computing Center (CC) of the Russian Academy of Sciences in Novosibirsk and the Institute of Mathematics of the Ludwig-Maximilians University (LMU) of Munich in the field of calculation of multiply scattered LIDAR signals was started. This cooperation was supported by the DFG (German Science Foundation), the DAAD (German Academic Exchange Office), the Ludwig-Maximilians University, and the DLR (German Space Research Establishment). This cooperation resulted in a refinement of a stochastic model for the description and simulation of the transport of polarized light and a new stochastic "cascade" model for the calculation of LIDAR signals for polarized light by variance reduction Monte Carlo methods. This was achieved by bringing together the different modeling and computing techniques used by the CC and the LMU.

1.2 The transport theoretic model

The modeling of the CC is based on the integral transport equation which is solved by a Neumann series. The iterates of the integral operator in the Neumann series are complicated iterated integrals. These integrals are calculated using variance reduction Monte Carlo methods; e.g. see Kalos et al. [20], Marchuk et al. [33], and Kargin et al. [21]. Using these methods, it is possible to calculate the iterated integrals of the Neumann series and, hence, to calculate the parts of the LIDAR signal of all scattering orders.

We shall briefly review the transport theoretic approach of the CC which is heuristic. Light propagation in the atmosphere is considered as a sequence of collisions of photons with the medium. When a collision takes place, absorption or scattering may occur, i.e. the photon may travel no further or it may leave the point of collision in a new direction. The straight path beween the two consequent collisions is called the free path, the angle between the previous and the new direction is called the scattering angle.

Let $x \in \mathbb{R}^3$ be the position and $\varphi \in S^2 := \{y \in \mathbb{R}^3 : \|y\| = 1\}$ be the direction of the path of the photon, $t \in \mathbb{R}_0^+$ the time, c the speed of light in the medium, $\sigma_s(x)$

the scattering coefficient, $\sigma_a(x)$ the absorption coefficient, $\sigma(x) := \sigma_s(x) + \sigma_a(x)$ the extinction coefficient, $\mu := \langle \varphi, \varphi' \rangle$ the cosine of the scattering angle, $g(\mu, x)$ the indicatrix, and $I(x, \varphi, t)$ the intensity of light. By definition, $I(x, \varphi, t) dS d\varphi dt$ is the average number of photons that cross a plane element dS perpendicular to the direction φ in the cone of directions $[\varphi, \varphi + d\varphi]$ during the time interval $[t, t + dt]$. The intensity satisfies the integro-differential transport equation:

$$\frac{1}{c}\frac{dI(x,\varphi,t)}{dt} + \varphi\,\frac{dI(x,\varphi,t)}{dx} + \sigma(x)\,I(x,\varphi,t) = \\ = \sigma(x)\int g(\langle\varphi,\varphi'\rangle)\,I(x,\varphi',t)\,d\varphi' + Q(x,\varphi,t).$$

This integro-differential equation is equivalent to the integral transport equation:

$$\begin{aligned}\psi(x,\varphi,t) &= \int\int\int K(x',\varphi',t' \to x,\varphi,t)\,\psi(x',\varphi',t')\,dt'd\varphi'dx' + \\ &\quad + \int\int Q(x',\varphi,t')\,L(x' \to x|\varphi)\,T(t' \to t|x,x')\,dt'dx'\end{aligned}$$

where $\psi(x, \varphi, t) := \sigma(X)I(x, \varphi, t)$ is called the collision density and

$$\begin{aligned}K(x',\varphi',t' \to x,\varphi,t) &:= S(\varphi' \to \varphi|x')\,L(x' \to x|\varphi)\,T(t' \to t|x,x'),\\ S(\varphi' \to \varphi|x') &:= \frac{g(\langle\varphi,\varphi'\rangle)}{2\pi},\\ L(x' \to x|\varphi) &:= \sigma(x)\,\exp\Big(\frac{-\tau(x' \to x|\varphi)}{\|x-x'\|^2}\,\delta(-\varphi + \frac{x-x'}{\|x-x'\|})\Big),\\ T(t' \to t|x,x') &:= \delta(t - t' + \frac{\|x-x'\|}{c}), \quad \text{and}\\ \tau(x' \to x|\varphi) &\quad\ \text{is the optical distance between } x \text{ and } x'.\end{aligned}$$

Again this integral equation is equivalent to the integral operator transport equation

$$\psi = \mathcal{K}\psi + \psi_0$$

where $\mathcal{K}$ is defined by the integral kernel K. This integral transport equation is solved by the Neumann series

$$\psi = \sum_{n=0}^{\infty} \mathcal{K}^n\,\psi_0$$

where $\mathcal{K}^n\,\psi_0$ may be interpreted as the contribution of the n–th scattering order. The signal of the light pulse received by the LIDAR is obtained from the scalar product

$$\langle\psi,\rho\rangle = \langle\sum_{n=0}^{\infty} \mathcal{K}^n\,\psi_0, \rho\rangle \qquad \text{(LE2)}$$

where ρ characterizes the receiver. The iterated integral $\langle \mathcal{K}^n \psi_0, \rho \rangle$ represents the n times scattered part of the LIDAR signal. The Equation (LE2) represents an exact multiple scattering LIDAR equation which is based on the transport theoretic approach. It is difficult, if not impossible to calculate these iterated integrals analytically or numerically. Variance reduction Monte Carlo methods are used to carry out these calculations. These variance reduction Monte Carlo methods solve the adjoint integral operator transport equation.

1.3 The stochastic process

The approach to simulate the transport of light used by the LMU is based on a stochastic model which describes the process of multiple scattering as a generalized Rayleigh's random walk, it is a general and precise mathematical description of the physical process of multiple scattering of light viewed as a "stochastic corpuscular multiple scattering process"; see Oppel et al. [38] and Kerscher et al. [23]. Also this stochastic model allows for deriving an exact multiple scattering LIDAR equation. The total LIDAR signal may be split up into the parts due to the different orders of scattering. Again, these parts may be expressed by complicated iterated integrals. Using these equations the double scattering LIDAR signal may be calculated fast and easily. The original stochastic model included polarisation implicitely (see Oppel et al [38].); a slight change of the model allows for introducing polarisation more explicitely and for easier calculation of the LIDAR signal with polarisation (see Kerscher et al. [23]).

First, we shall briefly review the stochastic process of corpuscular multiple scattering without explicite description of polarisation. Later, we shall introduce the stochastic model of this process with explicite description of polarisation. Based on these models we shall obtain exact multiple scattering LIDAR equations. These models and these formulas allow for calculating the LIDAR signal by (direct) Monte Carlo methods, but in a very inefficient way only. To improve the efficiency of the Monte Carlo simulation we introduce variance reduction methods (such as local estimates, scattering splitting, and exponential transforms) and we switch from the stochastic model of the type of a generalized Rayleigh's random walk to a much more complicated stochastic model of a "stochastic multiple scattering cascade process" which describes the variance reduction methods, reproduces the exact multiple scattering LIDAR equation, and guarantees fast calculation of the LIDAR signal with controlled finite variance.

To introduce our stochastic model of the stochastic process of corpuscular multiple scattering, we assume that light is corpuscular and that photons which are scattered by particles of the atmosphere travel along straight lines from one point of scattering to the next.

Figure 1.1: A photon starting in x_0 in the direction of φ_0.

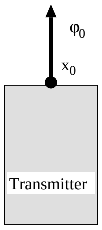

Let us consider a photon which is situated in $x_0 \in \mathbb{R}^3$ starting in the direction of $\varphi_0 \in S^2$ at the time $t = t_0$ (see Figure 1.1) where $S^2 := \{y \in \mathbb{R}^3 : \|y\| = 1\}$ denotes the set of all directions in $\mathbb{R}^3$. This photon will travel along the halfline $\{x_0 + t\varphi_0 : t \in \mathbb{R}_0^+\}$ pointing from x_0 in the direction of φ_0. After some time t it will be scattered at $x_{(1)} := x_0 + ct_1\varphi_0$ in the direction of $\varphi_1 \in S^2$ (see Figure 1.2).

Figure 1.2: A photon starting in x_0 in the direction of φ_0, scattered at $x_{(1)}$ into the direction of φ_1.

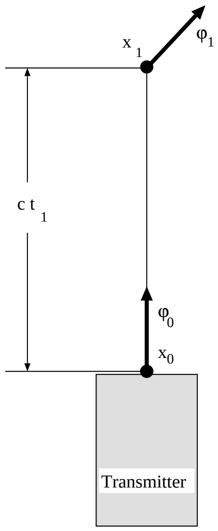

Then it will travel along the halfline $\{x_{(1)} + t\varphi_1 : t \in \mathbb{R}_0^+\}$ pointing from the first scattering point $x_{(1)}$ in the direction of φ_1. Again, after some time t_2 it will be scattered at $x_{(2)} := x_{(1)} + ct_2\varphi_1$ in the direction of $\varphi_1 \in S^2$ (see Figure 1.3).

Then it will travel along the halfline $\{x_{(2)} + t\varphi_2 : t \in \mathbb{R}_0^+\}$ from the second scattering point $x_{(2)}$ in the direction of φ_2, and so on. The path of a multiply scattered photon starting at the time t_0 is determined by its scattering sequence $(x_0, \varphi_0, t_0; t_1, \varphi_1; t_2, \varphi_2; \ldots)$ (see Figure 1.4).

Figure 1.3: A photon starting in x_0 in the direction of φ_0, scattered at position $x_{(1)}$ into the direction of φ_1, and then at $x_{(2)}$ into the direction of φ_2.

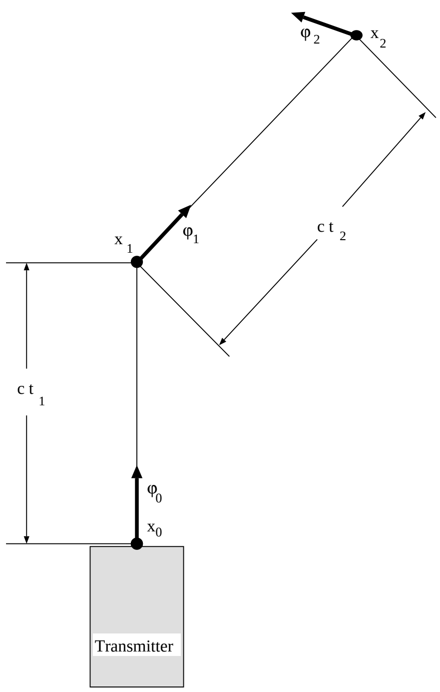

The times t_n between the scattering events and the scattering directions φ_n are realizations of random variables T_n and Φ_n, respectively. The distribution of T_n depends on the possibly locally variable extinction coefficient $\sigma : \mathbb{R}^3 \to \mathbb{R}_0^+$ along the halfline $\{x_{(n)} + t\varphi_n : t \in \mathbb{R}_0^+\}$, hence the distribution depends on the "history" $(x_0, \varphi_0, t_0; t_1, \varphi_1; t_2, \varphi_2; \ldots; t_n, \varphi_n)$ We call this distribution the "n–th extinction distribution" and denote it by

$$E_n(x_0, \varphi_0; t_1, \varphi_1; t_2, \varphi_2; \ldots; t_n, \varphi_n; \cdot) \quad : \quad \mathfrak{B}(\mathbb{R}_0^+) \to [0,1]$$

where $\mathfrak{B}(.)$ is the corresponding Borel σ–algebra. In many applications we may assume that it is a generalized exponential distribution determined by σ, i.e. for all t we have

$$E_n(x_0, \varphi_0; t_1, \varphi_1; t_2, \varphi_2; \ldots; t_n, \varphi_n; [0,t]) :=$$
$$:= \int_0^t \sigma(x_{(n-1)} + c\tau\varphi_{n-1}) \exp\Big(- \int_0^\tau \sigma(x_{(n-1)} + cs\varphi_{n-1}) ds\Big) d\tau.$$

The distribution of Φ_n depends on the kind of scatterer at the n–th scattering point $x_{(n)}$, on the direction φ_{n-1}, (on the polarization,) and on the wavelength; hence it depends on the history $(x_0, \varphi_0, t_0; t_1, \varphi_1; t_2, \varphi_2; \ldots; t_{n-1}, \varphi_{n-1}; t_n)$. We

Figure 1.4: The path of a multiply scattered photon starting in x_0 in the direction of φ_0.

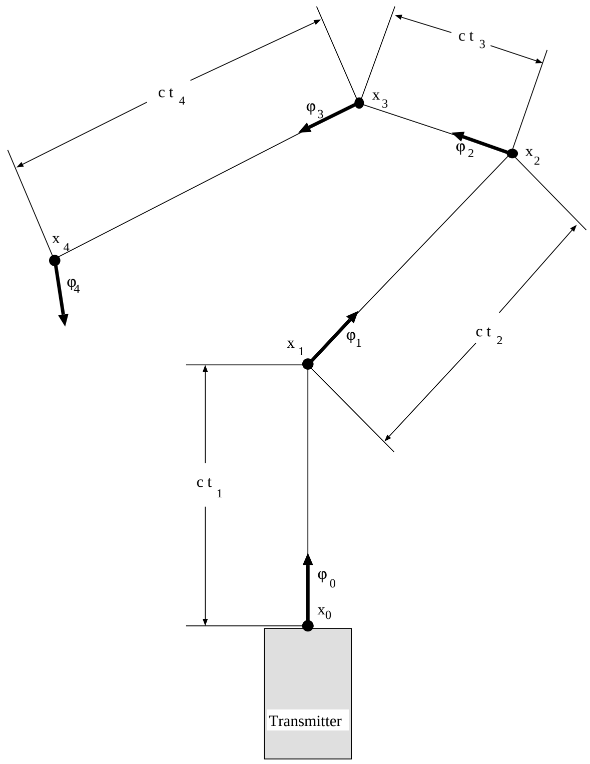

denote the "n–th scattering distribution" by

$$P_n(x_0, \varphi_0; t_1, \varphi_1; t_2, \varphi_2; \ldots; t_{n-1}, \varphi_{n-1}; t_n; \cdot) \quad : \quad \mathfrak{B}(S^2) \to [0,1]$$

$P_n(x_0, \varphi_0; t_1, \varphi_1; t_2, \varphi_2; \ldots; t_{n-1}, \varphi_{n-1}; t_n; B)$ is the probability that a photon with the history $(x_0, \varphi_0, t_0; t_1, \varphi_1; t_2, \varphi_2; \ldots; t_{n-1}, \varphi_{n-1}; t_n)$ is scattered at $x_{(n)}$ in the direction of $\varphi_n \in B$ where B is a Borel subset of S^2.

The stochastic process of corpuscular multiple scattering is determined by the sequence $((E_n, P_n) : n \in \mathbb{N})$ of the transition probabilities of the extinction distributions and of the scattering distributions: together with some starting distribution $\tau : \mathfrak{B}(\mathbb{R}^3 \times S^2 \times \mathbb{R}_0^+) \to [0,1]$ characterizing the cross–sectional, directional, and longitudenal shape of the transmitted pulse this sequence $((E_n, P_n) : n \in \mathbb{N})$ determines *a probability measure* $\mathbb{P}^\tau$ on the space of the infinite scattering sequences $(x_0, \varphi_0, t_0; t_1, \varphi_1; t_2, \varphi_2; \ldots)$; for more details see Oppel et al. [38].

1.4 The first stochastic LIDAR equation

Let X_t be the random variable denoting the position of the photon at time t, let Φ_t be the random variable denoting the direction of the photon at time t, and let N_t be the random variable denoting the number of scatterings having occured before time t. The field of view (FOV) of the receiver, its inertia, and the length of the LASER pulse define a set PPFOV $\in \mathbb{R}^3 \times S^2$ (which we call the "pulse-pupilla field of view") such that the LIDAR signal registered by the receiver at time t is characterized by the probability of the photon to be in the pulse-pupilla field of view of the receiver at the time t, i.e. this probability is equal to (see Oppel et al. ....)

$$\begin{aligned}\mu_\tau(t, \mathrm{PPFOV}) &:= \mathbb{P}^\tau((X_t, \Phi_t) \in \mathrm{PPFOV}) \\ &= \sum_{n=0}^{\infty} \mu_{\tau,n}(t, \mathrm{PPFOV}) \qquad \text{(LE3)}\end{aligned}$$

where

$$\begin{aligned}&\mu_{\tau,n}(t, \mathrm{PPFOV}) := \mathbb{P}^\tau((X_t, \Phi_t) \in \mathrm{PPFOV}; N_t = n) = \\ &= \mathbb{P}^\tau((X_t, \Phi_t) \in \mathrm{PPFOV}; \sum_{i=0}^{n} T_i \le t < \sum_{i=0}^{n+1} T_i) \\ &= \int 1_{\{(X_t,\Phi_t)\in\ \mathrm{PPFOV}\}}(\omega)\, 1_{\{N_t=n\}}\ \mathbb{P}^\tau(d\omega) \\ &= \int\limits_{\mathbb{R}^3\times S^2\times \mathbb{R}_0^+} \int\limits_{\mathbb{R}_0^+}\int\limits_{S^2} \cdots \int\limits_{\mathbb{R}_0^+}\int\limits_{S^2} 1_{\ \mathrm{PPFOV}}(x_{(n,t)}, \varphi_n) 1_{[0,t]}(\sum_{i=0}^{n} t_i)\ 1_{[t,\infty]}(\sum_{i=0}^{n+1} t_i) \\ &\qquad E_{n+1}(x_0, \varphi_0; t_1, \varphi_1; t_2, \varphi_2; \ldots; t_n, \varphi_n; dt_{n+1}) \\ &\qquad P_n(x_0, \varphi_0; t_1, \varphi_1; t_2, \varphi_2; \ldots; t_{n-1}, \varphi_{n-1}; t_n; d\varphi_n) \\ &\qquad P_1(x_0, \varphi_0; t_1; d\varphi_1)\ E_1(x_0, \varphi_0; dt_1)\ \tau(d(x_0, \varphi_0, t_0))\end{aligned}$$

where

$$x_{(n,t)} \ := \ x_0 + \sum_{i=1}^{n} t_i \varphi_{i-1} + c(t - \sum_{i=0}^{n} t_i)\varphi_n.$$

Equation (LE3) represents an exact multiple scattering LIDAR equation describing the multiply scattered LIDAR signal at time t. It is possible to obtain the classical LIDAR equation from this exact multiple scattering LIDAR equation as the single scattering part of the signal; for details see Oppel et al. [38]. The multiple integral describes the n-th scattering order of the multiple scattering LIDAR signal at time t, it can be evaluated using numerical, analytical, and Monte Carlo methods or it can be approximated by properly motivated simplifications of these equations.

1.5 A first comparison

During the first period of the cooperation the results of the algorithms used by the CC and the LMU/DLR where compared where this was possible. This comparison showed that the two completely different approaches had results which agreed not only qualitatively, but also quantitatively almost perfectly. Figure 1.5 shows results of such a comparison. Still existing small diferences are due to differences in modeling the transmitter and the receiver, to different discretization techniques, and to variance produced by the Monte Carlo method.

Figure 1.5: Comparison of double scattering return signals.

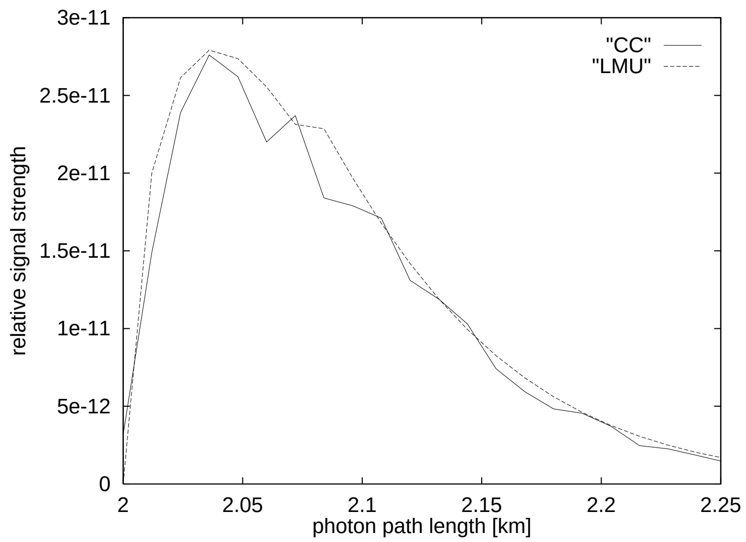

1.6 The revised stochastic LIDAR equation

During the second period of the cooperation we analysed the two exact multiple scattering LIDAR equations (LE2) and (LE3) which were obtained by the two different approaches. Masoud Noormohammadian observed that the two formulas consisting each of a series of iterated integrals could be transformed into each other. Some agreements concerning the modeling of the transmitted beam and the receiver had to be made.

The Equation (LE3) is based on the stoping rule N_t counting the number of scattering events until the time point t and on the concept of the pulse–pupilla field of view modeling the receiver and properties of the pulse by a spatial and directional domain. The multiple scattering LIDAR signal is given by the probability of the sets of scattering sequences ω such that the vector $(X_t(\omega), \Phi_t(\omega))$ of its position $X_t(\omega)$ and its direction $\Phi_t(\omega)$ is within the pulse-pupilla field of view. This probability represents the amount of multiply scattered light being registered by the receiver at the time t. $N_t(\omega)$ is the number of scattering events for the scattering sequence ω before the time t. The interpretation of this pulse-pupilla field of view is based on the spatial extension and the inertia of the receiver and on the pulse length and, hence, on some time interval.

Therefore, it is very natural to try to express an exact multiple scattering LIDAR equation in terms of some kind of intensity of multiply scattered light passing through some receiver surface area within a certain (e.g. short) time interval $\mathcal{T}$. We shall do this using several versions of the concept of flux and a new stoping rule N which counts the number of scattering events before reception. To give an example of such an exact multiple scattering LIDAR equation based on the concept of flux, let us consider a receiver centered in $x_R := (0,0,0)$ looking into the direction of $n_R := (0,0,1)$ with the circular effective receiver area $A_R := \{x \in \mathbb{R}^3 : \langle x, n_R \rangle = 0 \text{ and } \|x - x_R\| \leq r_R\}$ with radius r_R and the field of view $\mathrm{FOV}_R \subset S^2$ (see Figure 1.6).

Figure 1.6: Geometry of a LIDAR receiver from the flux point of view.

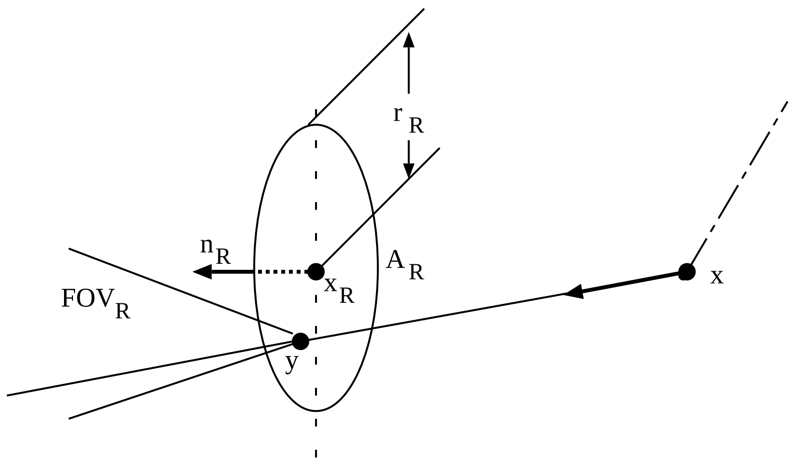

The flux is a common concept in physics. The flux of a radiative or scattering source at a point x will produce at a (small) receiver centered at x_R will dependend on its radiative or scattering properties (here given by the scattering distribution) and on the angle of the line combining it with x_R, i.e. on $\langle x - x_R, n_R \rangle$. Furthermore, the flux will proportional to the inverse of the square of its distance from x_R. To avoid (mathematical and technical) problems, the flux usually is truncated by some properly chosen constant Θ. What is measured by a receiver is the integral over the flux.

For a scattering sequence $\omega := (x_0, \varphi_0, t_0; t_1, \varphi_1; t_2, \varphi_2; \ldots)$ we denote by

$$
\begin{aligned}
N(\omega) & \quad \text{the number of the last scattering point,} \\
X(\omega) & := x_0 + \sum_{i=1}^{N(\omega)} cT_i(\omega)\Phi_{i-1}(\omega) \\
& \quad \text{the last scattering point} \\
& \quad \text{where } T_i(\omega) = t_i \text{ and } \Phi_{i-1}(\omega) = \varphi_{i-1} \text{ and,} \\
\Phi(\omega) & := \Phi_{N(\omega)+1}(\omega)
\end{aligned}
$$

the last direction of scattering before passing through the receiver. Then we obtain

$$
\begin{aligned}
\mu_{\tau,\Theta}(\mathcal{T}, \mathrm{FOV}_R) &:= \mathbb{E}^\tau(g(\mathcal{T}, \Theta; \cdot)) \\
&= \int g(\mathcal{T}, \Theta; \omega)\, \mathbb{P}^\tau(d\omega) \qquad \text{(LE4)}
\end{aligned}
$$

$$
\text{where} \quad g(\mathcal{T}, \Theta; \omega) := \min\{\Theta, \frac{\langle \Phi(\omega), n_R\rangle}{\langle X(\omega), n_R\rangle^2}\}\; I(\omega)
$$

$$
\text{and} \quad I(\omega) := 1_{\mathcal{T}}\Big(\sum_{i=0}^{N(\omega)} T_i(\omega) - \frac{\langle X(\omega), n_R\rangle}{\langle \Phi(\omega), n_R\rangle}\Big)
$$

and

$$
\begin{aligned}
\mu_{\tau,\Theta}(\mathcal{T}, \mathrm{FOV}_R) &= \sum_{n=0}^{\infty} \mu_{\tau,\Theta,n}(\mathcal{T}, \mathrm{FOV}_R) \\
\text{where} \quad \mu_{\tau,\Theta,n}(\mathcal{T}, \mathrm{FOV}_R) &:= \int g(\mathcal{T}, \Theta; \omega)\, 1_{N=n}(\omega)\, \mathbb{P}^\tau(d\omega).
\end{aligned}
$$

This is the exact multiple scattering LIDAR equation based on the Θ-truncated normed flux. The first part of Equation (LE 4) is the total multiple scattering LIDAR signal containing all orders of scattering. $\mu_{\tau,\Theta,n}(\mathcal{T}, \mathrm{FOV}_R)$ is the n–th order scattering part of it. The integral is taken over the set Ω of all scattering sequences. The probability measure $\mathbb{P}^\tau$ is defined as in Equation (LE3) for the corpuscular multiple scattering process defined by the sequence $((E_n, P_n) : n \in \mathbb{N})$ with the starting distribution τ. As in (LE3) the integral over Ω with respect to $\mathbb{P}^\tau$ may be written as an iteration of integrations over the "marginal" spaces with respect to the Markov kernels E_n and P_n and the starting distribution τ.

Using versions of such modified flux based multiple scattering LIDAR equations in the framework of the stochastic corpuscular multiple scattering process, it was possible to show that the transport theoretic approach and the stochastic approach to describe multiple scattering are equivalent, at least in many cases as we shall show (see Section 2.4).

1.7 The variance reduction Monte Carlo methods

During the third period of the cooperation Andrei Starkov adapted the CC variance reduction Monte Carlo methods to the simulation of a monostatic LIDAR and implemented a FORTRAN code for the calculation of multiply scattered LIDAR return signals which allows for calculating the contributions of all orders of scattering. On the basis of this code Masoud Noormohammadian and Andrei Starkov developed an improved ANSI–C code. These variance reduction Monte Carlo methods use splitting techniques which are adapted to the special configuration of the LIDAR.

The process of light propagation in the atmosphere can be simulated by Monte Carlo simulation based on the stochastic model of the stochastic corpuscular multiple scattering process. However, using such a Monte Carlo simulation for the calculation of LIDAR signals is very ineffective since only a few photons will arrive at the comparably tiny receiver. At least 70 million pathes of photons would have to be calculated by such a Monte Carlo simulation to obtain a signal of the quality of the ones in Figure 1.7. Variations of such Monte Carlo methods often result in a bias. For the construction of unbiased and variance reducing Monte Carlo simulations weight methods are used. They are based on employing "non-physical" probability distributions. These distributions are constructed properly from a priori information of the photon's importance. The variance reduction computational schemes are based on the simulation of the transport of a large number of photons with relatively low weight in interesting regions and of only a small number of photons with relatively high weight in unimportant regions.

The splitting techniques used in our variance reduction methods are "point splitting" and "scattering splitting".The point splitting technique is a history dependent combination of "exponential transform" and "splitting in collision points". The scattering splitting technique increases the number of photons scattered towards the receiver.

Hence, the applied variance reduction method means a transition from the Monte Carlo simulation of the stochastic corpuscular multiple scattering process to the Monte Carlo simulation of an artificial process which is a pretty complicated "stochastic multiple scattering cascade process"; see Figure 1.8. This transformation of the relatively simple stochastic corpuscular multiple scattering process into the pretty complicated stochastic multiple scattering cascade process results in a (possibly) tremendous increase of the speed and considerable decrease of the variance of the associated Monte Carlo simulations. We shall make precise this transformation of these stochastic processes and the associated formulas for the multiply scattered LIDAR signal and point out the relation of the stochastic

Figure 1.7: Multiply scattered LIDAR signals (variance reduction MC).

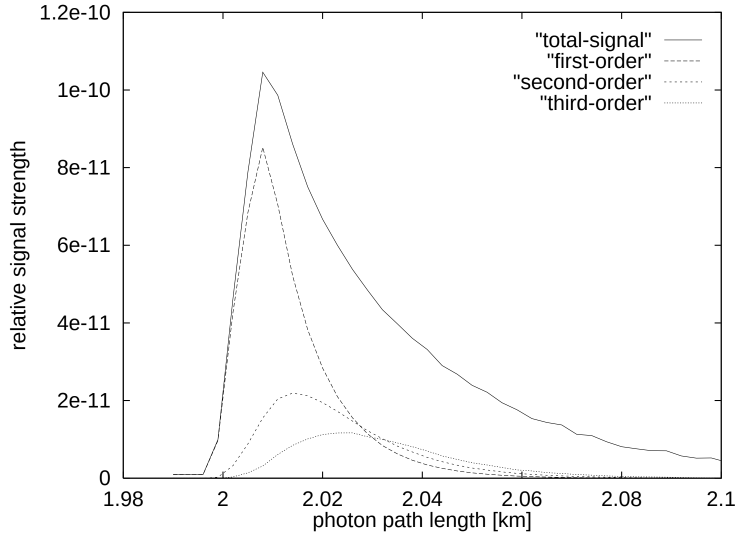

multiple scattering cascade process to the implemented variance reduction Monte Carlo methods.

The transformation of the stochastic multiple scattering process into the more complicated stochastic multiple scattering cascade process is a consequence of techniques applied to calculate the very complicated integrals in the exact multiple scattering LIDAR equations of the type of Equation (LE4). These techniques are essentially the following:

- to transform the integrands and the densities of the integrating Markov kernels appropriately
- to integrate the integral partially analytically
- to split the integral into parts and to modify these parts
- to introduce additional integrations artificially

This has to be done such that the integrals are not changed. However, if it is possible, the variance should be reduced. Calculating these transformed integrals by Monte Carlo simulation according to their new form then means:

- to design new Monte Carlo procedures which are based on the new Markov kernels
- these Monte Carlo procedures will yield unbiased and variance reduced estimates of the multiply scattered LIDAR signal.

Figure 1.8: Visualization of the cascade process (showing scattering splitting only).

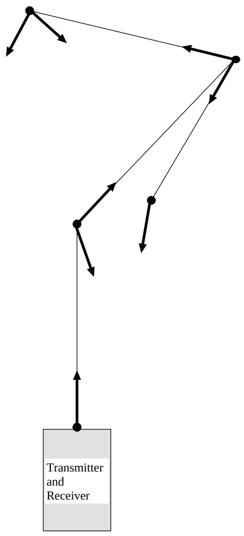

Besides the above mentioned splitting techniques we apply the methods of "local estimates" and of "exponential transforms".

The method of local estimates is based on two ideas: The first idea is to calculate the most inner integration analytically. This integral describes the extinction on the way from the last scattering point of a photon (characterized by the scattering sequence ω) to the receiver. This term will be the exponential factor used in the exponential transform. The second idea is based on the fact that for given last scattering point before reception the direction of the photon after this scattering event is uniquely determined by the point where it hits the receiver plane. This transformation produces an estimate which adds for every scattering event some amount to the LIDAR signal. (This method should not be applied if the radius of the receiver is too large.)

The method of the exponential transform is combined with point splitting and a randomisation procedure (which sometimes is called "Russian roulette"): The density of the extinction distribution is multiplied by a quotient equal to 1. The nominator of this quotient is of exponential type and is taken as the new density. The quotient Q of the old density and the denominator will be either larger or smaller than 1 according to the direction of the photon (represented by the scattering sequence ω). If Q is smaller than 1, then by the randomisation an expected number of $1-Q$ photons is simulated. If Q is larger than 1, then by the randomisation an expected number of Q photons is simulated. From the scalar product in the flux version of the multiple scattering LIDAR equation (LE4) it follows that the photon moves away from the receiver for $Q < 1$ and moves towards the receiver for $Q > 1$. Hence, we enlarge the number of photons moving towards the receiver and diminish the number of photons moving away from the receiver.

Splitting in collision points transforms one photon in many, say n, photons with the same history and observes these photons independently given this history. Taking the arithmetic mean will yield the same (conditional) expectation and reduces the (conditional) variance by the factor $1/n$.

Beam scattering splitting occurs in a selectable neighborhood of the transmitted beam and splits a photon moving away from the receiver into exactly two photons. The first photon will be scattered within a selectable cone coaxial to the incident direction in the direction of the receiver. The second photon will be scattered in a direction outside of this cone. The weights for the two photons will be chosen in such a way that they are smaller than 1 and that the scattering densities are constant inside and outside the cone. This means that a photon moving away from the receiver will be scattered such that at least one of the new photons will be scattered towards the receiver and, hence, the (conditional) probability of being received is increased. A photon moving towards the receiver is not splitted.

1.8 The polarisation

Until now we did not consider polarisation explicitely. Now we want to extend the stochastic corpuscular multiple scattering process to describe also effects of polarisation. This extension will be done by introducing Stokes vectors to describe the state of polarisation and polarized phase functions to characterize the scattering distributions. We shall obtain a model of a stochastic polarized multiple scattering process. Again, this stochastic polarized multiple scattering process is transformed into an associated stochastic polarized corpuscular multiple scattering cascade process. And this process will be the basis of the variance reduction Monte Carlo method for the calculation of the polarized multiple scattering LIDAR signal.

Again, we shall design this Monte Carlo method for a monostatic LIDAR with conical and ringshaped fields of view. Such a LIDAR is the multichannel polarisation Micro–LIDAR of the DLR. The design and the implementation of the computer codes for these new variance reduction Monte Carlo methods have been done by Martin Kerscher and Masoud Noormohammadian. We shall present the details of the mathematical constructions, the computer codes, and many calculations of LIDAR signals.

For the description of polarisation we use modified Stokes vectors according to Chandrasekhar [10]: $ST := (I_{\|}, I_{\perp}, U, V)^T$ where $I := I_{\|} + I_{\perp}$ denotes the intensity. The Stokes vector is defined with respect to a reference plane. This plane of reference is given by the direction of propagation $\varphi \in S^2$ (where S^2 denotes the unit sphere in $\mathbb{R}^3$) and a reference vector $\rho \in S^2$ with $\rho \perp \varphi$; see van de Hulst [19], §5.11.

We define the normed Stokes vector:

$$\begin{aligned} st &:= (i_{\|}, i_{\perp}, u, v)^T \\ &:= \begin{cases} (\frac{I_{\|}}{I}, \frac{I_{\perp}}{I}, \frac{U}{I}, \frac{V}{I})^T & \text{for } I \neq 0, \\ (0,0,0,0) & \text{for } I = 0. \end{cases} \end{aligned}$$

In the expanded (stochastic polarized corpuscular multiple scattering) model the path of a polarized photon is characterized by its starting point x_0, its starting direction φ_0, its initial state of polarization st_0 (given as a normed Stokes vector), the reference vector ρ_0, and by the sequences $(t_n : n \in \mathbb{N})$, $(\varphi_n : n \in \mathbb{N})$, $(st_n : n \in \mathbb{N})$, and $(\rho_n : n \in \mathbb{N})$, of the time intervals t_n between the $(n-1)$–th and the n–th scattering, the directions φ_n, the Stokes vectors st_n, and the reference vectors ρ_n after the n–th scattering, respectively (see Figure 1.9). We call this sequence

$$\omega := (x_0, \varphi_0, st_0, \rho_0, t_0; t_1, \varphi_1, st_1, \rho_1; t_2, \varphi_2, st_2, \rho_2; \ldots)$$

the *infinite polarized multiple scattering sequence.*

The extinction transition probabilities E_n are not changed with respect to the unpolarized case and are independent of the Stokes vectors:

$$\begin{aligned} &E_n(x_0, \varphi_0, st_0, \rho_0; t_1, \varphi_1, st_1, \rho_1; \ldots; t_{n-1}, \varphi_{n-1}, st_{n-1}, \rho_{n-1}; \cdot) := \\ &:= E_n(x_0, \varphi_0; t_1, \varphi_1; \ldots; t_{n-1}, \varphi_{n-1}; \cdot). \end{aligned}$$

Again, E_n is given by a generalized exponential distribution, following as a consequence of the Beer-Lambert law.

The scattering transition probabilities P_n, however, depend on the Stokes vectors and the reference vectors:

$$P_n(x_0, \varphi_0, st_0, \rho_0; t_1, \varphi_1, st_1, \rho_1; \ldots; t_{n-1}, \varphi_{n-1}, st_{n-1}, \rho_{n-1}; t_n; \cdot).$$

To show how this transition probability has to be changed with respect to the unpolarized case we first discuss single scattering of polarized light with special attention to spherical particles.

The scattering of a polarized photon with the reference plane (ρ, φ) and the Stokes vector st at the point x into the direction of φ' can be expressed by two matrix multiplications:

$$ST' := \mathcal{M}(\theta) \mathcal{L}(\phi)\, st.$$

Figure 1.9: The path of a photon starting in x_0 in the direction of φ_0 with the normed Stokes vector st_0 and the reference vector ρ_0.

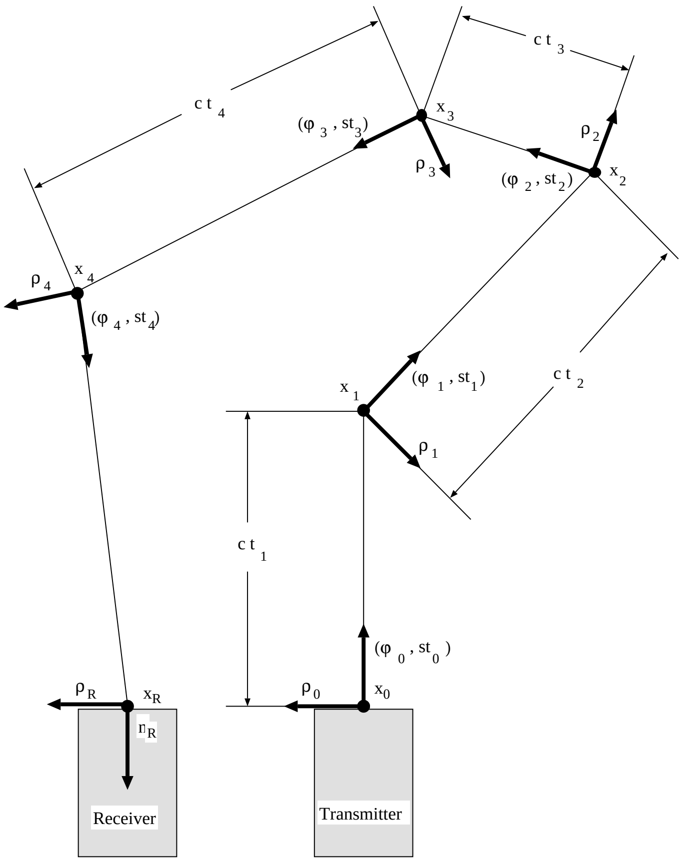

Here $\theta \in [0, \pi]$ is the elevation angle between the incident direction φ and the scattered direction φ' of the photon. $\phi \in [0, 2\pi]$ describes the azimuth angle between the plane of reference (ρ, φ) before the scattering and the plane of reference (ρ', φ') after the scattering, which is equal to the scattering plane (φ, φ'); see Figure 1.10.

$\mathcal{L}(\phi)$ is the matrix for the rotation of the Stokes vector (see Chandrasekhar [10] and Appendix 6.1.3):

$$\mathcal{L}(\phi) \;:=\; \begin{pmatrix} \cos^2(\phi) & \sin^2(\phi) & \frac{1}{2}\sin(2\phi) & 0 \\ \sin^2(\phi) & \cos^2(\phi) & -\frac{1}{2}\sin(2\phi) & 0 \\ -\sin(2\phi) & \sin(2\phi) & \cos(2\phi) & 0 \\ 0 & 0 & 0 & 1 \end{pmatrix}.$$

$\mathcal{M}(\theta)$ is the Mueller matrix for the transformation of the Stokes vector; see van

Figure 1.10: The geometry for single scattering of polarized light.

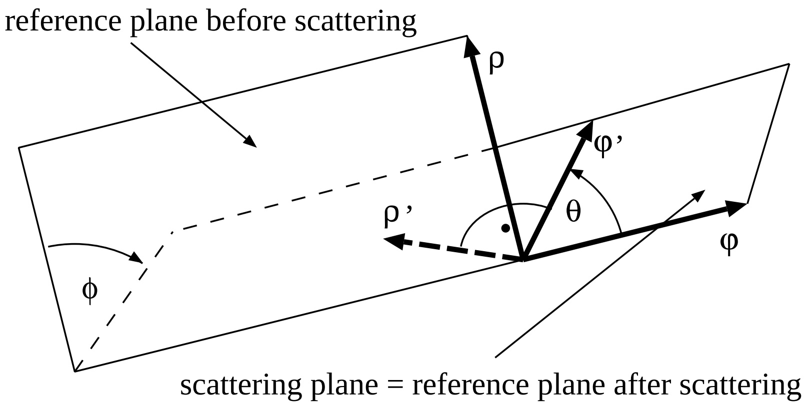

de Hulst [19], §5.14). For spherical particles the Mueller matrix is

$$\mathcal{M}(\theta) \;:=\; \begin{pmatrix} m_{11}(\theta) & 0 & 0 & 0 \\ 0 & m_{22}(\theta) & 0 & 0 \\ 0 & 0 & m_{33}(\theta) & -m_{43}(\theta) \\ 0 & 0 & m_{43}(\theta) & m_{33}(\theta) \end{pmatrix};$$

(see Deirmendjian [12], §3.2 and §3.3 and Appendix 6.1.6). We obtain the intensity $I' = I'_{||} + I'_{\perp}$ after the scattering from iterated matrix multiplication:

$$\begin{aligned} I'(\theta, \phi, st) \;&=\; \tfrac{1}{2}(m_{11}(\theta) + m_{22}(\theta)) + \\ &\tfrac{1}{2}(m_{11}(\theta) - m_{22}(\theta)) \Big((2i_{||} - 1)\cos(2\phi) + u \sin(2\phi) \Big). \end{aligned}$$

With the normalisation condition of the Mueller matrix for Mie particles (see Deirmendjian [12], §3.3) we get:

$$\int_0^{2\pi}\int_0^{\pi} I'(\theta, \phi, st)\, \sin(\theta)\, d\theta\, d\phi \;=\; 4\pi.$$

Now we are able to define the *polarized phase function* ph_{pol}:

$$ph_{pol}(\theta, \phi, st) \;:=\; \frac{I'(\theta, \phi, st)}{4\pi}.$$

The polarized phase function is the density of the scattering distribution which gives us the scattering transition probability

$$P_n(x_0, \varphi_0, st_0, \rho_0; t_1, \varphi_1, st_1, \rho_1; \ldots; t_{n-1}, \varphi_{n-1}, st_{n-1}, \rho_{n-1}; t_n; \cdot).$$

For the simulation we need to factorize the probability density ph_{pol}. With the marginal density

$$ph_1(\theta) \quad := \quad \int_0^{2\pi} ph_{pol}(\theta, \phi, st)\, d\phi = \frac{1}{4}\Big(m_{11}(\theta) + m_{22}(\theta)\Big),$$

and the conditional density

$$ph_2(\phi, st \mid \theta) \quad := \quad \begin{cases} \dfrac{ph_{pol}(\theta, \phi, st)}{ph_1(\theta)} & \text{for } ph_1(\theta) \neq 0, \\ 0 & \text{for } ph_1(\theta) = 0. \end{cases}$$

we get

$$ph_{pol}(\theta, \phi, st) \quad = \quad ph_1(\theta) \cdot ph_2(\phi, st \mid \theta),$$

and for $ph_1(\theta) \neq 0$

$$\begin{aligned} & ph_2(\phi, st \mid \theta) = \\ & \quad = \frac{1}{2\pi} + \frac{1}{2\pi}\, \frac{m_{11}(\theta) - m_{22}(\theta)}{m_{11}(\theta) + m_{22}(\theta)} \Big(\, (2i_{\|} - 1)\cos(2\phi) + u \sin(2\phi)\, \Big). \end{aligned}$$

For unpolarized scattering we use the well–known unpolarized phase function $ph_{unpol}(\theta) = ph_1(\theta)/(2\pi)$, which is independent of ϕ. We see that the deviation of ph_{pol} from ph_{unpol} is proportional to $(m_{11}(\theta) - m_{22}(\theta))\, /\, (m_{11}(\theta) + m_{22}(\theta))$. Figure 1.11 shows that this deviation is significant.

The Stokes vector st_n after the n–th scattering event is obtained from the photon history

$$(x_0, \varphi_0, st_0, \rho_0, t_0; t_1, \varphi_1, st_1; \ldots; t_{n-1}, \varphi_{n-1}, st_{n-1}, \rho_{n-1}; t_n, \varphi_n)$$

by the iterated transformation with $\mathcal{M}(\theta)\,\mathcal{L}(\phi)$. After each step the Stokes vector ST' has to be normed.

Again, we construct from the sequence $((E_n, P_n) : n \in \mathbb{N})$ of extinction and scattering distributions and from some initial distribution (describing the transmitted pulse and the receiver) a probability measure on the space of all infinte polarized multiple scattering sequences. This probability measure determines the stochastic polarized corpuscular multiple scattering process. Furthermore, we obtain an exact polarized multiple scattering LIDAR equation. We shall describe the details of the construction of this process and the derivation of the associated LIDAR equation in detail (see Chapter 2).

Again, the stochastic polarized corpuscular multiple scattering process is transformed into a stochastic polarized multiple scattering cascade process which enables us obtain a highly efficient variance reduction Monte Carlo method for the

Figure 1.11: $(m_{11}(\theta) - m_{22}(\theta)) \,/\, (m_{11}(\theta) + m_{22}(\theta))$ of a C1–cloud.

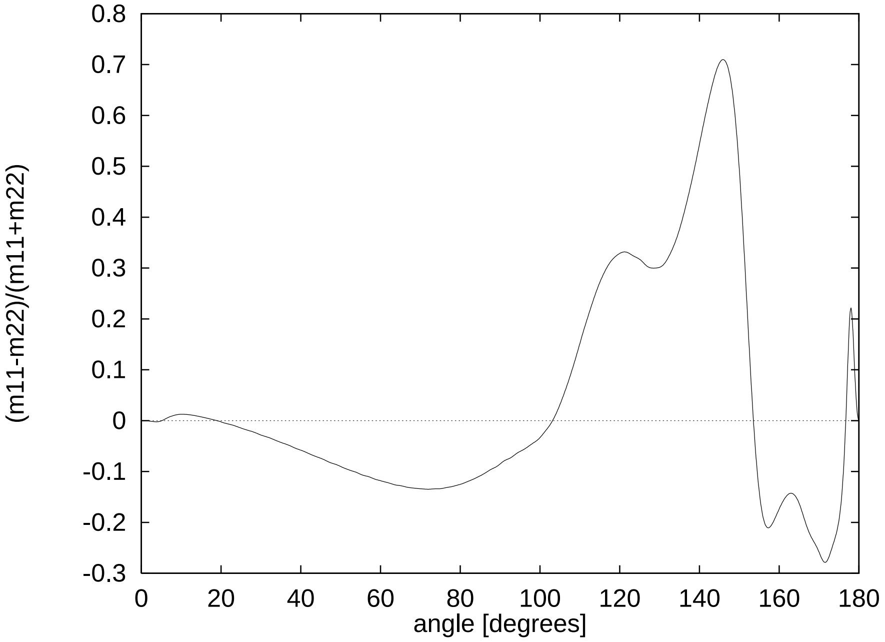

calculation of the exact polarized LIDAR signal containing all orders of scattering. Of course, the additional time needed for taking polarisation into account is considerable.

We shall describe the construction of the stochastic polarized corpuscular multiple scattering cascade process and its connection to the stochastic polarized multiple scattering process (see Chapter 2) and the code of the variance reduction Monte Carlo method in detail (see Chapter 4 and Appendix 6.7). Furthermore, we shall present a number of calculations for ground-based, and airborne LIDAR applications (see Chapter 5).

1.9 Recent calculations and various comparisons

During the last years we contributed with simulations to the following topics:

- simulations of polarized and unpolarized LIDAR signals of various configurations of C1 clouds published in:
  - "A Stochastic Model and Monte Carlo Sampling of LIDAR Returns" in MUSCLE 6 Proceedings; Oppel et al. [39].

  - "Polarized Multiply Scattered LIDAR Returns" in MUSCLE 7 Proceedings and Optical Review; Kerscher et al. [23].
  - "A Stochastic and a Variance Reduction MC method for the Calculation of Light Transport" in Applied Physics; Bissonette et al. [2].
  - and in this report in Chapter 5.

- simulations for space–based LIDAR systems were calculated and presented in:
  - "A Stochastic Model and Monte Carlo Sampling of LIDAR Returns" in MUSCLE 6 Proceedings; Oppel et al. [39].
  - "A Stochastic and a Variance Reduction MC method for the Calculation of Light Transport" in Applied Physics; Bissonette et al. [2].
  - a more detailled and extended version within an internal paper of the DLR (1994).

- comparisons and justification of our model / simulations for several standard situation with other scientists:
  - "LIDAR Multiple Scattering from Clouds" in Applied Physics; Bissonnette et al. [2].
  - not published exchange of data and comparison of this data with M. Wiegner and P. Bruscaglioni in the framework of the above mentioned publication in Applied Physics.

- test of simplified models with respect to multiple scattering for the measurement within Cirrus clouds:
  - "The Influence of Multiple Scattering from Ice Clouds and a New Ultra–highspeed Inversion Algorithm for Lidar Signals" in Ruppersberg et al. [42].
  - publication of the complete data of this Ruppersberg–LMU comparison (with discussion of the comparison) in Noormohammadian [37] Chapter 3 and 4.1.

- sensitivity analysis: The calculations for a C1–cloud sensitivity analysis are discussed in this report in Section 5.2.

- inversion methods: Discussed in this report.

- simulation of LIDAR signals from advective and radiative fogs of different thickness. Application of the knowledge obtained by this data to design a prototype of an expert system to handle the "automatic" detection of the fog visibility using a multisensor system:

- "Expertensysteme zur Datenanalyse" in Prooceedings of LASER '93"
- the complete simulated data used to design the expert system is presented in Noormohammadian [37] Chapter 3 and Section 4.2 .

Additionally, our program (`rbs`) was used by M. Wiegner and P. Voelger (Meteorological Institute of the Ludwig Maximilians University Munich) to investigate the relevance of multiple scattering in space based LIDAR measurents and in ground based Aerosol measurements. These simulations were especially helpful for a first evaluation of the possibilities of the planed European satelite ATLID.

1.10 First Conclusions

Simulations of multiply scattered LIDAR signals are important for many reasons:

1. It is necessary to judge the influence of multiple scattering on the inversion procedures based on the classical LIDAR equation. We mentioned this problem in Section 1.1 of this Chapter. The DLR part of the report about the DFG project MUSCLE contains more details and many calculations supporting the need for exact multiple scattering LIDAR equations (and for inversion procedures based on such exact LIDAR equations).

2. It is necessary to judge the quality of approximative multiple scattering LIDAR equations in various environmental situations. Some of these approximative multiple scattering comprise only some orders of multiple scattering, and this only in form of a simple and rough estimate. Nevertheless, they may be very effective in certain environmental situations. Whereas in other situations they may fail completely. To check the range of validity of such approximative multiple scattering LIDAR equations, their results have to be compared with the very exact, but computer time consuming variance reduced Monte Carlo simulations.

3. For designing new LIDAR equipment it is extremely helpful to analyse the complex relations of hardware parameters and environmental parameters with respect to the LIDAR signal. For example, the influence of multiple scattering differs considerably for airborne, ground-based, and space-based LIDARs for simple geometric reasons: the shape of the region where multiple scattering is "observed" by the receiver differs from a narrow cone over a broader cone to a wide cone base, respectively. As a consequence of this the amount of influence of multiple scattering varies from only some over considerable to absolutely dominant and the orders of multiple scattering vary from few low (2–3) over some higher (2–10) to very many high (2–100) orders, respectively. Furthermore, depolarisation depends heavily on the orders of multiple scattering.

4. To have LIDAR signals with exactly known environmental parameters is essential for testing methods for the evaluation of such signals. Especially, since the inversion procedures known to us all are are extremely discontinuous (i.e. the inversion problems are ill-posed) in the presence of multiple scattering.

5. Some very generally applicable and powerful inversion prodedures need as a prerequisite methods for the arbitrarily exact calculation of multiply scattered LIDAR signals.

1.11 Outlook and inversions

The ultimate purpose of in situ or remote LIDAR sensing of the atmosphere is the determination of the microphysical parameters which are important for meteorologists. For example, such parameters are extinction, absorption, phase, particle number density, particle size, shape, and orientation.

Again the most simple way of evaluating multiply scattered LIDAR signals is to compare them with an appropriate set of calculated multiple scattering LIDAR signals. It is very hard, if not impossible, to draw conclusions on the wanted parameters only by such inspection. One reason for that is the huge number of parameters (e.g. of the phase function) entering the exact multiple scattering LIDAR equation.

Procedures which allow for extracting such parameters from one or several (e.g. FOV, wavelength, polarisation) LIDAR signals are called inversion procedures. Usually such inversion procedures are obtained from solving the exact multiple scattering LIDAR equation for the wanted parameters. Of course, many parameters enter the exact multiple scattering LIDAR equation. Only under additional assumptions on the values of the other environmental parameters this equation will be uniquely solvable for one or a few of these parameters. But usually in applications the values of these fixed parameters will not be known. Furthermore, these inversion procedures will be very sensitive to variations of the fixed parameters. Hence, these inversion methods are often extremely unreliable. A sensitivity analysis of the procedure is needed to judge the quality of the inversion.

We have designed, implemented, and applied inversion algorithms which are based on random search and include a sensitivity analysis: Each set of environmental parameters is a vector p in some subset P of an n-dimensional Euclidian space. A random search procedure chooses a vector p in the set P at random according to some (properly chosen) probability law (which may depend on the history of the search process). To this parameter vector p the multiple scattering LIDAR signal is calculated by variance reduced Monte Carlo simulation. This simulated signal is then compared to the given (e.g. measured) multiple scattering LIDAR signal. For comparison we can use functionals describing the distance between the measured and the simulated signal appropriately (e.g. by a Chebyshev norm for some interval, a weighted L_2–norm). If we shall use an efficient random search procedure (e.g. uniform random search, uniform search on circles with adapted radius, genetic algorithms; Kiefer-Wolfowitz procedure), we shall find regions of parameter vectors which are "solutions" of our inversion problem.

Such random search procedures may be designed to be very efficient. Of course, many comparisons have to be made (by the computer). Much computing time is needed, since every single variance reduction Monte Carlo simulation of a multiple scattering LIDAR signal is time consuming (which can be reduced a little bit by starting simulations with higher variance and reducing the variance progressively). A by–product of the random search procedure is a sensitivity analysis of the dependence of the solution on the parameters. This is done by noting the progress of approximation of the distance between the measured and the simulated signal for the inspected parameters during the search process.

Chapter 2

Stochastic approach

2.1 The multiple scattering process for polarized light

In this section we shall present a stochastic model for the description of the polarized multiple light scattering process at athmospheric particles (cf. Oppel et al. [38], $ 4 or Noormohammadian [37]). This process may be divided in elementary (single) scatering processes in a canononical fashion. For polarized light such a single scattering process is discussed in the appendix 6.1. We show that the multiple scattering process, more exact the position–direction process describing the nth scattering position and the nth scattering direction, is a Markov process.

If not explicitely stated, we use the expressions in the sense given in the symbol table.

Motivation 2.1.1 In our model we asume that we are able to describe a light beam with photons which travel along straight lines and get scattered at atmospheric particles, i.e. molecules, ice crystals, water droplets or dust particles. The assumptions made in using this picture are the *single particle* and the *independent scattering ??* assumption. For a discussion see Oppel et al. [38], $ 2 and $ 3.

For the description of the stochastic model we look at a photon starting at time t_0 in point $x_0 \in \mathbb{R}^3$ with direction of propagation $\varphi_0 \in S^2$ and normed Stokes vector $st_0 \in Pol$ (see Figure 2.1). For the full specification of the Stokes vector we need the reference vector $\rho_0 \in S^2$ with $\rho_0 \perp \varphi_0$. ρ_0 determines together with φ_0 the reference plane (see definition 6.1.1). The tupel?? $\omega_0 := (x_0, \varphi_0, st_0, \rho_0, t_0)$ is describing a LIDAR sender at position x_0 emitting an exact collimated beam into direction φ_0 with polarisation according to the Stokes vector st_0 and the reference plane (ρ_0, φ_0). This photon travels wit the speed of light c along the halfline starting in x_0 into the direction φ_0. After time $\omega_1 := t_1$ the photon is getting scattered or absorbed at the point $x_{(1)} := x_0 + c\, t_1\, \varphi_0$ into the direction φ_1. In the case of scattering the photon gets a new Stokes vector st_1 with reference vector ρ_1, $\rho_1 \perp \varphi_1$. We define $\omega_2 := (\varphi_1, st_1, \rho_1)$. Afterwards the photon is moving along the halfline starting in $x_{(1)}$ into the direction φ_1 with constant velocity c.

Again after time $\omega_3 := t_2$ the photon gets scattered (or absorbed) at position $x_{(2)} := x_{(1)} + ct_2\varphi_1$ into direction φ_2 and Stokes vector st_2 and reference vector ρ_2, $\rho_2 \perp \varphi_2$. We define $\omega_4 := (\varphi_2, st_2, \rho_2)$.

The path of a photon is uniquely described with the scattering sequence:

$$\begin{aligned} \omega &:= (\omega_0, \omega_1, \omega_2, \omega_3, \omega_4, \dots) \\ &:= \Big((x_0, \varphi_0, st_0, \rho_0, t_0); t_1, \varphi_1, st_1, \rho_1; t_2, \varphi_2, st_2, \rho_2; \dots\Big). \end{aligned}$$

Figure 2.1 is illustrating this situation.

Figure 2.1: The path of a multiply scattered photon starting in x_0 in the direction of φ_0, with Stokes vector st_0 and reference vector ρ_0.

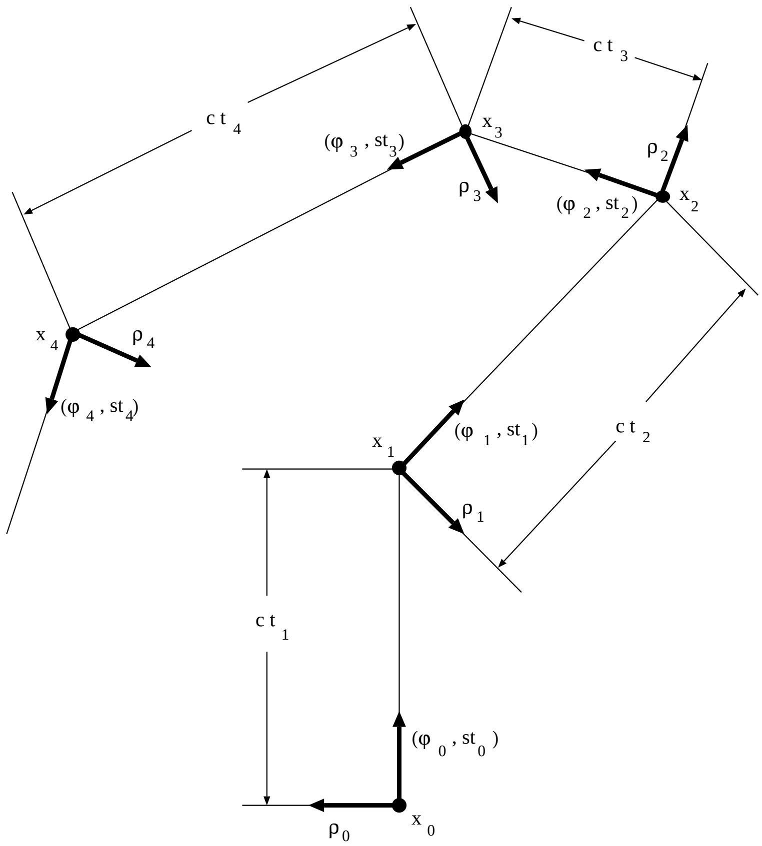

2.1.1 The stochastic process

In this section we define the stochastic model of the process of multiple scattering.

Definition and Remark 2.1.2 (Physical scattering process) Let $c \in \mathbb{R}^+$ be a fixed constant. We define for each $i \in \{1,2,3\}$, $k \in \mathbb{N}$ and $l, n \in \mathbb{N}_0$ with $l \leq n$:

$$\Omega_{01} := \mathbb{R}^3, \quad \Omega_{02} := S^2, \quad \Omega_{03} := Pol, \quad \Omega_{04} := S^2, \quad \Omega_{05} := \mathbb{R}_0^+$$

$$\Omega_0 := \Omega_{01} \times \Omega_{02} \times \Omega_{03} \times \Omega_{04} \times \Omega_{05},$$

$$\Omega_{k,dir} := S^2_\infty, \quad \Omega_{k,pol} := Pol, \quad \Omega_{k,ref} := S^2,$$

$$\Omega_k := \begin{cases} \mathbb{R}^+_{0,\infty}, & \text{if } k \text{ is odd,} \\ \Omega_{k,dir} \times \Omega_{k,pol} \times \Omega_{k,ref}, & \text{if } k \text{ is even,} \end{cases}$$

$$\Omega^{(n)} := \prod_{m=0}^{n} \Omega_m \quad \text{and} \quad \Omega := \prod_{m=0}^{\infty} \Omega_m$$

On these sets we have the σ–algebras:

$$\mathfrak{K}_{0i} := \mathfrak{B}(\Omega_{0i}),\ \ \mathfrak{K}_0 := \mathfrak{B}(\Omega_0),$$

$$\mathfrak{K}_{2k,dir} := \mathfrak{B}(\Omega_{2k,dir}),\ \ \mathfrak{K}_{2k,pol} := \mathfrak{B}(\Omega_{2k,pol}),\ \ \mathfrak{K}_{2k,ref} := \mathfrak{B}(\Omega_{2k,ref}),$$

$$\mathfrak{K}_k := \begin{cases} \mathfrak{B}(\Omega_k), & \text{if } k \text{ is odd,} \\ \mathfrak{K}_{k,dir} \otimes \mathfrak{K}_{k,pol} \otimes \mathfrak{K}_{k,ref} & \text{if } k \text{ is even,} \end{cases}$$

$$\mathfrak{K}^{(n)} := \bigotimes_{m=0}^{n} \mathfrak{K}_m \ \text{ and } \ \mathfrak{K} := \bigotimes_{m=0}^{\infty} \mathfrak{K}_m.$$

The constant c is the speed of a photon, i.e. the speed of light in the medium. From now on we assume that c is the speed of light in vacuum which is a good approximation for atmospherical situations. Therefore different medias only cause different extinction and transition distributions (see section 2.3) and not different light speeds. These mathematical definitions are describing the following physical quantities (see Figure 2.1):

Ω_{01}	the set of the starting positions x_0,
Ω_{02}	the set of the starting directions φ_0,
Ω_{03}	the set of the normed Stokes vectors st_0 of the starting photon,
Ω_{04}	the set of the reference vectors ρ_0 of the starting photon,
Ω_{05}	the set of the starting times t_0,
Ω_{2k-1}	the set of the time intervalls between the $(k-1)$–th and the k–th scattering event,
$\Omega_{2k,dir}$	the set of the directions of propagation φ_k after the k–th scattering event,
$\Omega_{2k,pol}$	the set of the normed Stokes vectors st_k after the k–th scattering event,
$\Omega_{2k,ref}$	the set of the reference vectors ρ_k after the k–th scattering event,
Ω_{2k}	the product set built from the directions of propagation φ_k and the Stokes vectors st_k after the k–th scattering event.

We are looking at the following projections:

$pr_{0i} : \Omega_0 \to \Omega_{0i}$	the canonical projection onto the set of the i–th component of Ω_0,

$pr_n : \Omega \to \Omega_n$	the canonical projection,
$pr_{dir} : \Omega_{2k} \to \Omega_{2k,dir}$	the canonical projection onto the set of directions of propagation,
$pr_{pol} : \Omega_{2k} \to \Omega_{2k,pol}$	the canonical projection onto the set of Stokes vectors,
$pr_{ref} : \Omega_{2k} \to \Omega_{2k,ref}$	the canonical projection onto the set of reference vectors,
$pr_{n,l} : \Omega^{(n)} \to \Omega_l$	the canonical projection onto the set of the l–th component,
$\pi_n : \Omega \to \Omega^{(n)}$	with $\omega := (\omega_m : m \in \mathbb{N}_0) \mapsto \pi_n(\omega) := (\omega_m : 0 \le m \le n)$.

The canonical projection is the projection onto a constituent of the product set.

Furthermore

$$E_k \in \mathfrak{M}(\Omega^{(2k-2)}, \Omega_{2k-1}) \qquad \text{and}$$
$$P_k \in \mathfrak{M}(\Omega^{(2k-1)}, \Omega_{2k}) \qquad \text{are given Markov kernels and}$$
$$\mathcal{P}_k \in \mathfrak{M}(\Omega^{(k-1)}, \Omega_k) \qquad \text{with} \quad \mathcal{P}_k := \begin{cases} E_{(k+1)/2}, & \text{if } k \text{ is odd,} \\ P_{k/2}, & \text{if } k \text{ is even.} \end{cases}$$

According to the disordered structure of the athmosphere (on small scales) the directions of propagation after the scattering and the time intervalls between two subsequent scattering events are random (see Oppel et al. [38] §2). This randomness is described with the Markov kernels (transition probabilities) E_k and P_k for $k \in \mathbb{N}$.

$E_k(\omega_0, \ldots, \omega_{2k-2}; A)$ is the probability that a photon with scattering sequence $(\omega_0, \ldots, \omega_{2k-2})$ is getting scattered the k–th time at the time $t_k = \omega_{2k-1} \in A \in \mathfrak{K}_{2k-1}$ after its $(k-1)$–th scattering event. $E_k(\omega_0, \ldots, \omega_{2k-2}; \{\infty\})$ is the probability that the photon doesn't get scattered any more (i.e. the medium (slab) has extinction 0).

$P_k(\omega_0, \ldots, \omega_{2k-1}; B)$ is the probability that a photon with scattering sequence $(\omega_0, \ldots, \omega_{2k-1})$ is getting scattered the k–th time in the direction of $\varphi_k = pr_{dir}(\omega_{2k})$ with the Stokes vector $st_k = pr_{pol}(\omega_{2k})$ and the reference vector $\rho_k = pr_{ref}(\omega_{2k})$ with $\omega_{2k} \in B \in \mathfrak{K}_{2k}$. $P_k(\omega_0, \ldots, \omega_{2k-1}; \{\overset{\mathrm{d}}{\infty}\} \times A)$ is for all $A \in \mathfrak{B}(\Omega_{2k,pol} \times \Omega_{2k,ref})$, $A \neq \emptyset$ the probability that the photon gets absorbed during the kth scattering.

According to the theorem of Ionescu–Tulcea (cf. Neveu [36], theorem 5.1.1 and corollary 2, p 194 and p 197) for each probability measure $\tau : \mathfrak{K}_0 \to [0,1]$ there exists only one probability measure $\mathbb{P}^\tau : \mathfrak{K} \to [0,1]$ such that for each rectangle $R := \bigcap_{m=0}^{n} pr_m^{-1}(K_m)$ with $K_m \in \mathfrak{K}_m$ and $n \in \mathbb{N}_0$ the following holds:

$$\mathbb{P}^\tau(R) \;=\; \int\limits_{K_0}\int\limits_{K_1}\dots\int\limits_{K_n} \mathcal{P}_n(\omega_0,\dots,\omega_{n-1};d\omega_n) \quad \dots \quad \mathcal{P}_1(\omega_0;d\omega_1) \quad \tau(d\omega_0).$$

For each $k \in \mathbb{N}$ we call

- Ω (provided with the product σ–algebra) the set of the *physical scattering sequences* $\omega \in \Omega$,
- E_k the *kth extinction probability*,
- P_k the *kth scattering probability*,
- $\mathbb{P}^\tau$ the *physical (multiple) scattering process with starting distribution* τ (or Rayleighs random flight).

Now we are able to define some random varaiables and sets we need later.

Definition and Remark 2.1.3 For $k \in \mathbb{N}$ and $n \in \mathbb{N}_0$ we define:

$$\mathfrak{P}_n \;:=\; \pi_n^{-1}(\mathfrak{K}^{(n)}),$$

$$\Psi_k \;:=\; \begin{cases} \mathbb{R}_0^+, & \text{if } k \text{ is odd,} \\ S^2 \times Pol \times S^2, & \text{if } k \text{ is even,} \end{cases}$$

$$\mathcal{X}_{(k)} \;:=\; \{\omega \in \Omega : pr_i(\omega) \in \Psi_i \text{ f"ur } i = 1,\dots,k\},$$

and

$$X_{(0)} := pr_{01} \circ pr_0, \quad \Phi_0 := pr_{02} \circ pr_0, \quad St_0 := pr_{03} \circ pr_0,$$

$$R_0 := pr_{03} \circ pr_0, \quad T_0 := pr_{05} \circ pr_0,$$

$$T_k := pr_{2k-1}, \quad St_k := pr_{pol} \circ pr_{2k}, \quad R_k := pr_{ref} \circ pr_{2k},$$

$$\Phi_k : \Omega \to S^2_\infty, \quad \Phi_k(\omega) := \begin{cases} pr_{dir} \circ pr_{2k}, & \text{if } \omega \in \mathcal{X}_{(2k)}, \\ \overset{\mathrm{d}}{\infty}, & \text{if } \omega \in \Omega \setminus \mathcal{X}_{(2k)}, \end{cases}$$

$$X_{(k)} : \Omega \to \mathbb{R}^3_\infty, \quad X_{(k)}(\omega) := \begin{cases} X_{(0)}(\omega) + c \sum\limits_{i=1}^{k} \Phi_{i-1}(\omega) T_i(\omega), & \text{if } \omega \in \mathcal{X}_{(2k-1)}, \\ \vec{\infty}, & \text{if } \omega \in \Omega \setminus \mathcal{X}_{(2k-1)}, \end{cases}$$

Directly from the definition follows for $k \in \mathbb{N}$ that $\mathcal{X}_{(k)} \in \mathfrak{P}_k$, $X_{(0)}$ is a $\mathfrak{P}_0$–$\mathfrak{K}_{01}$ mesurable, Φ_0 is a $\mathfrak{P}_0$–$\mathfrak{K}_{02}$ measurable, St_0 is a $\mathfrak{P}_0$–$\mathfrak{K}_{03}$ measurable, R_0 is a $\mathfrak{P}_0$–$\mathfrak{K}_{04}$ measurable, T_0 is a $\mathfrak{P}_0$–$\mathfrak{K}_{05}$ measurable, Φ_k is a $\mathfrak{P}_{2k}$–$\mathfrak{K}_{2k,dir}$ measurable, St_k

is a $\mathfrak{P}_{2k}$–$\mathfrak{K}_{2k,pol}$ measurable, R_k is a $\mathfrak{P}_{2k}$–$\mathfrak{K}_{2k,ref}$ measurable, T_k is a $\mathfrak{P}_{2k-1}$–$\mathfrak{K}_{2k-1}$ measurable and $X_{(k)}$ is a $\mathfrak{P}_{2k-1}$–$\mathfrak{B}(\mathbb{R}^3_\infty)$ measurable mapping.

For $\omega \in \Omega$ and $k \in \mathbb{N}$ we get:

$\mathcal{X}_{(2k-1)}$	the set of photons which get scattered k times at least (especially the photons which did not get absorbed until the kth scattering)
$X_{(0)}(\omega)$	the starting position of the photon,
$\Phi_0(\omega)$	the starting direction of the photon,
$St_0(\omega)$	the normed Stokes vector of the starting photon,
$R_0(\omega)$	the reference vector of the starting photon,
$T_0(\omega)$	the starting time of the photon (see the definition of the emitting puls of the LIDAR in Definition 2.2.1),
$\Phi_k(\omega)$	the direction of the photon after the k–th scattering if $\Phi_k(\omega) \in S^2$
$St_k(\omega)$	the normed Stokes vector of the photon after the k–th scattering
$R_k(\omega)$	the reference vector of the photon after the k–th scattering
$T_k(\omega)$	the time between the $(k-1)$–th and the k–th scattering event if $T_k(\omega) \in \mathbb{R}^+_0$,
$X_{(k)}(\omega)$	the k–th scattering position if $X_{(k)}(\omega) \in \mathbb{R}^3$.

Since for $k \in \mathbb{N}$ the functions $X_{(0)}$, Φ_0, St_0, R_0, T_0, Φ_k, St_k, R_k, T_k and $X_{(k)}$ only depend on the first $2k$ or $2k+1$ coordinate(s), we use the same notation if the functions are defined on the according sets $\Omega^{(0)}$, $\Omega^{(2k-1)}$ or $\Omega^{(2k)}$.

2.1.2 The markov property

Theorem 2.1.4 (Markov property) For $E \in \mathfrak{M}(\mathbb{R}^3_\infty \times S^2_\infty, \mathbb{R}^+_{0,\infty})$ and $P \in \mathfrak{M}(\mathbb{R}^3_\infty \times S^2_\infty \times \mathit{Pol} \times S^2, S^2_\infty \times \mathit{Pol} \times S^2)$ with:

$$\begin{aligned} E(x,\varphi;\,\cdot\,) &= \delta_\infty(\,\cdot\,), \quad \text{if } (x,\varphi) \in (\mathbb{R}^3_\infty \times S^2_\infty) \setminus (\mathbb{R}^3 \times S^2) \text{ and} \\ P(x,\varphi,st,\rho;\,\cdot\,) &= \Big(\delta_{\underset{\infty}{\mathrm{d}}} \times \delta_{st} \times \delta_\rho\Big)(\,\cdot\,) \\ &\quad\ \text{if } (x,\varphi,st,\rho) \in (\mathbb{R}^3_\infty \times S^2_\infty \times \mathit{Pol} \times S^2) \setminus (\mathbb{R}^3 \times S^2 \times \mathit{Pol} \times S^2), \end{aligned}$$

and E_k, P_k for all $k \in \mathbb{N}$, τ and $\mathbb{P}^\tau$ given according to Definition 2.1.2 and if with $A \in \mathfrak{K}_{2k-1}$, $B \in \mathfrak{K}_{2k}$, $\omega_{(2k-2)} \in \Omega^{(2k-2)}$ and $\omega_{(2k-1)} \in \Omega^{(2k-1)}$ the following is valid:

$$\begin{aligned} E_k(\omega_{(2k-2)};A) &= E\Big(X_{(k-1)}(\omega_{(2k-2)}),\Phi_{k-1}(\omega_{(2k-2)});A\Big), \\ P_k(\omega_{(2k-1)};B) &= P\Big(X_{(k)}(\omega_{(2k-1)}),\Phi_{k-1}(\omega_{(2k-1)}),St_{k-1}(\omega_{(2k-1)}),R_{k-1}(\omega_{(2k-1)});B\Big). \end{aligned}$$

Then the stochastic process $(X_{(n)},\Phi_n,St_n,R_n):n\in\mathbb{N}_0)$ on the probability space $(\Omega,\mathfrak{K},\mathbb{P}^\tau)$ fulfils the weak Markov property.

Proof: T

his is follows directly from the statements 1 and 4 of Theorem 6.3.4.

2.1.3 The stopping rules

Definition and Remark 2.1.5 (Stopping time) For $t\in\mathbb{R}_0^+$ we define:

$$N_t:\Omega\to\mathbb{N}_{0,\infty},\quad\text{with}\quad N_t(\omega):=\begin{cases}\inf\Big\{j\in\mathbb{N}_0:t<\sum\limits_{i=1}^{j+1}T_i(\omega)\Big\}, & \text{if } \{\ldots\}\neq\emptyset,\\ \infty, & \text{if } \{\ldots\}=\emptyset,\end{cases}$$

$$X_t:\Omega\to\mathbb{R}^3_\infty,\quad\text{with}\quad X_t(\omega):=\begin{cases}X_{(N_t(\omega))}(\omega)+c\,\Phi_{N_t(\omega)}\Big(t-\sum\limits_{i=1}^{N_t(\omega)}T_i(\omega)\Big), & \text{if } \omega\in\mathcal{X}_t,\\ \vec{\infty}, & \text{if } \omega\in\Omega\setminus\mathcal{X}_t,\end{cases}$$

with

$$\mathcal{X}_t:=\{\omega\in\Omega:pr_i(\omega)\in\Psi_i \text{ for } i=1,\ldots,2N_t(\omega)\}\ \cap\ \{\omega\in\Omega:N_t(\omega)\in\mathbb{N}\}.$$

For $\omega\in\Omega$ and $t\in\mathbb{R}_0^+$ we get:

$\mathcal{X}_t$	the set of photons not beeing absorbed until the time t after a finite number of scattering,
$N_t(\omega)$	the number of scattering events until the time t, if $N_t(\omega)\in\mathbb{N}_0$,
$X_t(\omega)$	the position of the photon at the time t, if $X_t(\omega)\in\mathbb{R}^3$.

For $t\in\mathbb{R}_0^+$ and $n\in\mathbb{N}_0$ we get:

$$\begin{aligned} \{N_t=n\} &\in \sigma\Big(\{T_1,\ldots,T_{n+1}\}\Big) \quad\subset\quad \mathfrak{P}_{2n+1}, \\ \{N_t=\infty\} &= \Omega\setminus\bigcup_{i\in\mathbb{N}_0}\{N_t=i\} \quad\in\quad \sigma\Big(\bigcup_{i\in\mathbb{N}_0}\mathfrak{P}_{2i+1}\Big), \\ \mathcal{X}_t &= \bigcup_{m\in\mathbb{N}_0}\bigcap_{k=1}^{2m}\Big(pr_k^{-1}(\Psi_k)\cap N_t^{-1}(\{m\})\Big) \quad\in\quad \mathfrak{K}. \end{aligned}$$

This means that N_t+1 is a stopping time with respect to the monoton increasing sequence $(\mathfrak{P}_{2k-1} : k \in \mathbb{N})$ of sub–σ–algebras of $\mathfrak{K}$ for $t \in \mathbb{R}_0^+$. X_t is $\mathfrak{K}$–$\mathfrak{B}(\mathbb{R}^3_\infty)$ measurable.

For each starting distribution τ the stochastic process $(X_t : t \in \mathbb{R}_0^+)$ on the probability space $(\Omega, \mathfrak{K}, \mathbb{P}^\tau)$ is describing the diffusion of the photons of the multiple scattering process.

The following lemmata characterize the stopping time N_t and are special cases of more general theorems similar to the theorems in Chapter 2 in Noormohammadian [37]. In the case of homogeneous fog it is possible to give the distribution of N_t explicitely (see Oppel et al. [38], p 63, for the unpolarized case).

Lemma 2.1.6 With the Definitions 2.1.2 and 2.1.3, $t_{\min} > 0$ and with $E_k\Big(\psi; [0, t_{\min}[\Big) = 0$ for all $k \in \mathbb{N}$ and $\psi \in \Omega^{(2k-2)}$ we get for all $t \in \mathbb{R}_0^+$:

$$\mathbb{P}^\tau\Big(N_t = \infty\Big) \;\leq\; \mathbb{P}^\tau\Big(N_t > t/t_{\min}\Big) \;=\; 0.$$

Lemma 2.1.7 With the Definitions 2.1.2 and 2.1.3 and σ and E_k for $k \in \mathbb{N}$ given according to 2.3.6 with

$$(\#) \qquad \begin{cases} \text{there is a } T > 0 \text{ and } \Sigma > 0, \text{ such that} \\[2mm] c\,\sigma(x+ct\varphi)\ \exp\Big(-\displaystyle\int_0^t c\,\sigma(x+cs\varphi)\,ds\Big) \;\leq\; c\,\Sigma\ exp\Big(-c\Sigma t\Big) \\[2mm] \text{for all } 0 \leq t < T \text{ and } (x,\varphi) \in \mathbb{R}^3 \times S^2 \end{cases}$$

we get $\mathbb{P}^\tau\Big(N_t = \infty\Big) = 0$ for all $t \in \mathbb{R}_0^+$.

Lemma 2.1.8 We use the Definitions 2.1.2 and 2.1.3. Furthermore let σ and E_k for $k \in \mathbb{N}$ be given according to theorem 2.3.6, and let K be a compact set in $\mathbb{R}^3 \equiv \Omega_{01}$ with $\tau \circ pr_{01}^{-1}(K) = 1$, then we get for all $t \in \mathbb{R}_0^+$ with $B_t(K) := \{x \in \mathbb{R}^3 : \inf_{y \in K} \|x-y\| \leq ct\}$:

$$\text{If } \sigma \Big| B_t(K) \text{ is bounded, then } \quad \mathbb{P}^\tau\Big(N_t = \infty\Big) = 0.$$

Remark 2.1.9 (”far distance”–hypothesis e.t.c) The assumptions of Lemma 2.1.6 describe the so called ”far distance”–hypothesis, this means that the time between two scattering events must not get arbitrary small. Physical arguments for this assumption are the finite number of scattering particles in a finite volume and the finite speed of light c (cf. Oppel et al. [38], §3 and S.27 or Marchuk et al. [33], p 19–21).

Instead in Lemma 2.1.7 we assume that we are able to estimate the density of the extinction distribution with the density of the exponential distribution (with constant extinction) from above.

On the basis of the preceeding considerations Lemma 2.1.8 characterizes environmental situations for an emitter with limited expansion which is emitting photons into a medium with limited extinction.

Now, we are able to conclude that in all relevant physical situations the assumptions of the Lemmata 2.1.6, 2.1.7 or 2.1.8 are fulfilled, i.e. $\mathbb{P}^\tau(N_t = \infty) = 0$ for all $t \in \mathbb{R}_0^+$. Therfore we get:

$$\begin{aligned} 0 \;\leq\; \mathbb{P}^\tau\Big(\sum_{k\in\mathbb{N}} T_k < \infty\Big) \;&=\; \mathbb{P}^\tau\Big(\bigcup_{t\in\mathbb{N}}\Big\{\sum_{k\in\mathbb{N}} T_k \leq t\Big\}\Big) \;=\; \mathbb{P}^\tau\Big(\bigcup_{t\in\mathbb{N}}\Big\{N_t = \infty\Big\}\Big) \\ &\leq\; \sum_{t\in\mathbb{N}} \mathbb{P}^\tau\Big(N_t = \infty\Big) \;\stackrel{\text{assumption}}{=}\; 0. \end{aligned}$$

This means, in all relevant physical situautions $\mathbb{P}^\tau$–almost surely only a finite number of scatterings occure in a finite time intervall.

2.2 The physical LIDAR equation for polarized light

Starting from the stochastic model for the description of the multiple scattering of polarized light (see Section 2.1) we now derive a time dependent and time independent LIDAR equation for the (normed) polarized flux.

2.2.1 The LIDAR transmitter and receiver

At first we define mathematically what we are calling a LIDAR:

Definition and Remark 2.2.1 (LIDAR transmitter and receiver) Let be $x_R \in \mathrm{IR}^3$, $\vec{n}_R \in S^2$, $\rho_R \in S^2$ with $\rho_R \perp \vec{n}_R$, $r_R \in \mathrm{IR}^+$, $S^2_R := \{\varphi \in S^2 : \langle \varphi, \vec{n}_R \rangle > 0\}$, $FOV_R \subset S^2_R$ an open set in S^2, and $\tau : \mathfrak{K}_0 \to [0,1]$ a probability measure.

The properties of the *LIDAR transmitter* are given by the starting distribution τ. τ determines the position and the direction distribution of the tarnsmitted beam, the time distribution of the transmitter puls and the Stokes vector of the transmitted beam.

Without any restriction of generality we define $x_R := (0,0,0)$ and $\vec{n}_R := (0,0,-1)$ in cartesian coordinates, i.e. we place the center of the LIDAR receiver in the origin of the coordinate system. We describe the *LIDAR receiver* by a receiver "field of view" (FOV_R) and the set

$$\begin{aligned} A_R &:= \{x \in \mathrm{IR}^3 : \langle x, \vec{n}_R \rangle = 0 \text{ and } \|x - x_R\| < r_R\} \\ &= \left\{(x_1, x_2, 0) \in \mathrm{IR}^3 : \sqrt{x_1^2 + x_2^2} < r_R\right\}, \end{aligned}$$

with

- A_R the effective receiver plane,
- x_R the center of the receiver,
- r_R the radius of the receiver,
- $\vec{n}_R$ the normal on the receiver plane A_R in receiving direction, and
- ρ_R the reference vector of the receiver.

With ρ_R and $\vec{n}_R$ the reference plane of the receiver is determined.

Figure 2.2: Geometry of the LIDAR receiver. In the picture we see $(x, \psi_1, t) \notin \mathcal{R}$ for $t \in \mathbb{R}_0^+$ and $(x, \psi_2, t) \in \mathcal{R}$ for $t > \|y - x\|/c$.

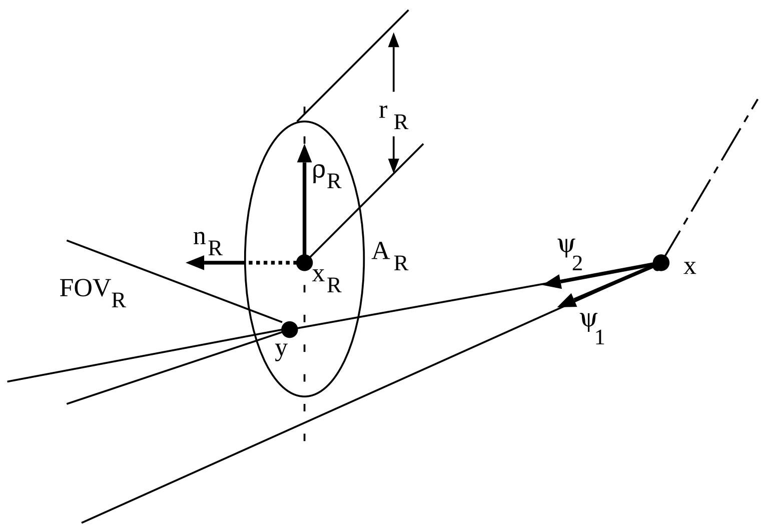

Furthermore:

$$
\begin{aligned}
\mathcal{H}^+ &:= \{x \in \mathbb{R}^3 : \langle x, \vec{n}_R \rangle > 0\}, \\
\mathcal{H}^- &:= \{x \in \mathbb{R}^3 : \langle x, \vec{n}_R \rangle < 0\}, \\
\mathcal{C}_x &:= \left\{ \psi \in S^2 : \psi = \frac{x' - x}{\|x' - x\|} \text{ with } x' \in A_R \right\} \quad \text{for all } x \in \mathcal{H}^+ \cup \mathcal{H}^-, \\
\mathcal{R} &:= \left\{ (x, \varphi, t) \in \mathbb{R}^3 \times S^2 \times \mathbb{R}_0^+ : x \in \mathcal{H}^-,\ \varphi \in \mathcal{C}_x \cap FOV_R \text{ and } t > \frac{-\langle x, \vec{n}_R \rangle}{c \cdot \langle \varphi, \vec{n}_R \rangle} \right\}, \\
\mathcal{N} &:= \{\omega \in \Omega : N(\omega) \in \mathbb{N}_0\}
\end{aligned}
$$

$$
N : \Omega \to \mathbb{N}_{0,\infty}, \quad \text{with} \quad N(\omega) := \begin{cases} \inf\{n \in \mathcal{N}_\omega\}, & \text{if } \mathcal{N}_\omega \neq \emptyset, \\ \infty, & \text{if } \mathcal{N}_\omega = \emptyset, \end{cases}
$$

$$
\Phi : \Omega \to S^2_\infty, \quad \text{with} \quad \Phi(\omega) := \begin{cases} \Phi_{N(\omega)}(\omega), & \text{if } \omega \in \mathcal{N}, \\ \stackrel{\mathrm{d}}{\infty}, & \text{if } \omega \in \Omega \setminus \mathcal{N}, \end{cases}
$$

$$
St : \Omega \to Pol, \quad \text{with} \quad \Phi(\omega) := \begin{cases} St_{N(\omega)}(\omega), & \text{if } \omega \in \mathcal{N}, \\ St_0, & \text{if } \omega \in \Omega \setminus \mathcal{N}, \end{cases}
$$

$$R : \Omega \to S^2, \quad \text{with} \quad R(\omega) := \begin{cases} R_{N(\omega)}(\omega), & \text{if } \omega \in \mathcal{N}, \\ R_0, & \text{if } \omega \in \Omega \setminus \mathcal{N}, \end{cases}$$

$$X : \Omega \to \mathbb{R}^3_\infty, \quad \text{with} \quad X(\omega) := \begin{cases} X_{(N(\omega))}(\omega), & \text{if } \omega \in \mathcal{N}, \\ \vec{\infty}, & \text{if } \omega \in \Omega \setminus \mathcal{N}. \end{cases}$$

According to Remark 2.1.9 in all relevant physical situations there $\mathbb{P}^\tau$–almost surely only a finite number of scatterings occure within a finite time intervall, i.e.:

$$\mathbb{P}^\tau\Big(\sum_{k \in \mathbb{N}} T_k < \infty \Big) \quad = \quad 0.$$

With that and since $N(\omega) < \infty$ already implies $\langle X(\omega), \vec{n}_R \rangle < 0$ and $\langle \Phi(\omega), \vec{n}_R \rangle > 0$, we are able to define that a photon with the scatering sequence $\omega \in \Omega$ is *registrated by the receiver*, i.e. it is *received*, if $N(\omega) < \infty$. Such a photon is in the receiver, i.e. $X_t(\omega) \in A_R$, at time

$$t \quad := \quad \left(\sum_{i=0}^{N(\omega)} T_i(\omega) \right) + \frac{-\langle X(\omega), \vec{n}_R \rangle}{c \cdot \langle \Phi(\omega), \vec{n}_R \rangle} \quad \in \quad \mathbb{R}^+.$$

We say the photon is *received at time t*. Especially for $\omega \in \Omega$ and $n \in \mathbb{N}_0$ we get:

$$\begin{aligned} N(\omega) = n \quad \Longleftrightarrow \quad & (X_{(n)}(\omega), \Phi_n(\omega), T_{n+1}(\omega)) \in \mathcal{R} \quad \text{and} \\ & (X_{(i)}(\omega), \Phi_i(\omega), T_{i+1}(\omega)) \in (\mathbb{R}^3 \times S^2 \times \mathbb{R}_0^+) \setminus \mathcal{R} \\ & \text{for all } i = 0, \ldots, n-1. \end{aligned}$$

This implies that the photon is received exactly when it is crossing the receiver (i.e. the receiver plane A_R) with direction $\psi \in FOV_R$ for the first time.

Let be:

- $\mathcal{H}^+$ the halfspace "behind the receiver",
- $\mathcal{H}^-$ the halfspace "in front of the receiver",
- $\mathcal{C}_x$ for $x \in \mathcal{H}^+ \cup \mathcal{H}^-$ the cone of the directions ψ, such that the halflines $\{x + ct\psi : t \in \mathbb{R}_0^+\}$ starting in x into the direction ψ intersect the receiver plane A_R,
- $\mathcal{R}$ the set of the tripeles (x, φ, t), such that the line from x to $x + ct\varphi$ is intersecting the receiver within the receiver FOV_R, if x is a point "in front of the receiver",
- $\mathcal{N}$ the set of photons which are received after a finite (or zero) number of scatterings,

and for $\omega \in \mathcal{N}$:

$N(\omega)$	the number scatterings until the photon is received ,
$X(\omega)$	the last position of the scattering before the photon is received, if $N(\omega) > 0$,
$\Phi(\omega)$	the direction of the photon after the scattering at the last scattering point"in front of the receiver" equal to the direction of the photon in the receiver,
$St(\omega)$	the Stokes vector of the photon after the scattering at the last scattering point"in front of the receiver", and
$R(\omega)$	the reference vector of the photon after the scattering at the last scattering point "in front of the receiver".

We get the following Lemma, its proof is given in the Appendix 6.4.

Lemma 2.2.2 1. $\mathcal{C}_x \cap FOV_R$ is an open set S^2 for all $x \in \mathcal{H}^+ \cup \mathcal{H}^-$.

2. $\mathcal{R}$ is an open set in $\mathbb{R}^3 \times S^2 \times \mathbb{R}_0^+$.

3. $N + 1$ is a stopping time with respect to the monotonically increasing sequence of sub–σ–algebras $(\mathfrak{P}_{2k-1})_{k\in\mathbb{N}}$ of $\mathfrak{K}$.

4. Φ, St, R and X are $\mathfrak{K}$–$\mathfrak{B}(S^2_\infty)$–, $\mathfrak{K}$–$\mathfrak{B}(Pol)$–, $\mathfrak{K}$–$\mathfrak{B}(S^2)$– or $\mathfrak{K}$–$\mathfrak{B}(\mathbb{R}^3_\infty)$–measurable, respectively.

2.2.2 The polarized flux

We now introduce the polarized photon flux (normed, time dependent, time independent) and the measuring time intervall. Both will be characterized further in the LIDAR equation (cf. theorem 2.2.6).

Definition and Remark 2.2.3 In Remark 6.1.1 we saw that a Stokes vector is always defined with respect to a reference plane. For given $\vec{n}_R \in S^2$ and $\rho_R \in S^2$ with $\vec{n}_R \perp \rho_R$ we get from the measurable mapping $\Gamma : S^2 \times S^2 \to [0,\pi]$ with

$$\Gamma(\varphi,\rho) \;:=\; \begin{cases} \arccos\Big(\langle n_R \times \rho_R, \varphi \times \rho\rangle\Big), & \text{if } \omega \in \mathcal{N} \text{ and } \varphi \in S^2_R, \\ 0, & \text{if } \omega \in \Omega \setminus \mathcal{N} \end{cases}$$

the angle between the reference plane of the photon after the last scattering in front of the receiver and the reference plane of the receiver, modulo π. This is

sufficient since we get according to Remark 6.1.3 that $\mathcal{L}(\phi) = \mathcal{L}(\phi + \pi)$. The orientation of the reference plane and scattering plane is preserved since for $\varphi \in S_R^2$ with Remark 2.2.1 and $N(\omega) < \infty$ we already get $\langle \Phi(\omega), \vec{n}_R \rangle > 0$.
The rotation of the Stokes vector after the last scattering in front of the receiver into the reference plane of the receiver is given with the rotation matrix $\mathcal{L}(\Gamma(\Phi(\omega), \omega))$) according to Remark 6.1.3.
In analogy to Lemma 6.1.9 and with Lemma 2.2.2.4 the mapping $\mathcal{L} \circ \Gamma \circ (\Phi, R)$ is welldefined and $\mathfrak{K} \otimes \mathfrak{B}(Pol)$–$\mathfrak{B}(Pol)$–measurable. (This mapping is according to the definition of *Pol* bounded in each component of the Stokes vector.)

Let $\Theta \in \mathbb{R}^+$ be a technical parameter and $\mathcal{T} \subset \mathbb{R}^+$ an open, bounded intervall. Then we define the mappings

$$
\begin{aligned}
f, f_\Theta &: \mathbb{R}^3_\infty \times S^2_\infty \times Pol \times S^2 \to \mathbb{R}^4 \quad \text{and} \\
f_{\mathcal{T}}, f_{\Theta,\mathcal{T}} &: \mathbb{R}^3_\infty \times S^2_\infty \times Pol \times S^2 \times \mathbb{R}^+_{0,\infty} \to \mathbb{R}^4
\end{aligned}
$$

with:

$$
f(x, \varphi, st, \rho) := \begin{cases} \langle \varphi, \vec{n}_R \rangle \cdot \mathcal{L}(\Gamma(\varphi, \rho)) \cdot st, & \\ & \text{if } (x, \varphi) \in \mathbb{R}^3 \times S^2, \\ (0,0,0,0), & \text{otherwise,} \end{cases}
$$

$$
f_\Theta(x, \varphi, st, \rho) := \begin{cases} \min\left\{\Theta \,,\, \dfrac{\langle \varphi, \vec{n}_R \rangle}{\langle x, \vec{n}_R \rangle^2}\right\} \cdot \mathcal{L}(\Gamma(\varphi, \rho)) \cdot st, & \\ & \text{if } (x, \varphi) \in \mathbb{R}^3 \times S^2 \\ & \text{and } \langle x, \vec{n}_R \rangle \neq 0, \\ (0,0,0,0), & \text{otherwise,} \end{cases}
$$

$$
f_{\mathcal{T}}(x, \varphi, st, \rho, t) := \begin{cases} \langle \varphi, \vec{n}_R \rangle \cdot 1_{\mathcal{T}}\left[t + \dfrac{-\langle x, \vec{n}_R \rangle}{c \cdot \langle \varphi, \vec{n}_R \rangle}\right] \cdot \mathcal{L}(\Gamma(\varphi, \rho)) \cdot st, & \\ & \text{if } (x, \varphi) \in \mathbb{R}^3 \times S^2, \\ & \text{and } \langle \varphi, \vec{n}_R \rangle \neq 0, \\ (0,0,0,0), & \text{otherwise,} \end{cases}
$$

$$
\not{f}_{\Theta,\mathcal{T}}(x,\varphi,st,\rho,t) \;:=\; \begin{cases} \min\left\{\Theta\ ,\ \dfrac{\langle\varphi,\vec{n}_R\rangle}{\langle x,\vec{n}_R\rangle^2}\right\}\ \cdot\ 1_{\mathcal{T}}\left[t+\dfrac{-\langle x,\vec{n}_R\rangle}{c\cdot\langle\varphi,\vec{n}_R\rangle}\right]\cdot \not{L}(\Gamma(\varphi,\rho))\cdot st, \\ \qquad\qquad \text{if } (x,\varphi)\in \mathbb{R}^3\times S^2 \\ \qquad\qquad \text{and } \langle x,\vec{n}_R\rangle\cdot\langle\varphi,\vec{n}_R\rangle\neq 0, \\ (0,0,0,0), \qquad \text{otherwise.} \end{cases}
$$

For $i\in\{1,2,3,4\}$ the mappings $\not{f}_i$, $\not{f}_{\Theta,i}$, $\not{f}_{\mathcal{T},i}$, and $\not{f}_{\Theta,\mathcal{T},i}$ are welldefined, measurable, and bounded with $\not{f}=(\not{f}_i)_{i=1,\ldots,4}$.

For $n\in\mathbb{N}_0$ we define the following mappings ξ, ξ_n, ξ_Θ, $\xi_{\Theta,n}$, $\xi_{\mathcal{T}}$, $\xi_{\mathcal{T},n}$, $\xi_{\Theta,\mathcal{T}}$, $\xi_{\Theta,\mathcal{T},n}:\Omega\to\mathbb{R}^4$:

$$
\begin{aligned}
\xi_\Theta(\omega) &:= \not{f}_\Theta\Big(X(\omega),\Phi(\omega),St(\omega),R(\omega)\Big), \\
\xi_{\Theta,n}(\omega) &:= \not{f}_\Theta\Big(X(\omega),\Phi(\omega),St(\omega),R(\omega)\Big)\quad 1_{\{N=n\}}(\omega), \\
\xi_{\Theta,\mathcal{T}}(\omega) &:= \not{f}_{\Theta,\mathcal{T}}\Big(X(\omega),\Phi(\omega),St(\omega),R(\omega),\sum_{i=0}^{N(\omega)}T_i(\omega)\Big), \\
\xi_{\Theta,\mathcal{T},n}(\omega) &:= \not{f}_{\Theta,\mathcal{T}}\Big(X(\omega),\Phi(\omega),St(\omega),R(\omega),\sum_{i=0}^{N(\omega)}T_i(\omega)\Big)\quad 1_{\{N=n\}}(\omega).
\end{aligned}
$$

Analogously for $n\in\mathbb{N}_0$ we define the mappings ξ, ξ_n, $\xi_{\mathcal{T}}$ and $\xi_{\mathcal{T},n}$ by replacing the mappings TWf_Θ or $\not{f}_{\Theta,\mathcal{T}}$ by $\not{f}$ or $\not{f}_{\mathcal{T}}$.

Lemma 2.2.4 Let $n\in\mathbb{N}_0$ and $\eta\in\{\xi,\ \xi_n,\ \xi_\Theta,\ \xi_{\Theta,n},\ \xi_{\mathcal{T}},\ \xi_{\mathcal{T},n},\ \xi_{\Theta,\mathcal{T}},\ \xi_{\Theta,\mathcal{T},n}\}$, then we get for all $i\in\{1,2,3,4\}$ (the i numerates the components of the Stokes vector):

1. η is $\mathfrak{K}$–$\mathfrak{B}(\mathbb{R}^4)$–measurable and bounded.
2. $0\leq \mathbb{E}^\tau(\eta_i)<\infty$.
3. $0\leq \mathrm{Var}^\tau(\eta_i)<\infty$.

(With $\mathbb{E}^\tau$ and Var^τ we denote the the expectation value and the variance with respect to the probability space $(\Omega,\mathfrak{K},\mathbb{P}^\tau)$), respectively.

Proof:

To 1: For $\omega\in\Omega\setminus\mathcal{N}$ we get $\Phi(\omega)\overset{\mathrm{d}}{=}\infty$ and therefore $\eta(\omega)=0$.
For $\omega\in\mathcal{N}$ we get according to the definition of N and $\mathcal{R}$, that $\langle\Phi(\omega),\vec{n}_R\rangle >$

0, i.e. $\eta(\omega) \geq 0$. With that we showed that η is welldefined. The remaining statements follow from the definition of η and from the boundedness of $\not\ell$, $\not\ell_{\mathcal{T}}$, $\not\ell_{\Theta}$ and $\not\ell_{\Theta,\mathcal{T}}$ (in each component).

To 2 and 3: Since $\mathbb{P}^{\tau}$ is a probability measure (cf. remark 2.1.2) the assertion follow directly from 1. ∎

Definition and Remark 2.2.5 (The polarized flux) By Lemma 2.2.4 the following expectation values are well defined and we call them according to Marchuk et al. [33], p 5:

$\mathbb{E}^{\tau}(\xi)$	*the time independent photon flux,*
$\mathbb{E}^{\tau}(\xi_{\Theta})$	*the normed (Θ–truncated) time independent photon flux,*
$\mathbb{E}^{\tau}(\xi_{\mathcal{T}})$	*the time dependent photon flux and*
$\mathbb{E}^{\tau}(\xi_{\Theta,\mathcal{T}})$	*the normed (Θ–truncated) time dependent photon flux.*

For $n \in \mathbb{N}_0$ we call

$$\mathbb{E}^{\tau}(\xi_n), \qquad \mathbb{E}^{\tau}(\xi_{\Theta,n}), \qquad \mathbb{E}^{\tau}(\xi_{\mathcal{T},n}) \quad \text{or} \quad \mathbb{E}^{\tau}(\xi_{\Theta,\mathcal{T},n})$$

the *n–times scattered portion* of $\mathbb{E}^{\tau}(\xi)$, $\mathbb{E}^{\tau}(\xi_{\Theta})$, $\mathbb{E}^{\tau}(\xi_{\mathcal{T}})$ or $\mathbb{E}^{\tau}(\xi_{\Theta,\mathcal{T}})$.

In the time dependent case and with $\omega \in \mathcal{N}$ the factor

$$1_{\mathcal{T}}\left[\left(\sum_{i=0}^{N(\omega)} T_i(\omega)\right) + \frac{-\langle X(\omega), \vec{n}_R\rangle}{c \cdot \langle \Phi(\omega), \vec{n}_R\rangle}\right]$$

is determining the photons which are crossing the receiver within the time intervall $\mathcal{T}$ (cf. Remark 2.2.1).
The factor

$$\frac{1}{\langle X(\omega), \vec{n}_R\rangle^2} = \frac{4\pi}{4\pi\langle X(\omega), \vec{n}_R\rangle^2}$$

is giving the norming factor of the flux $\langle \Phi(\omega), \vec{n}_R\rangle$ in the relation of the surface of the unit sphere to the surface of the sphere with radius exactly the distance of the last scattering position to the receiver plane. (Remember: the center x_R of the receiver is in the origin.) With this norming we get a pole at $\langle X(\omega), \vec{n}_R\rangle \to 0$, therefore it is necessary to truncate the flux with Θ. Then we call:

$\mathcal{T}$	the measuring time intervall
Θ	the maximum distance normed signal which is receivable by the LIDAR.

2.2.3 The LIDAR equation for polarized light

The following theorem gives us the representation of the polarized photon flux (normed, time dependent, time independent) (for unpolarized light see Noormohammadian [37]):

Theorem 2.2.6 (Physical LIDAR equation for polarized light) Let $\overline{\mathcal{R}} := (\mathbb{R}^3 \times S^2 \times \mathbb{R}_0^+) \setminus \mathcal{R}$ and $\mathcal{R}$ be defined according to Definition 2.2.1 and Θ, $\mathcal{T}$ be defined according to Definition 2.2.5. Then we get for all $j \in \{1,2,3,4\}$:

$$
\begin{aligned}
\mathbb{E}^\tau(\xi_\Theta) &= \sum_{n\in\mathbb{N}_0} \mathbb{E}^\tau(\xi_{\Theta,n}) \qquad \text{and} \\
\mathbb{E}^\tau(\xi_{\Theta,\mathcal{T}}) &= \sum_{n\in\mathbb{N}_0} \mathbb{E}^\tau(\xi_{\Theta,\mathcal{T},n}), \qquad \text{with} \\
\mathbb{E}^\tau(\xi_{\Theta,n}) &= \Big(\mathbb{E}^\tau(\xi_{\Theta,n,j})\Big)_{j=1,\dots,4} \quad , \\
\mathbb{E}^\tau(\xi_{\Theta,\mathcal{T},n}) &= \Big(\mathbb{E}^\tau(\xi_{\Theta,\mathcal{T},n,j})\Big)_{j=1,\dots,4} \quad , \\
\mathbb{E}^\tau(\xi_{\Theta,n,j}) &= \int_{\Omega_0}\int_{\Omega_1}\int_{\Omega_2}\cdots\int_{\Omega_{2n}}\int_{\Omega_{2n+1}} \not{p}_{\Theta,j}(x_{(n)},\varphi_n,st_n,\rho_n)\; 1_{\mathcal{R}}(x_{(n)},\varphi_n,t_{n+1}) \\
&\quad \left(\prod_{i=0}^{n-1} 1_{\overline{\mathcal{R}}}(x_{(i)},\varphi_i,t_{i+1})\right) \quad E_{n+1}((x_0,\varphi_0,t_0);t_1,\varphi_1;\dots;t_n,\varphi_n;dt_{n+1}) \\
&\quad P_n((x_0,\varphi_0,st_0,\rho_0,t_0);t_1,\varphi_1,st_1,\rho_1;\dots;t_n;d(\varphi_n,st_n,\rho_n)) \\
&\quad \dots \quad P_1((x_0,\varphi_0,st_0,\rho_0,t_0);t_1;d(\varphi_1,st_1,\rho_1)) \quad E_1((x_0,\varphi_0,t_0);dt_1) \\
&\quad \tau(d(x_0,\varphi_0,st_0,\rho_0,t_0)), \\
\mathbb{E}^\tau(\xi_{\Theta,\mathcal{T},n,j}) &= \int_{\Omega_0}\int_{\Omega_1}\int_{\Omega_2}\cdots\int_{\Omega_{2n}}\int_{\Omega_{2n+1}} \not{p}_{\Theta,\mathcal{T},j}\left(x_{(n)},\varphi_n,st_n,\rho_n,\sum_{i=0}^{n} t_i\right)\; 1_{\mathcal{R}}(x_{(n)},\varphi_n,t_{n+1}) \\
&\quad \left(\prod_{i=0}^{n-1} 1_{\overline{\mathcal{R}}}(x_{(i)},\varphi_i,t_{i+1})\right) \quad E_{n+1}((x_0,\varphi_0,t_0);t_1,\varphi_1;\dots;t_n,\varphi_n;dt_{n+1}) \\
&\quad P_n((x_0,\varphi_0,st_0,\rho_0,t_0);t_1,\varphi_1,st_1,\rho_1;\dots;t_n;d(\varphi_n,st_n,\rho_n))
\end{aligned}
$$

$$\ldots \quad P_1((x_0,\varphi_0,st_0,\rho_0,t_0);t_1;d(\varphi_1,st_1,\rho_1))$$

$$E_1((x_0,\varphi_0,t_0);dt_1) \quad \tau(d(x_0,\varphi_0,st_0,\rho_0,t_0)), \qquad \text{and}$$

$$x_{(i)} \;:=\; x_0 + \sum_{j=1}^{i} ct_j\varphi_{j-1} \quad \text{for all } i \in \mathbb{N}_0.$$

For $n \in \mathbb{N}_0$ we are able to define the components of $\mathbb{E}^\tau(\xi)$ and $\mathbb{E}^\tau(\xi_n)$ or $\mathbb{E}^\tau(\xi_{\mathcal{T}})$ and $\mathbb{E}^\tau(\xi_{\mathcal{T},n})$ in complete analogy to $\mathbb{E}^\tau(\xi_\Theta)$ and $\mathbb{E}^\tau(\xi_{\Theta,n})$ or $\mathbb{E}^\tau(\xi_{\Theta,\mathcal{T}})$ and $\mathbb{E}^\tau(\xi_{\Theta,\mathcal{T},n})$ by interchanging the functions $\not{f}_\Theta$ or $\not{f}_{\Theta,\mathcal{T}}$ with $\not{f}$ or $\not{f}_{\mathcal{T}}$, as done in Definition 2.2.3.

We call the formulas

$\mathbb{E}^\tau(\xi) =$	$\left(\mathbb{E}^\tau(\xi_j)\right)_{j=1,\ldots,4}$	*the time independent, "physical" LIDAR equation,*
$\mathbb{E}^\tau(\xi_\Theta) =$	$\left(\mathbb{E}^\tau(\xi_{\Theta,j})\right)_{j=1,\ldots,4}$	*the normed (Θ truncated), time independent "physical" LIDAR equation,*
$\mathbb{E}^\tau(\xi_{\mathcal{T}}) =$	$\left(\mathbb{E}^\tau(\xi_{\mathcal{T},j})\right)_{j=1,\ldots,4}$	*the time dependent, "physical" LIDAR equation, and*
$\mathbb{E}^\tau(\xi_{\Theta,\mathcal{T}}) =$	$\left(\mathbb{E}^\tau(\xi_{\Theta,\mathcal{T},j})\right)_{j=1,\ldots,4}$	*the normed (Θ truncated), time dependent "physical" LIDAR equation,*

for polarized ligth.

Proof:

We show the above only for $\mathbb{E}^\tau(\xi_{\Theta,\mathcal{T}})$ and $\mathbb{E}^\tau(\xi_{\Theta,\mathcal{T},n})$ with $n \in \mathbb{N}_0$. The remaining statements follow analogously.
From the descriptions from above and from the definition of $\mathcal{R}$, $\overline{\mathcal{R}}$, N and $\not{f}_{\Theta,\mathcal{T}}$ for $\omega \in \Omega$ we get:

$$N(\omega) \;=\; \infty \quad \Longrightarrow$$

$$\not{f}_{\Theta,\mathcal{T}}\Big(X(\omega),\Phi(\omega),St(\omega),R(\omega),\sum_{i=0}^{N(\omega)} T_i(\omega)\Big) \;=$$

$$= \not{f}_{\Theta,\mathcal{T}}\Big(\vec{\infty},\overset{\mathrm{d}}{\infty},St(\omega),R(\omega),\sum_{i=0}^{\infty} T_i(\omega)\Big) \;=\; (0,0,0,0).$$

From the measurability of N and the boundedness of $\not{f}_{\Theta,\mathcal{T},j}$ we get for $j \in \{1,2,3,4\}$:

$$\mathbb{E}^\tau(\xi_{\Theta,\mathcal{T},j}) \;=\; \sum_{n\in\mathbb{N}_0} \mathbb{E}^\tau(\xi_{\Theta,\mathcal{T},n,j})$$

$$= \sum_{n \in \mathbb{N}_0} \int_{\Omega} \not p_{\mathcal{T},j}\Big(X_{(n)}(\omega), \Phi_n(\omega), St_n(\omega), R_n(\omega), \sum_{i=0}^{n} T_i(\omega)\Big)$$
$$1_{\{N=n\}}(\omega)\ \mathbb{P}^\tau(d\omega)$$

and for $n \in \mathbb{N}_0$ according to Remark 2.2.1:

$$\begin{aligned} \mathbb{E}^\tau(\xi_{\Theta,\mathcal{T},n,j}) \;&=\; \int_{\Omega} \not p_{\Theta,\mathcal{T},j}\Big(X_{(n)}(\omega), \Phi_n(\omega), St_n(\omega), R_n(\omega), \sum_{i=0}^{n} T_i(\omega)\Big) \\ &\qquad 1_{\mathcal{R}}\Big(X_{(n)}(\omega), \Phi_n(\omega), T_{n+1}(\omega)\Big) \\ &\qquad \Big(\prod_{i=0}^{n-1} 1_{\overline{\mathcal{R}}}\Big(X_{(i)}(\omega), \Phi_i(\omega), T_{i+1}(\omega)\Big)\Big)\ \mathbb{P}^\tau(d\omega). \end{aligned}$$

Since for $n \in \mathbb{N}_0$ the integrands are $\mathfrak{P}_{2n+1}$–$\mathfrak{B}(\mathbb{R})$–measurable (see Lemma 2.2.2) we immediately get the assertion for $\mathbb{E}^\tau(\xi_{\Theta,\mathcal{T},n,j})$ from the theorem of Ionescu–Tulcea (cf. Neveu [36], theorem 5.1.1, or Oppel et al. [38] section A.2, theorem 2) and from the factorization theorem (cf. Gänßler–Stute [15], Theorem 1.2.24). ■

2.3 The extinction and scattering distribution

In this section we study the Markov kernels E_k and P_k for $k \in \mathbb{N}$. For this purpose we introduce the terms "generalized exponential distribution", "extinction distribution", "phase function", and "scattering distribution".

2.3.1 The extinction distribution

At first we define the extinction distribution. According to the Beer–Lambert law, it has the form of a generalized exponential distribution (cf. Oppel et al. [38] §3).

Definition and Remark 2.3.1 (Generalized exponential distribution) Let $\Sigma : \mathbb{R}_0^+ \to \mathbb{R}_0^+$ be a Borel measurable and on $\mathbb{R}_0^+$ locally Lesbesgue integrable function with $\int_{\mathbb{R}_0^+} \Sigma(s)\, ds \ = \ \infty$. The mapping

$$\mathcal{E}_\Sigma : \mathbb{R} \to [0,1], \quad \text{with} \quad \mathcal{E}_\Sigma(t) \ := \ \begin{cases} 1 - \exp\Big(- \int\limits_0^t \Sigma(s)\, ds\Big), & \text{falls } t \geq 0, \\ 0, & \text{falls } t < 0, \end{cases}$$

has the following properties (cf. Oppel et al. [38]):

1. $\mathcal{E}_\Sigma$ is a distribution function with $\mathcal{E}_\Sigma(t) = 0$ for all $t \leq 0$.
2. $\mathcal{E}_\Sigma$ is absolutely continnious and in $\mathbb{R}$ almost everywhere differntiable.
3. $\mathcal{E}_\Sigma(t) \ = \ \int\limits_0^t \Sigma(s) \ \exp\Big(- \int\limits_0^s \Sigma(r)\, dr\Big)\, ds \quad \text{for all } t \in \mathbb{R}_0^+.$

We call the probability measure $\varepsilon_\Sigma : \mathfrak{B}(\mathbb{R}) \to [0,1]$, uniquely determined by $\mathcal{E}_\Sigma$, the *generalized exponential distribution with extinction* Σ.

Definition 2.3.2 (Extinction distribution) Let $\sigma : \mathbb{R}^3 \to \mathbb{R}_0^+$ be a Borel measurable function such that for all $(x, \varphi) \in \mathbb{R}^3 \times S^2$:

1. $\int\limits_{\mathbb{R}_0^+} \sigma(x + s\varphi)\, ds \ = \ \infty \quad \text{and}$
2. $\sigma(x + \cdot\, \varphi) \quad$ is a locally integrable function on $\mathbb{R}_0^+$,

then we call the mapping $E_\sigma : (\mathbb{R}^3 \times S^2) \times \mathfrak{B}(\mathbb{R}_0^+) \to [0,1]$ with:

$$E_\sigma(x,\varphi;A) \;:=\; \varepsilon_{\Sigma_{x,\varphi}}(A)$$

extinction distribution with extinction σ where we define for $(x,\varphi) \in \mathbb{R}^3 \times S^2$:

$$\Sigma_{x,\varphi} : \mathbb{R}_0^+ \to \mathbb{R}_0^+, \quad \text{with} \quad \Sigma_{x,\varphi}(t) := c\,\sigma(x + ct\varphi).$$

For $(x,\varphi) \in \mathbb{R}^3 \times S^2$ and $a, b \in \mathbb{R}_0^+$ with $a < b$, $E_\sigma(x,\varphi;[a,b])$ gives the probability that a photon which travels along the halfline $\{x + ct\varphi : t > 0\}$ gets scattered between the point $x + ca\varphi$ and $x + cb\varphi$.

Furthermore, we define the mapping $E'_\sigma : (\mathbb{R}^3 \times S^2) \times \mathfrak{B}(\mathbb{R}_0^+) \to \mathbb{R}_0^+$

$$E'_\sigma(x,\varphi;A) \;:=\; c\,\sigma(x) \int_A \exp\Big(-\int_0^t c\,\sigma(x + cs\varphi)\,ds\Big)\,dt$$

which we need for the construction of the transport integral operator (see Definition 2.4.1 and 2.4.4).

In the following Lemma 2.3.3 we give some of the properties of E_σ and E'_σ which we need later (the proof is in appendix 6.5).

Lemma 2.3.3 Let $\sigma : \mathbb{R}^3 \to \mathbb{R}_0^+$ be as in Definition 2.3.2 Then we get:

1. E_σ is a transition probability from $\Big((\mathbb{R}^3 \times S^2), \mathfrak{B}(\mathbb{R}^3 \times S^2)\Big)$ to $\Big(\mathbb{R}_0^+, \mathfrak{B}(\mathbb{R}_0^+)\Big)$.

2. For $A \in \mathfrak{B}(\mathbb{R}_0^+)$ and $(x,\varphi) \in \mathbb{R}^3 \times S^2$ we get:

$$E_\sigma(x,\varphi;A) \;=\; \int_A c\,\sigma(x + cs\varphi)\,\exp\Big(-\int_0^s c\,\sigma(x + cr\varphi)\,dr\Big)\,ds.$$

3. E'_σ is well defined.

4. $E'_\sigma(\,\cdot\,;A)$ is Borel measurable for all $A \in \mathfrak{B}(\mathbb{R}_0^+)$.

5. $E'_\sigma(x,\varphi;\,\cdot\,)$ is a σ–finite measure for all $(x,\varphi) \in \mathbb{R}^3 \times S^2$.

2.3.2 The scattering distribution

We derive the scattering distribution using the phase function. The phase function may be derived from electromagnetic theory (cf. Oppel et al. [38], §2). A derivation of the polarized phasefunction for spherical particles is give in Appendix 6.1 in Remark 6.1.8 (cf. Kerscher et al. [23])

Definition and Remark 2.3.4 (Scattering distribution) Let θ and ϕ defined as in Definition 6.1.13; θ denotes the elevation angle between the incident beam direction and the scattered direction and ϕ the azimuthal angle between the plane of reference before and after the scattering. In the following we will describe both the functions and the variables (angles) with θ und ϕ.

According to Definition 6.1.8 we get for the polarized phase function

$$\int_0^{2\pi}\int_0^{\pi} ph_{pol}(x,\theta,\phi,st)\,\sin(\theta)\,d\theta\,d\phi = 1.$$

Furthermore, let $p : \mathbb{R}^3 \to [0,1]$ be a Borel–measurable mapping. Then we define the mapping $P_p : (\mathbb{R}^3 \times S^2 \times \mathit{Pol} \times S^2) \times \mathfrak{B}(S^2 \times \mathit{Pol} \times S^2) \to [0,1]$ with

$$P_p(x,\varphi,st,\rho;B) \;:=\; (1-p(x)) \int\limits_B ph_{pol}\Big(x,\theta(\varphi,\varphi'),\phi(\varphi,\rho,\varphi'),st\Big)$$
$$\Big(\lambda \times \delta_{N(x,\theta(\varphi,\varphi'),\phi(\varphi,\rho,\varphi'),st)\cdot \mathcal{M}(x,\theta(\varphi,\varphi'))\cdot \mathcal{L}(\phi(\varphi,\rho,\varphi'))\cdot st} \times \delta_{Rot_2(\varphi,\rho,\varphi')\cdot\rho}\Big)\;\Big(d(\varphi',st',\rho')\Big).$$

Here $\mathcal{L}$ denotes the rotation of the Stokes vector according to Definition 6.1.3, $\mathcal{M}$ the Mueller matrix for the scattering according to Definition 6.1.4, N the norming according to Definition 6.1.5, and Rot_2 the rotation matrix according to Definition 6.1.15.

Because $0 \le p \le 1$ and the measurability of p and ph we optain from Lemma 6.2.3 that P_p is a sub–Markov kernel from $(\mathbb{R}^3 \times S^2 \times \mathit{Pol} \times S^2, \mathfrak{B}(\mathbb{R}^3 \times S^2 \times \mathit{Pol} \times S^2))$ to $(S^2 \times \mathit{Pol} \times S^2, \mathfrak{B}(S^2 \times \mathit{Pol} \times S^2))$.

The Stokes vector of the scattered photon

$$st' \;=\; N(x,\theta(\varphi,\varphi'),\phi(\varphi,\rho,\varphi'),st)\cdot \mathcal{M}(x,\theta(\varphi,\varphi'))\cdot \mathcal{L}(\phi(\varphi,\rho,\varphi'))\cdot st$$

is uniquely determined with probability 1 by the direction of the scattered photon φ' and by (φ,st,ρ) of the incoming photon. Likewise the reference vector of the scattered photon

$$\rho' = Rot_2(\varphi,\rho,\varphi')\cdot\rho$$

is determined with probability 1 by the direction φ' of the scattered photon and by (φ,ρ) of the incoming photon.

For $(x,\varphi,st,\rho) \in \mathbb{R}^3 \times S^2 \times \mathit{Pol} \times S^2$ and $B \in \mathfrak{B}(S^2 \times \mathit{Pol} \times S^2), B \neq \emptyset$ we call

- $$\int_B ph_{pol}\Big(x, \theta(\varphi,\varphi'), \phi(\varphi,\rho,\varphi'), st\Big)$$
$$\Big(\lambda \times \delta_{N(x,\theta(\varphi,\varphi'),\phi(\varphi,\rho,\varphi'),st)\cdot \mathcal{M}(x,\theta(\varphi,\varphi'))\cdot \mathcal{L}(\phi(\varphi,\rho,\varphi'))\cdot st} \times \delta_{Rot_2(\varphi,\rho,\varphi')\cdot\rho}\Big)\ \Big(d(\varphi', st', \rho')\Big).$$
  the probability that a photon incoming with the direction φ, the Stokes vector st, the reference vector ρ is scattered at the position x will travel in the direction $\varphi' \in pr_{dir}(B)$,

- $1 - p(x)$
  the "local probability" that the photon is scattered at the position x, and

- $p(x)$
  the "local probability" that the photon is absorbed at the position x.

We may interprete the definition of P_p in the following sense:
Every photon is getting a weight factor $1 - p(x)$ after the scattering. In the average we now calculate only the scattered photons. With the definition of P_p we are formally not able to differentiate between absorbed and non absorbed photons. To achieve this we have to look at a Markov cernels P_k from Definition 2.3.6.

Definition and Remark 2.3.5 Defining $ph_D(x,\theta) := \frac{1}{4}\Big(m_1(x,\theta) + m_2(x,\theta)\Big)$, we are able to write ph_{pol} in the following way:

$$\begin{aligned} ph_{pol}(x,\theta,\phi,st) &= \frac{1}{2\pi}\, ph_D(x,\theta) + \\ &\quad + \frac{1}{8\pi}\Big(m_1(x,\theta) - m_2(x,\theta)\Big)\Big((2i_1 - 1)\cos(2\phi) + u\sin(2\phi)\Big). \end{aligned}$$

We call ph_D the *phase function according to Deirmendjian* which is sufficient for the determination of the scattering distribution of unpolarized light (see Noormohammadian [37] and Deirmendjian [12]). We see that there is a dependence of ph_{pol} from ϕ and st for $m_1(x,\theta) - m_2(x,\theta) \neq 0$, In this case the scattering distribution of polarized light differs from the scattering distribution of unpolarized light. In Figure 2.3 we see that $m_1(x,\theta) - m_2(x,\theta)/m_1(x,\theta) + m_2(x,\theta)$ for a C1–cloud (see Deirmendjian [12]) is differing significantly from 0. See Paragraph 6.1.3, too.

2.3.3 The Markov kernels E_k and P_k

The Markov kernels E_k and P_k in Theorem 2.1.4 and Theorem 2.2.6 are very general. We now give the connection with the physically motivated scattering and exctinction distribution defined above.

Figure 2.3: $m_1(x,\theta)-m_2(x,\theta)/m_1(x,\theta)+m_2(x,\theta)$ of a C1–Cloud (wavelength 1.064 μm)

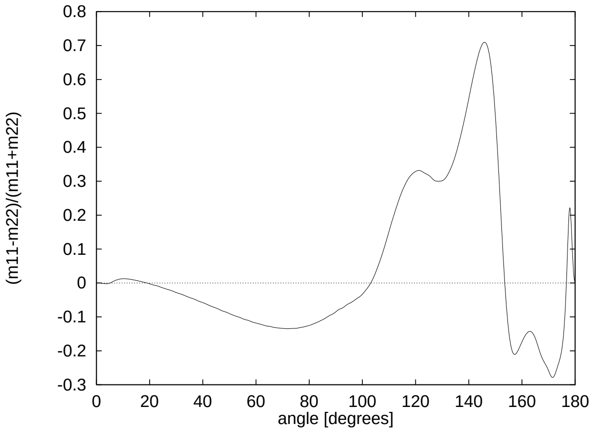

Definition and Remark 2.3.6 (The Markov kernels E_k and P_k) For $k \in \mathbb{N}$, $A \in \mathfrak{K}_{2k-1}$, $B \in \mathfrak{K}_{2k}$, $\psi \in \Omega^{(2k-2)}$ und $\omega \in \Omega^{(2k-1)}$ (see Theorem 2.1.4) we define

$$E_k(\psi\,;A) \;:=\; \begin{cases} E_\sigma\Big(X_{(k-1)}(\psi),\Phi_{k-1}(\psi);A\cap \mathbb{R}_0^+\Big), \\ \qquad\qquad \text{if } \Big(X_{(k-1)}(\psi),\Phi_{k-1}(\psi)\Big)\in \mathbb{R}^3\times S^2, \\ \delta_\infty(A), \qquad \text{otherwise,} \end{cases}$$

$$P_k(\omega\,;B) \;:=\; \begin{cases} p(x)\delta_{\overset{\mathrm{d}}{\infty}}(pr_{dir}(B))+ \\ +P_p\Big(X_{(k)}(\omega),\Phi_{k-1}(\omega),St_{k-1}(\omega),R_{k-1}(\omega);B\cap S^2\times Pol\times S^2\Big), \\ \qquad\qquad \text{for } \Big(X_{(k)}(\omega),\Phi_{k-1}(\omega),St_{k-1}(\omega),R_{k-1}(\omega)\Big)\in \\ \qquad\qquad\qquad \in \mathbb{R}^3\times S^2\times Pol\times S^2, \\ \delta_{\overset{\mathrm{d}}{\infty}}(pr_{dir}(B)), \qquad \text{otherwise.} \end{cases}$$

That Markov kernels have the properties as of Theorem 2.1.4.

2.4 Connections with transport theory

With the definitions of the Markov kernels E_k and P_k from Section 2.3 we give two versions, the "collision density" and "scattering density" model, of the description of the photon flux in the form of a scalar product $\langle f, g\rangle$, where f is a Neuman series describing the LIDAR receiver. This enables us to interprete f as a solution of an integral equation of the second kind as used in the description of the photon flux in the transport theoretic approach (cf. Marchuk et al. [33]).

2.4.1 The transport integral operators

With the definitions of the extinction and the scattering distribution of Section 2.3 we are able to define the following Markov kernels which we characterize in Lemma 2.4.3 (the proof is analogue to the proof of Lemma 1.3.6 given by Noormohammadian [37] for the unpolarized case) and which we use for the construction of the (adjoint) transport integral operators in Definition 2.4.4.

Definition 2.4.1 Let $\sigma : \mathbb{R}^3 \to \mathbb{R}_0^+$ and $p : \mathbb{R}^3 \to [0,1]$ be as in Definition 2.3.2 and 2.3.4. Then we define the following mappings $\mathcal{P}_c, \mathcal{P}_s, \mathcal{P}_c^*, \mathcal{P}_s^* : (\mathbb{R}^3 \times S^2 \times Pol \times S^2) \times \mathfrak{B}(\mathbb{R}^3 \times S^2 \times Pol \times S^2) \to \mathbb{R}_{0,\infty}^+$ with

$$\begin{aligned}
\mathcal{P}_c(x,\varphi,st,\rho;C) &:= \int\limits_{\mathbb{R}_0^+}\int\limits_{S^2}\int\limits_{Pol}\int\limits_{S^2} 1_C(x-ct'\varphi,\varphi',st',\rho') \\
&\qquad P_p(x-ct'\varphi,\varphi,st,\rho;d(\varphi',st',\rho')) \quad E'_\sigma(x,-\varphi;dt'), \\
\mathcal{P}_s(x,\varphi,st,\rho;C) &:= \int\limits_{S^2}\int\limits_{\mathbb{R}_0^+}\int\limits_{Pol}\int\limits_{S^2} 1_C(x-ct'\varphi',\varphi',st',\rho') \\
&\qquad E'_\sigma(x,-\varphi';dt') \quad P_p(x,\varphi,st,\rho;d(\varphi',st',\rho')), \\
\mathcal{P}_c^*(x,\varphi,st,\rho;C) &:= \int\limits_{S^2}\int\limits_{\mathbb{R}_0^+}\int\limits_{Pol}\int\limits_{S^2} 1_C(x+ct'\varphi',\varphi',st',\rho') \\
&\qquad E_\sigma(x,\varphi';dt') \quad P_p(x,\varphi,st,\rho;d(\varphi',st',\rho')), \\
\mathcal{P}_s^*(x,\varphi,st,\rho;C) &:= \int\limits_{\mathbb{R}_0^+}\int\limits_{S^2}\int\limits_{Pol}\int\limits_{S^2} 1_C(x+ct'\varphi,\varphi',st',\rho') \\
&\qquad P_p(x+ct'\varphi,\varphi,st,\rho;d(\varphi',st',\rho')) \quad E_\sigma(x,\varphi;dt').
\end{aligned}$$

Definition 2.4.2 With the functions θ and ϕ according to Definition 6.1.13 and with the definition of the polarized phase function in Definition 6.1.8 we define the following measurable mapping:

$$ph \;:\; \mathbb{R}^3 \times S^2 \times Pol \times S^2 \times S^2 \to \mathbb{R}_0^+ \quad \text{with}$$
$$ph(x,\varphi,\rho,\varphi',st) \;:=\; ph_{pol}(x,\theta(\varphi,\varphi'),\phi(\varphi,\rho,\varphi'),st)$$

Lemma 2.4.3

1. $\mathcal{P}_c$, $\mathcal{P}_s$, $\mathcal{P}_c^*$ and $\mathcal{P}_s^*$ are welldefined mappings.
2. $\mathcal{P}_c(\,\cdot\,;C)$ and $\mathcal{P}_s(\,\cdot\,;C)$ are Borel measurable for all $C \in \mathfrak{B}(\mathbb{R}^3 \times S^2 \times Pol \times S^2)$.
3. $\mathcal{P}_c(x,\varphi,st,\rho;\,\cdot\,)$ and $\mathcal{P}_s(x,\varphi,st,\rho;\,\cdot\,)$ are σ–finite measures for all $(x,\varphi,st,\rho) \in \mathbb{R}^3 \times S^2 \times Pol \times S^2$.
4. $\mathcal{P}_c^*$ and $\mathcal{P}_s^*$ are sub–Markov kernels from $\Big((\mathbb{R}^3 \times S^2 \times Pol \times S^2), \mathfrak{B}(\mathbb{R}^3 \times S^2 \times Pol \times S^2)\Big)$ to $\Big((\mathbb{R}^3 \times S^2 \times Pol \times S^2), \mathfrak{B}(\mathbb{R}^3 \times S^2 \times Pol \times S^2)\Big)$.
5. For $(x,\varphi,st,\rho) \in \mathbb{R}^3 \times S^2 \times Pol \times S^2$ and $C \in \mathfrak{B}(\mathbb{R}^3 \times S^2 \times Pol \times S^2)$ we get:

$$\begin{aligned}
&\mathcal{P}_c^*(x,\varphi,st,\rho;C) = \\
&= \int\limits_{\mathbb{R}^3\setminus\{x\}} \int\limits_{S^2} \int\limits_{Pol} \int\limits_{S^2} 1_C(x',\varphi',st',\rho') \quad \Big(1-p(x)\Big) \quad ph(x,\varphi,\rho,\varphi',st) \\
&\qquad \frac{1}{2\pi\|x'-x\|^2} \quad \sigma(x') \quad \exp\Big(-\int\limits_0^{\|x'-x\|} \sigma(x+s\varphi')\,ds\Big) \quad \delta_{Rot_2(\varphi,\rho,\varphi')\cdot\rho}(d\rho') \\
&\qquad \delta_{N(x,\theta(\varphi,\varphi'),\phi(\varphi,\rho,\varphi'),st)\cdot\mathcal{M}(x,\theta(\varphi,\varphi'))\cdot\mathcal{L}(\phi(\varphi,\rho,\varphi'))\cdot st}(dst') \quad \delta_{\frac{x'-x}{\|x'-x\|}}(d\varphi') \quad dx',
\end{aligned}$$

$$\begin{aligned}
&\mathcal{P}_s^*(x,\varphi,st,\rho;C) = \\
&= \int\limits_{\mathbb{R}^3\setminus\{x\}} \int\limits_{S^2} \int\limits_{Pol} \int\limits_{S^2} 1_C\Big(x+\|x'-x\|\varphi,\varphi',st',\rho'\Big) \quad \Big(1-p(x+\|x'-x\|\varphi)\Big) \\
&\qquad ph\Big(x+\|x'-x\|\varphi,\rho,\varphi',st\Big) \quad \frac{1}{2\pi\|x'-x\|^2} \quad \sigma\Big(x+\|x'-x\|\varphi\Big) \\
&\qquad \exp\Big(-\int\limits_0^{\|x'-x\|} \sigma(x+s\varphi)\,ds\Big) \quad \delta_{Rot_2(\varphi,\rho,\varphi')\cdot\rho}(d\rho') \\
&\qquad \delta_{N(x,\theta(\varphi,\varphi'),\phi(\varphi,\rho,\varphi'),st)\cdot\mathcal{M}(x,\theta(\varphi,\varphi'))\cdot\mathcal{L}(\phi(\varphi,\rho,\varphi'))\cdot st}(dst') \quad \delta_{\frac{x'-x}{\|x'-x\|}}(d\varphi') \quad dx'.
\end{aligned}$$

Now, we introduce the time independent and time dependent transport integral operators, respectively, for the "collision density" and "scattering density" model. In Lemma 2.4.5 and Remark 2.4.6 we shall eludicate these terms. Later we shall use these transport integral operators to define the time independent and time dependent photon flux.
We shall use the symbols L^1, L^∞, $L^1_{\mathcal{T}}$, $L^\infty_{\mathcal{T}}$ and $\langle\,\cdot\,,\,\cdot\,\rangle$, $\|\,\cdot\,\|$, $\langle\,\cdot\,,\,\cdot\,\rangle_{\mathcal{T}}$ and $\|\,\cdot\,\|_{\mathcal{T}}$ in a sense explained in the table of symbols.

Definition 2.4.4 (Transport integral operators) With $\overline{\mathcal{R}}$ according to Theorem 2.2.6 and $\mathcal{P}_c, \mathcal{P}_s, \mathcal{P}^*_c, \mathcal{P}^*_s$ as in Definition 2.4.1 we define:

$$
\begin{aligned}
K_c \quad &: \quad L^1 \to L^1, \quad \text{with} \quad f \mapsto K_c f, \quad \text{and}\\
&K_c f(x,\varphi,st,\rho) :=\\
&:= \int\limits_{\mathbb{R}^3\times S^2\times Pol\times S^2} f(x',\varphi',st',\rho') \quad \mathcal{P}_c\Big(x,\varphi,st,\rho; d(x',\varphi',st',\rho')\Big),
\end{aligned}
$$

$$
\begin{aligned}
K_s \quad &: \quad L^1 \to L^1, \quad \text{with} \quad f \mapsto K_s f, \quad \text{and}\\
&K_s f(x,\varphi,st,\rho) :=\\
&:= \int\limits_{\mathbb{R}^3\times S^2\times Pol\times S^2} f(x',\varphi',st',\rho') \quad 1_{\overline{\mathcal{R}}}(x',\varphi',\|x'-x\|/c)\\
&\qquad\qquad \mathcal{P}_s\Big(x,\varphi,st,\rho; d(x',\varphi',st',\rho')\Big),
\end{aligned}
$$

$$
\begin{aligned}
K_{c,\mathcal{T}} \quad &: \quad L^1_{\mathcal{T}} \to L^1_{\mathcal{T}}, \quad \text{with} \quad f_{\mathcal{T}} \mapsto K_{c,\mathcal{T}} f_{\mathcal{T}}, \quad \text{and}\\
&K_{c,\mathcal{T}}\, f_{\mathcal{T}}(x,\varphi,st,\rho,t) :=\\
&:= \int\limits_{\mathbb{R}^3\times S^2\times Pol\times S^2} f_{\mathcal{T}}\Big(x',\varphi',st',\rho',t-\|x'-x\|/c\Big)\\
&\qquad\qquad \mathcal{P}_c\Big(x,\varphi,st,\rho; d(x',\varphi',st',\rho')\Big),
\end{aligned}
$$

$$
\begin{aligned}
K_{s,\mathcal{T}} \quad &: \quad L^1_{\mathcal{T}} \to L^1_{\mathcal{T}}, \quad \text{with} \quad f_{\mathcal{T}} \mapsto K_{s,\mathcal{T}} f_{\mathcal{T}}, \quad \text{and}\\
&K_{s,\mathcal{T}}\, f_{\mathcal{T}}(x,\varphi,st,\rho,t) :=\\
&:= \int\limits_{\mathbb{R}^3\times S^2\times Pol\times S^2} f_{\mathcal{T}}\Big(x',\varphi',st',\rho',t-\|x'-x\|/c\Big) \quad 1_{\overline{\mathcal{R}}}(x',\varphi',\|x'-x\|/c)\\
&\qquad\qquad \mathcal{P}_s\Big(x,\varphi,st,\rho; d(x',\varphi',st',\rho')\Big).
\end{aligned}
$$

We call

K_c *the time independent "collision density" transport integral operator,*

K_s *the time independent "scattering density" transport integral operator,*

$K_{c,\mathcal{T}}$ *the time dependent "collision density" transport integral operator,*

$K_{s,\mathcal{T}}$ *the time dependent "scattering density" transport integral operator.*

The technical proof of the following lemma may be done in the same way as in the unpolarized case given in Noormohammadian [37] for Lemma 1.3.8.

Lemma 2.4.5 With the assumptions of Definition 2.4.4 we get:

1. K_c, K_s, $K_{c,\mathcal{T}}$ and $K_{s,\mathcal{T}}$ are well defined.
2. K_c, K_s, $K_{c,\mathcal{T}}$ and $K_{s,\mathcal{T}}$ are linear bounded operators with $\|K_c\|$, $\|K_s\|$, $\|K_{c,\mathcal{T}}\|_{\mathcal{T}}$, $\|K_{s,\mathcal{T}}\|_{\mathcal{T}} \leq 1$.
3. The adjoint operators K_c^*, $K_s^* : L^\infty \to L^\infty$ of K_c and K_s respectively and the adjoint operators $K_{c,\mathcal{T}}^*$, $K_{s,\mathcal{T}}^* : L_{\mathcal{T}}^\infty \to L_{\mathcal{T}}^\infty$ of $K_{c,\mathcal{T}}$ and $K_{s,\mathcal{T}}$ respectively exist and are linear and bounded.
4. For all $(x, \varphi, st, \rho) \in \mathrm{I\!R}^3 \times S^2 \times Pol \times S^2$, $t \in \mathrm{I\!R}_0^+$, $g \in L^\infty$ and $g_{\mathcal{T}} \in L_{\mathcal{T}}^\infty$ we get:

$$K_c^* g(x, \varphi, st, \rho) =$$
$$= \int\limits_{\mathrm{I\!R}^3 \times S^2 \times Pol \times S^2} g(x', \varphi', st', \rho') \quad \mathcal{P}_c^*\Big(x, \varphi, st, \rho; d(x', \varphi', st', \rho')\Big),$$

$$K_s^* g(x, \varphi, st, \rho) =$$
$$= \int\limits_{\mathrm{I\!R}^3 \times S^2 \times Pol \times S^2} g(x', \varphi', st', \rho') \quad 1_{\overline{\mathcal{R}}}(x, \varphi, \|x' - x\|/c)$$
$$\mathcal{P}_s^*\Big(x, \varphi, st, \rho; d(x', \varphi', st', \rho')\Big),$$

$$K_{c,\mathcal{T}}^*\, g_{\mathcal{T}}(x, \varphi, st, \rho, t) =$$
$$= \int\limits_{\mathrm{I\!R}^3 \times S^2 \times Pol \times S^2} g_{\mathcal{T}}\Big(x', \varphi', st', \rho', t + \|x' - x\|/c\Big)$$
$$\mathcal{P}_c^*\Big(x, \varphi, st, \rho; d(x', \varphi', st', \rho')\Big),$$

$$K_{s,\mathcal{T}}^*\, g_{\mathcal{T}}(x, \varphi, st, \rho, t) =$$

$$= \int\limits_{\mathbb{R}^3\times S^2\times Pol\times S^2} g_{\mathcal{T}}\Big(x', \varphi', st', \rho', t + \|x'-x\|/c\Big) \quad 1_{\overline{\mathcal{R}}}(x, \varphi, \|x'-x\|/c)$$
$$\mathcal{P}_s^*\Big(x, \varphi, st, \rho; d(x', \varphi', st', \rho')\Big).$$

Figure 2.4: Principle of the "scattering density" (left) and "collision density" model (right).

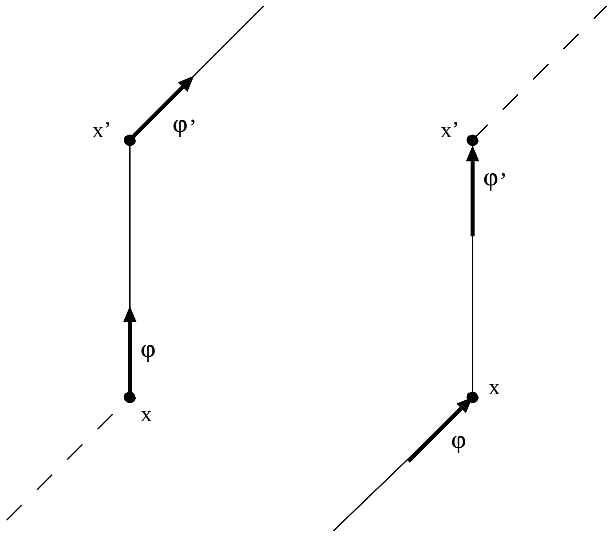

Remark 2.4.6 Since the transport integral operator K_c is equivalent to the operator K defined by Marchuk et al. [33], p.12 (see although Remark 2.4.11) we call the representation of the photon flux with K_c und $K_{c,\mathcal{T}}$ the "collision density" model. In the "collision density" model (i.e. with the adjoint operator K_c^* or $K_{c,\mathcal{T}}^*$) we determine at first the new direction and then the time until the next scattering, i.e. the next scattering position x' (cf. right sketch in figure 2.4).

With the adjoint operators K_s^* and $K_{s,\mathcal{T}}^*$ we simulate the time until the next scattering and therefore the position of the next scattering x' and then the direction φ' of the photon. This is the reversed order as in the "collision density" model. We call this model using the operators K_s and $K_{s,\mathcal{T}}$ the "scattering density" model (cf. left sketch in figure 2.4).

2.4.2 The scattering density model

The following theorem allows us to write the photon flux in the scattering density model as a scalar product of the receiver function and the transmitter function. The proof is given in Appendix 6.6.

Theorem 2.4.7 (photon flux in the "scattering density" model) Let $\mathcal{H}^+$, $\mathcal{R}$, τ and $\not{f}$, $\not{f}_\Theta, \ldots$, ξ, $\xi_\Theta, \ldots$ as in definition 2.2.1 and 2.2.3 and σ, E_σ, p, P_p and K_s, $K_{s,\mathcal{T}}$ as in definition 2.3.2, 2.3.4 and 2.4.4. Furthermore let E_k and P_k be as in Definition 2.3.6.

Let f be a $\lambda_3 \times \lambda \times \lambda_{Pol} \times \lambda$ density of the probability measure

$$\mathfrak{B}(\mathbb{R}^3 \times S^2 \times Pol \times S^2) \to [0,1]$$

with

$$A \;\mapsto\; \left(\tau \circ (X_{(0)}, \Phi_0, St_0, R_0)^{-1}\right)(A),$$

and let $f_\mathcal{T}$ be a$\lambda_3 \times \lambda \times \lambda_{Pol} \times \lambda \times \lambda_1$ density of the probability measure

$$\mathfrak{B}(\mathbb{R}^3 \times S^2 \times Pol \times S^2 \times \mathbb{R}) \to [0,1]$$

with

$$A \;\mapsto\; \tau\left(A \cap (\mathbb{R}^3 \times S^2 \times Pol \times S^2 \times \mathbb{R}_0^+)\right).$$

We define the mappings $g, g_\Theta : \mathbb{R}^3 \times S^2 \times Pol \times S^2 \to \mathbb{R}^4$ and $g_\mathcal{T}, g_{\Theta,\mathcal{T}} : \mathbb{R}^3 \times S^2 \times Pol \times S^2 \times \mathbb{R} \to \mathbb{R}^4$ with

$$\begin{aligned}
g(x,\varphi,st,\rho) &:= \int\limits_{\mathbb{R}_0^+} \not{f}(x,\varphi,st,\rho) \quad 1_\mathcal{R}(x,\varphi,t') \quad E_\sigma(x,\varphi;dt'),\\
g_\Theta(x,\varphi,st,\rho) &:= \int\limits_{\mathbb{R}_0^+} \not{f}_\Theta(x,\varphi,st,\rho) \quad 1_\mathcal{R}(x,\varphi,t') \quad E_\sigma(x,\varphi;dt'),\\
g_\mathcal{T}(x,\varphi,st,\rho,t) &:= \int\limits_{\mathbb{R}_0^+} \not{f}_\mathcal{T}(x,\varphi,st,\rho,t) \quad 1_\mathcal{R}(x,\varphi,t') \quad E_\sigma(x,\varphi;dt'),\\
g_{\Theta,\mathcal{T}}(x,\varphi,st,\rho,t) &:= \int\limits_{\mathbb{R}_0^+} \not{f}_{\Theta,\mathcal{T}}(x,\varphi,st,\rho,t) \quad 1_\mathcal{R}(x,\varphi,t') \quad E_\sigma(x,\varphi;dt').
\end{aligned}$$

Then we get for all $n \in \mathbb{N}_0$:

1. $f \in L^1, \; f_\mathcal{T} \in L^1_\mathcal{T}$ and $g, g_\Theta \in L^\infty, \; g_\mathcal{T}, g_{\Theta,\mathcal{T}} \in L^\infty_\mathcal{T}$.

2. $\mathbb{E}^\tau(\xi_n) \;=\; \left\langle {K_s}^n f \,,\, g \right\rangle, \quad \mathbb{E}^\tau(\xi) \;=\; \sum\limits_{m \in \mathbb{N}_0} \left\langle {K_s}^m f \,,\, g \right\rangle.$

3. $\mathbb{E}^\tau(\xi_{\Theta,n}) \;=\; \left\langle {K_s}^n f \,,\, g_\Theta) \right\rangle, \quad \mathbb{E}^\tau(\xi_\Theta) \;=\; \sum\limits_{m \in \mathbb{N}_0} \left\langle {K_s}^m f \,,\, g_\Theta \right\rangle.$

4. $\mathbb{E}^\tau(\xi_{\mathcal{T},n}) \;=\; \left\langle (K_{s,\mathcal{T}})^n f_\mathcal{T} \,,\, g_\mathcal{T} \right\rangle_\mathcal{T}, \quad \mathbb{E}^\tau(\xi_\mathcal{T}) \;=\; \sum\limits_{m \in \mathbb{N}_0} \left\langle (K_{s,\mathcal{T}})^m f_\mathcal{T} \,,\, g_\mathcal{T} \right\rangle_\mathcal{T}.$

5. $\mathbb{E}^\tau(\xi_{\Theta,\mathcal{T},n}) \;=\; \left\langle (K_{s,\mathcal{T}})^n f_\mathcal{T} \,,\, g_{\Theta,\mathcal{T}} \right\rangle_\mathcal{T}, \quad \mathbb{E}^\tau(\xi_{\Theta,\mathcal{T}}) \;=\; \sum\limits_{m \in \mathbb{N}_0} \left\langle (K_{s,\mathcal{T}})^m f_\mathcal{T} \,,\, g_{\Theta,\mathcal{T}} \right\rangle_\mathcal{T}.$

Remark 2.4.8 The following sketch shows the principle of the proof for statement 5 of Theorem 2.4.7:

$$\begin{array}{ccccc}
\Big\langle\ f_{\mathcal{T}}\ , & K^*_{s,\mathcal{T}} & \cdots & K^*_{s,\mathcal{T}} & g_{\Theta,\mathcal{T}}\ \Big\rangle_{\mathcal{T}} \\
\tau & \mathcal{P}^*_s & \cdots & \mathcal{P}^*_s & \\
\overbrace{(x_0,\varphi_0,st_0,\rho_0,t_0)} & \overbrace{\xrightarrow{E_1}\ t_1\ \xrightarrow{P_1}\ (\varphi_1,st_1,\rho_1)} & \cdots & \overbrace{\xrightarrow{E_n}\ t_n\ \xrightarrow{P_n}\ (\varphi_n,st_n,\rho_n)} & \overbrace{\xrightarrow{E_{n+1}}\ t_{n+1}}
\end{array}$$

In the Theorem 2.4.7 we assume that the extinction probability E_k for $k \in \mathbb{N}$, depending on the point of the last scattering $x_{(k-1)}$ and the direction of propagation φ_{k-1}, has the form of a generalized exponential distribution determined by the extinction $\sigma(x_{(k-1)} + \cdot\, \varphi_{k-1})$ along the half line $\{x_{(k-1)} + s\,\varphi_{k-1} : s \in \mathbb{R}_0^+\}$. In addition we assume that the photon gets scattered again after the $(k-1)$th scattering with probability 1.
These assumptions are justifed by the Beer–Lambert law (cf. Oppel et al. [38], §3). Therefore, σ depends on the (mass) density, the shape, and the refractive index of the scattering particle at a given wavelength.

Furthermore, the scattering distribution P_k for $k \in \mathbb{N}$ depends only on the last scattering point $x_{(k)}$, the direction of propagation φ_{k-1}, the Stokes vector st_{k-1} and the reference vector ρ_{k-1} of the incoming beam (cf. Theorem 2.1.4).

Theorem 2.4.7 implies, that we are **always** able (i.e. in all relevant physical situations) to express the time(in)dependent (normed and Θ truncated) photon flux in the "scattering density" model as a scalar product of a function describing the LIDAR sender by a Neumann series. We may interpretate this Neumann series as a solution of an integral equation of the second kind related to the transport equation given in Marchuk et al. [33], §2 or 3.1. The transport integral operator in the time independent case K_s and in the time dependent case $K_{s,\mathcal{T}}$ is **<u>not</u>** equivalent to the transport integral operator given by Marchuk et al. [33], S.12 (see although Remark 2.4.11).

2.4.3 The collision density model

We need the following lemma to prove under certain assumptions a similar theorem for the "collision density" model. The proof of the lemma is left to the reader.

Lemma 2.4.9 Let $x \in \mathbb{R}^3$, $\varphi \in S^2$, $t \in \mathbb{R}_0^+$ and $y := x + ct\varphi$. Then we get with the expression according to Definition 2.2.1 and Theorem 2.2.6:

1. If $y \in \mathbb{R}^3 \setminus \mathcal{H}^+$, then $(x, \varphi, t) \in \overline{\mathcal{R}}$.
2. If $x \in \mathcal{H}^-$, then the following statements are equivalent:
   (a) $(x, \varphi, t) \in \mathcal{R}$.
   (b) $y \in \mathcal{H}^+, \varphi \in FOV_R$ and $-\varphi \in \mathcal{C}_y$.

The proof of the following theorem is given in Appendix 6.6.

Theorem 2.4.10 (photon flux in the "collision density" model) Let $\mathcal{H}^+$, FOV_R, $\mathcal{C}_x$, τ and $\not{f}$, $\not{f}_{\mathcal{T}}, \ldots$, ξ, $\xi_{\mathcal{T}}, \ldots$ be as in definition 2.2.1 and 2.2.3, let σ, E_σ and p, P_p, and K_c, $K_{c,\mathcal{T}}$ be as in definition 2.3.2, 2.3.4 and 2.4.4, let $\mathcal{H} := \mathbb{R}^3 \setminus (\mathcal{H}^+ \cup \mathcal{H}^-)$ and let E_k and P_k as in definition 2.3.6. Furthermore, we assume

$$p(x) = 1 \text{ for all } x \in \mathcal{H}^+, \qquad \tau\Big((\mathcal{H}^- \times S^2 \times \mathbb{R}_0^+) \cup (\mathcal{H} \times FOV_R \times \mathbb{R}_0^+)\Big) = 0$$

In addition let f be a $\lambda_3 \times \lambda \times \lambda_{Pol} \times \lambda$ density of the probability measure

$$\begin{aligned} &\mathfrak{B}(\mathbb{R}^3 \times S^2 \times Pol \times S^2) \to [0,1] \quad \text{with} \\ A \;&\mapsto\; \Big((\tau \times E_1) \circ (X_{(0)}, \Phi_0, St_0, R_0)^{-1}\Big)(A), \end{aligned}$$

and let $f_{\mathcal{T}}$ be a $\lambda_3 \times \lambda \times \lambda_{Pol} \times \lambda \times \lambda_1$ density of the probability measure

$$\begin{aligned} &\mathfrak{B}(\mathbb{R}^3 \times S^2 \times Pol \times S^2 \times \mathbb{R}) \to [0,1] \quad \text{with} \\ B \;&\mapsto\; \Big((\tau \times E_1) \circ (X_{(0)}, \Phi_0, St_0, R_0, T_0 + T_1)^{-1}\Big)\Big(B \cap (\mathbb{R}^3 \times S^2 \times Pol \times S^2 \times \mathbb{R}_0^+)\Big). \end{aligned}$$

We define the mappings $g : \mathbb{R}^3 \times S^2 \times Pol \times S^2 \to \mathbb{R}^4$ and $g_{\mathcal{T}} : \mathbb{R}^3 \times S^2 \times Pol \times S^2 \times \mathbb{R} \to \mathbb{R}^4$ with

$$\begin{aligned} g(x, \varphi, st, \rho) &:= 1_{\mathcal{H}^+}(x) \;\; 1_{FOV_R}(\varphi) \;\; 1_{\mathcal{C}_x}(-\varphi) \;\; \not{f}(x, \varphi, st, \rho), \\ g_{\mathcal{T}}(x, \varphi, st, \rho, t) &:= 1_{\mathcal{H}^+}(x) \;\; 1_{FOV_R}(\varphi) \;\; 1_{\mathcal{C}_x}(-\varphi) \;\; \not{f}_{\mathcal{T}}(x, \varphi, st, \rho, t). \end{aligned}$$

Then we get for all $n \in \mathbb{N}_0$:

1. $f \in L^1, \;\; f_{\mathcal{T}} \in L^1_{\mathcal{T}}$ and $g \in L^\infty, \;\; g_{\mathcal{T}} \in L^\infty_{\mathcal{T}}$.
2. $\mathbb{E}^\tau(\xi_n) \;=\; \Big\langle\, K_c{}^n\, f \,,\, g \,\Big\rangle, \quad \mathbb{E}^\tau(\xi) \;=\; \sum_{m \in \mathbb{N}_0} \Big\langle\, K_c{}^m\, f \,,\, g \,\Big\rangle.$
3. $\mathbb{E}^\tau(\xi_{\mathcal{T},n}) \;=\; \Big\langle\, (K_{c,\mathcal{T}})^n\, f_{\mathcal{T}} \,,\, g_{\mathcal{T}} \,\Big\rangle_{\mathcal{T}}, \quad \mathbb{E}^\tau(\xi_{\mathcal{T}}) \;=\; \sum_{m \in \mathbb{N}_0} \Big\langle\, (K_{c,\mathcal{T}})^m\, f_{\mathcal{T}} \,,\, g_{\mathcal{T}} \,\Big\rangle_{\mathcal{T}}.$

Remark 2.4.11 The following sKetch illustrates the principle of the proof of Theorem 2.4.10 (statement 3):

$$\Big\langle \quad f_{\mathcal{T}} \quad , \qquad\qquad K^*_{c,\mathcal{T}} \qquad\qquad \cdots \qquad\qquad K^*_{c,\mathcal{T}} \qquad\qquad g_{\mathcal{T}} \quad \Big\rangle_{\mathcal{T}}$$

$$\overbrace{(x_0,\varphi_0,st_0,\rho_0,t_0) \xrightarrow{E_1} t_1}^{\tau \times E_1} \quad \overbrace{\xrightarrow{P_1} (\varphi_1,st_1,\rho_1) \xrightarrow{E_2} t_2}^{\mathcal{P}^*_c} \quad \overset{\cdots}{\cdots} \quad \overbrace{\xrightarrow{P_n} (\varphi_n,st_n,\rho_n) \xrightarrow{E_{n+1}} t_{n+1}}^{\mathcal{P}^*_c}$$

In Theorem 2.4.10 and its proof we see that the assumptions about the extinction and the scattering distributions made in Theorem 2.4.7 are not sufficient. It is therefore necessary to make **additional assumptions** about the absorbtion and the LIDAR transmitter if we want to express the not normed photon flux in an analogue way as in the scattering density model (see Remark 2.4.8).
These additional assumptions (mainly the halfspace "behind" the receiver has to absorb all photons with probability 1) guarantee that we are able to determine, wether a photon has been received from the last direction of propagation and the position of absorbtion behind the receiver (see Lemma 2.4.9).

In general it is <u>not</u> possible to express the normed time independent and the time dependent photon flux with the operators $\boldsymbol{K}_c$ and $\boldsymbol{K}_{c,\mathcal{T}}$ since there is no possibility to express the denominator $\langle x_n, \varphi_n \rangle^2$ in terms of the $(n+1)--$th "scattering" position (i.e. the position of absorbtion "behind" the receiver) and the n–th direction of propagation.

The representation of the time dependent and time independent photon flux given here corresponds to the representation of the photon flux given by Marchuk et al. [33], pp18 (compare the representation of the density $k(x', x)$ on p12 by Marchuk with the representation of $\mathcal{P}^*_c$ in statement 5 of Lemma 2.4.3 together with Lemma 2.4.5). That means the transport integral operator K_c is exactly the operator K used by Marchuk in §2 and 3.

Chapter 3

Variance reduction

The theory of the variance reduction is an extension of the theory given in Noormohammadian [37] Chapter 2. This extension will be discussed in detail in the forthcoming DLR Forschungsbericht.

Chapter 4

The Monte Carlo program

4.1 The normed time dependent polarized photon flux in the program pbs

In this section we describe the program `pbs` we use for the calculation of multiple scattered LIDAR returns based on the stochastic model described in Chapter 2, using the variance reduction Monte Carlo techniques described in Chapter 3. This means the program `pbs` is calculating the normed (Θ–truncated) time dependent polarized photon flux $\mathbb{E}_{\rho\times\widetilde{\mathbb{P}}^{\tau}}(\widetilde{\xi}_{\Theta,\mathcal{T}_n})$ according to the normed time dependent LIDAR equation given for the unpolarized case in Noormohammadian [37], Chapter 2.

Now we specify in detail the variables used in the calculation of the normed time dependent polarized photon flux within the program `pbs`:

4.1.1 The LIDAR receiver and transmitter in the programs pbs

Definition 4.1.1 (LIDAR receiver in `pbs`) Let $x_R := (0,0,0) \in \mathbb{R}^3$, $\vec{n}_R := (0,0,-1) \in S^2$, $\varphi_R \in S^2$, $\rho_R \in S^2$ with $\varphi_R \perp \rho_R$, $\alpha_R \in [0,\pi/2]$, and $r_R \in \mathbb{R}_0^+$. Furthermore, let A_R be as in Definition 2.2.1. Then the LIDAR receiver is defined by:

$$FOV_R \;:=\; \Big\{\varphi \in S^2 : \langle \varphi, -\varphi_R\rangle > \cos(\alpha_R)\Big\}$$

`pbs` fixes the center of the LIDAR receiver x_R in the origin of the cartesian coordinate system in $\mathbb{R}^3$ with fixed normal $\vec{n}_R$ and free selectable receiver radius r_R. The receiver field of view FOV_R has the form of a cone coaxial to the "line of vision" $-\varphi_R$ with divergence α_R (see Figure 4.1).

Care has to be taken in choosing r_R since the estimate used for the determination of the photon flux does not lead to variance reduction in any case. Especially for the determination of the photon flux through the entire receiver plane or for "big" r_R other estimates have to be used

φ_R, ρ_R, α_R and r_R are read in from the `pbs` input file (see Paragraph 4.2.2). The condition $\varphi_R \perp \rho_R$ is checked during initialization.

Definition 4.1.2 (LIDAR transmitter in `pbs`) Let $\vec{n}_R$ be as in Definition 4.1.1 and let $x_T \in \mathbb{R}^3$, $\vec{n}_T := \vec{n}_R$, $\varphi_T \in S^2$, $\rho_T \in S^2$ with $\varphi_T \perp \rho_T$, $st_T \in Pol$, $\alpha_T \in [0,\pi/2]$ and $r_T, s_T \in \mathbb{R}_0^+$. Then the LIDAR transmitter in `pbs` is given by:

$$\begin{aligned} A_T \;&:=\; \Big\{x \in \mathbb{R}^3 : \langle x - x_T, \vec{n}_T\rangle = 0 \text{ and } \|x - x_T\| < r_T\Big\}, \\ FOV_T \;&:=\; \Big\{\varphi \in S^2 : \langle \varphi, \varphi_T\rangle > \cos(\alpha_T)\Big\}. \end{aligned}$$

Figure 4.1: The receiver in the program `pbs`.

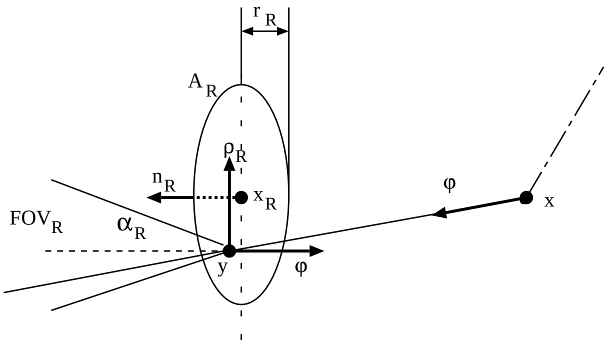

Figure 4.2: The transmitter in the program `pbs`.

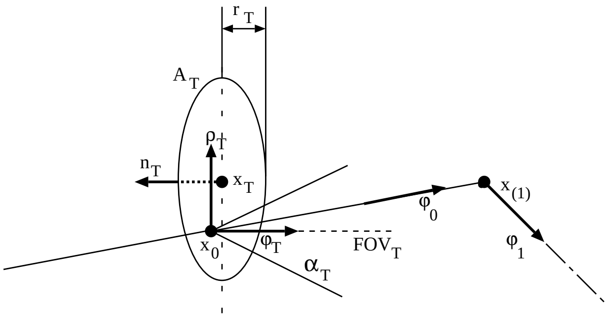

The starting distribution τ is defined in the following way:

$$\tau : \widetilde{\mathfrak{K}}_0 \to [0,1] \quad \text{with} \quad \tau(A) := (\rho_{x,T} \times \rho_{\theta,T} \times \rho_{\phi,T} \times \rho_{t,T})(A)$$

where

- $\rho_{x,T}$ is the density of the normed uniform distribution on A_T with respect to the Lesbesgue measure on the plane $\{x \in \mathbb{R}^3 : \langle x - x_T, \vec{n}_T \rangle = 0\}$,
- $\rho_{\theta,T}$ is the density of the normed uniform distribution on $[0, \alpha_T]$ with respect to λ_1,
- $\rho_{\phi,T}$ is the density of the normed uniform distribution on $[0, 2\pi]$ with respect to λ_1, and
- $\rho_{t,T}$ is the density of the normed uniform distribution on $[0, s_T/c]$ with respect to λ_1.

`pbs` simulates the starting position x_0 of the photon according to the uniform distribution on the disc determined by the center x_T, the normal vector $\vec{n}_T := \vec{n}_R$

and the radius r_T. The direction of propagation φ_0 is determined by the elevation angle θ choosen according to the uniform distribution on $[0, \alpha_T]$ and the azimuthal angle ϕ chosen according to the uniform distribution on $[0, 2\pi]$ in the following way (see Definition 6.1.15 and Figure 4.2):

$$\varphi_0 = Rot_1'(\varphi_T, \rho_T, \theta, \phi) \cdot \varphi_T$$

With φ_T, ρ_T, st_T, and φ_0 we calculate the Stokes vector st_0 and the reference vector ρ_0 in the following way (see Definition 6.1.3 and Definition 6.1.15):

$$\begin{aligned} st_0 &= L(\phi) \cdot st_T \\ \rho_0 &= Rot_2(\varphi_T, \rho_T, \varphi_0) \cdot \rho_T \end{aligned}$$

For the distribution of the starting time we use the uniform distribution on the interval $[0, s_T/c]$ (rectangular puls) with c standing for the speed of light.

x_T, φ_T, ρ_T, st_T, α_T, r_T and s_T are read in from the `pbs` input file (see Paragraph 4.2.2). The condition $\varphi_T \perp \rho_T$ is checked during initialization.

Definition 4.1.3 (Measuring time intervals in `pbs`) Let be c as in Definition 2.1.2 and let be $s_{\min}, s_{\max} \in \mathbb{R}^+$ with $s_{\min} < s_{\max}$ and $N_{\mathcal{T}} \in \mathbb{N}$. Then `pbs` is using the measuring time intervals defined the following way for $n = 1, \ldots, N_{\mathcal{T}}$ (see Definition 2.2.3):

$$\begin{aligned} \mathcal{T}_n &:= \left]\frac{s_{\min,n}}{c}, \frac{s_{\max,\mathrm{n}}}{c}\right[, \\ s_{\min,n} &:= s_{\min} + \frac{n-1}{N_{\mathcal{T}}} \cdot (s_{\max} - s_{\min}), \\ s_{\max,n} &:= s_{\min} + \frac{n}{N_{\mathcal{T}}} \cdot (s_{\max} - s_{\min}). \end{aligned}$$

This means `pbs` is calculating the normed, time dependent, polarized photon flux for each of the $N_{\mathcal{T}}$ measuring time intervals corresponding to the "intersection" $(\mathcal{T}_n : n \in N_{\mathcal{T}})$ of the complete measuring time interval $]s_{\min}/c, s_{\max}/c[$. Therefore, the time resolution of the simulated LIDAR backscatter signal is $(s_{\max} - s_{\min})/(c \cdot N_{\mathcal{T}})$.

$s_{\min}$ and $s_{\max}$ are the minimum and maximum photon path length (often called range) we are interested in. $s_{\min}$, $s_{\max}$, $N_{\mathcal{T}}$ and are read in from the `pbs` input file (see Paragraph 4.2.2).

4.1.2 The extinction and scattering distribution in the program `pbs`

Definition 4.1.4 (Extinction distribution in `pbs`) Let be x_R and $\vec{n}_R$ as in Definition 4.1.1. Furthermore, let be $N_S \in \mathbb{N}$, $d_1, \ldots, d_{N_S-1} \in \mathbb{R}$ with $d_1 < \ldots < d_{N_S-1}$, and $\sigma_1, \ldots, \sigma_{N_S} \in \mathbb{R}_0^+$. Then the extinction distribution is obtained from the extinction σ in `pbs` by the following definition:

$$\sigma : \mathbb{R}^3 \to \mathbb{R}_0^+ \quad \text{with} \quad \sigma(x) := \sum_{k=1}^{N_S} 1_{\mathcal{H}_k}(x) \cdot \sigma_k,$$

where

$$\mathcal{H}_1 \ := \ \begin{cases} \mathbb{R}^3 & \text{for } N_S = 1, \\ \{x \in \mathbb{R}^3 : \langle x - x_R, \vec{n}_R \rangle \leq d_1\} & \text{else,} \end{cases}$$

$$\mathcal{H}_k \ := \ \left\{x \in \mathbb{R}^3 : d_{k-1} < \langle x - x_R, \vec{n}_R \rangle \leq d_k\right\} \quad \text{for } k = 2, \ldots, N_S - 1,$$

$$\mathcal{H}_{N_S} \ := \ \begin{cases} \mathbb{R}^3 & \text{for } N_S = 1, \\ \{x \in \mathbb{R}^3 : d_{N_S-1} < \langle x - x_R, \vec{n}_R \rangle\} & \text{else.} \end{cases}$$

Obviously we get:

$$\mathbb{R}^3 = \bigcup_{i=1}^{N_S} \mathcal{H}_i \quad \text{and} \quad \mathcal{H}_i \cap \mathcal{H}_j = \emptyset \quad \text{for } i, j \in \{1, \ldots, N_S\} \text{ with } i \neq j.$$

In the sense of Definition 2.3.2 σ is well–defined since condition i) of Definition 2.3.2 is fulfilled if we choose σ constant and everywhere greater 0 outside the sphere around x_T (see Definition 4.1.2) with radius $s_T + s_{\max}$. We are always able to do so, since we always stop the underlying Markov process $((X_{(n)}, \Phi_n) : n \in \mathbb{N}_0)$ on the probability space $(\Omega, \mathfrak{K}, \mathbb{P}^\tau)$ from Section 2.1 at the latest at time $(s_T + s_{\max})/c$.

With the program `pbs` we simulate N_S homogeneous "slabs", this implies constant extinction σ_i within the slab $\mathcal{H}_i$ for $i = 1, \ldots, N_S$. The planes between the slabs are choosen to be parallel to the receiver plane $\{x \in \mathbb{R} : \langle x - x_R, \vec{n}_R \rangle = 0\}$ (see Figure 4.3). The case $N_S = 1$, $N_S = 2$, and $N_S > 2$ we call *uniform fog*, *uniform halfspaces*, and *uniform slabs*, respectively.

The σ_k are read in from the `pbs` input file (see Paragraph 4.2.2).

Definition 4.1.5 (Mueller matrix and scattering distribution in `pbs`)
Let be $N_S, \mathcal{H}_1, \ldots, \mathcal{H}_{N_S}$ as in Definition 4.1.4. Furthermore, let $q_1, \ldots, q_{N_S} \in [0, 1]$, $N_{ph_1}, \ldots, N_{ph_{N_S}} \in \mathbb{N} \setminus \{1\}$, $\alpha_{i,1}, \ldots, \alpha_{i,N_{ph_i}} \in [0, 180]$ with $0 =: \alpha_{i,1} < \alpha_{i,j} < \alpha_{i,N_{ph_i}} := 180$ and $m_{11,(i,1)}, \ldots, m_{11,(i,N_{ph_i})} \in \mathbb{R}_0^+$, $m_{22,(i,1)}, \ldots, m_{22,(i,N_{ph_i})} \in \mathbb{R}_0^+$,

Figure 4.3: Sketch of the environmental situation in the program `pbs`.

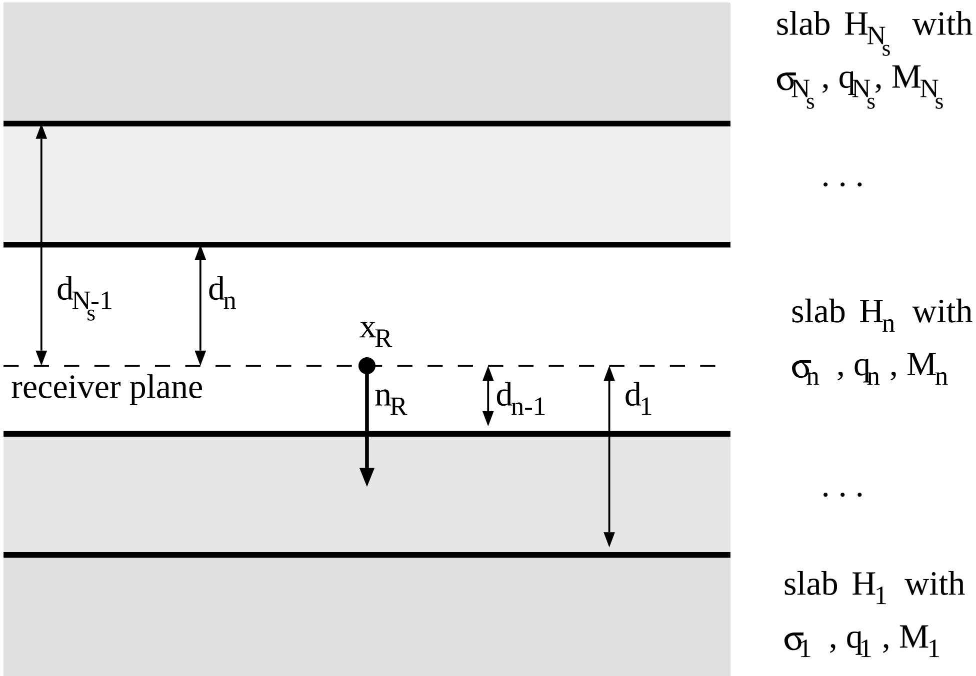

$m_{33,(i,1)}, \ldots, m_{33,(i,N_{ph_i})} \in \mathbb{R}$, and $m_{43,(i,1)}, \ldots, m_{43,(i,N_{ph_i})} \in \mathbb{R}$. Hence, we define with the absorbtion probability

$$p \ : \ \mathbb{R}^3 \to [0,1], \quad \text{with} \quad p(x) := \sum_{k=1}^{N_S} 1_{\mathcal{H}_k}(x) \cdot (1 - q_k),$$

and with the polarized phase function (see Definition 6.1.8)

$$\begin{aligned} ph_{pol} \ &: \ \mathbb{R}^3 \times [0,\pi] \times [0,2\pi] \times Pol \to \mathbb{R}_0^+ \quad \text{with} \\ ph_{pol}&(x,\theta,\phi,st) := \\ &= \sum_{i=1}^{N_S} 1_{\mathcal{H}_i}(x) \, \frac{1}{4\pi} \Big[\tfrac{1}{2}(m_{11,(i)}(x,\theta) + m_{22,(i)}(x,\theta)) + \\ &\quad + \tfrac{1}{2}(m_{11,(i)}(x,\theta) - m_{22,(i)}(x,\theta)) \Big(\, (2i_{\|} - 1)\cos(2\phi) + u\sin(2\phi) \, \Big) \Big] \end{aligned}$$

a scattering distribution P_p according to Definition 2.3.4 in the program `pbs`. ph_{pol} has to satisfy the norming condition for all $st \in Pol$ and $x \in \mathbb{R}^3$.

$$4\pi \ = \ \int_0^{2\pi}\!\!\int_0^{\pi} ph_{pol}(x,\theta,\phi,st) \, d\theta \, d\phi$$

We used the definition

$$m_{11,(i)} \quad : \quad [0,\pi] \rightarrow \mathbb{R}_0^+ \quad \text{with}$$

$$m_{11,(i)}(\vartheta) \quad := \quad \sum_{j=1}^{N_{ph_i}-1} 1_{[\vartheta_{i,j},\,\vartheta_{i,j+1}]}(\vartheta) \cdot \left(\frac{\vartheta_{i,j+1} - \vartheta}{\vartheta_{i,j+1} - \vartheta_{i,j}} \cdot (m_{11,(i,j)} - m_{11,(i,j+1)}) + m_{11,(i,j+1)} \right)$$

for $m_{22,(i)} : [0,\pi] \rightarrow \mathbb{R}_0^+$, $m_{33,(i)} : [0,\pi] \rightarrow \mathbb{R}$, and $m_{43,(i)} : [0,\pi] \rightarrow \mathbb{R}$, respectively, and $\vartheta_{i,j} := \alpha_{i,j} \cdot \pi/180$ for $j = 1,\ldots,N_{ph_i}$. The m are components of a Mueller matrix $\mathcal{M}$ of the shape (see Definition 6.1.6)

$$\mathcal{M}_{(i,j)} \quad := \quad \begin{pmatrix} m_{11,(i,j)} & 0 & 0 & 0 \\ 0 & m_{22,(i,j)} & 0 & 0 \\ 0 & 0 & m_{33,(i,j)} & -m_{43,(i,j)} \\ 0 & 0 & m_{43,(i,j)} & m_{33,(i,j)} \end{pmatrix}$$

For $i = 1,\ldots,N_S$ and $x \in \mathcal{H}_i$ the value of $m_{11}(x,\cdot\,) = m_{11,(i)}(\cdot\,)$ is calculated with linear interpolation from the supporting points $((\alpha_{i,j},\, m_{11,(i,j)}) : j = 1,\ldots,N_{ph_i})$, m_{22}, m_{33}, and m_{43}, respectively. Each homogenous slab $\mathcal{H}_i$ has its own Mueller matrix $\mathcal{M}$, its own survival probability q_i (the absorbtion probability is $p_i = 1-q_i$, q_i is read in from the `pbs` input file) and its own extinction σ_i (see although Figure 4.3 and Definition 4.1.4). Each Mueller matrix has to be provided in a seperate file, the name of this file is given in the `pbs` input file (see Paragraph 4.2.2). The file must have the following structure:

$$\begin{array}{ccccc} \alpha_{i,1} & m_{11,(i,1)} & m_{22,(i,1)} & m_{33,(i,1)} & m_{43,(i,1)} \\ \vdots & \vdots & \vdots & \vdots & \vdots \\ \alpha_{i,N_{ph_i}} & m_{11,(i,N_{ph_i})} & m_{22,(i,N_{ph_i})} & m_{33,(i,N_{ph_i})} & m_{43,(i,N_{ph_i})} \end{array}$$

Lines starting with # and lines at the end of the file (i.e. after N_{ph_i} valid lines) are ignored (this may be used for comments). The separation characters may be either (multiple) spaces or (multiple) tabs.

4.1.3 The Monte Carlo parameters used in `pbs`

Two of the variance reduction schemes, exponential transform and scattering splitting, are controllable via parameters in the input file. The adjustment of these parameters is in some situations crucial for the success i.e. the unbiased estimation of the LIDAR signal. It is not possible to give standard values which work well for all aplications. For each situation (geometry, extinction, phase function) the Monte Carlo paramters have to be adjusted again. We want to emphasize that a non careful use of these parameters may result in a *misleading* or even a *wrong* LIDAR signal. This is definitely not "Plug and Play" and will never be!

Definition 4.1.6 (Monte Carlo parameters for scattering splitting)
Choose $\tilde{\gamma} \in]0, \pi/2[$. $\tilde{\gamma}$ is the (elevation) angle where we split the S^2 in the forward and backward partsphere (see Figure 4.4).

Figure 4.4: The forward and backward partsphere used in scattering splitting.

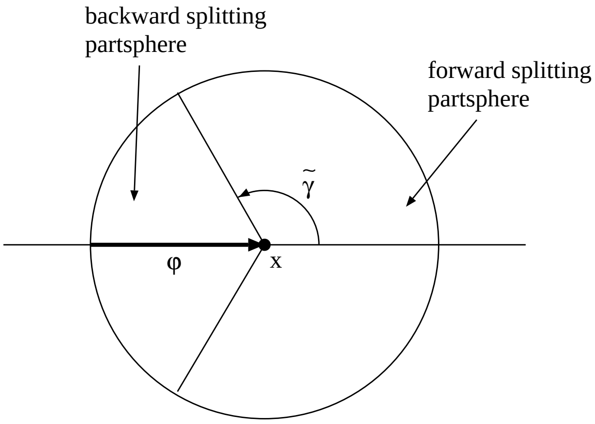

$\tilde{\gamma}$ is read in from the `pbs` input file (see Paragraph 4.2.2, $\tilde{\gamma}$ must be given in degrees). In the unpolarized case we are free to choose arbitrary $\tilde{\gamma}$ (see Noormohammadian [37]), for polarisation $\tilde{\gamma}$ has to be greater than a minimum angle $\widetilde{\gamma_{min}}$ During the initialization this condition is checked and if $\tilde{\gamma} < \widetilde{\gamma_{min}}$, $\tilde{\gamma}$ is set to $\widetilde{\gamma_{min}}$. The really used $\tilde{\gamma}$ is reported in the output file of `pbs` (see Paragraph 4.2.3).

Since "scattering splitting" is costly in computational time, we use scattering splitting not for each scattering. In the following we define where we use it.

Let be x_R, φ_R and $\vec{n}_R$ as in Definition 4.1.1 and d_1 as in Definition 4.1.4. Furthermore, let be $\tilde{\alpha}, \tilde{\beta} \in]0, \pi/2[$ and $\tilde{r} \in \mathbb{R}_0^+$.
Now we define the "splitting region" $\tilde{\mathcal{K}}$, i.e. the region where we perform scattering splitting if scattering occurs (see Figure 4.5, 4.6 and 4.7).

$$
\begin{aligned}
\tilde{\mathcal{K}} &:= (\tilde{\mathcal{K}}_1 \times S^2) \cap \tilde{\mathcal{K}}_2, \quad \text{with} \\
\tilde{\mathcal{K}}_1 &:= \Big\{ x \in \mathbb{R}^3 : \langle \tilde{\psi}_x, \varphi_R \rangle - \|\tilde{\psi}_x\| \cdot \cos(\tilde{\alpha}) > 0 \Big\}, \\
\tilde{\mathcal{K}}_2 &:= \Big\{ (x, \varphi) \in \mathbb{R}^3 \times S^2 : \langle \tilde{\varphi}_x, \varphi \rangle - \|\tilde{\varphi}_x\| \cdot \cos(\tilde{\beta}) > 0 \Big\}
\end{aligned}
$$

and for $x \in \mathbb{R}^3$:

$$
\begin{aligned}
\tilde{\psi}_x &:= x - \Big(x_R + (\tilde{r}/\tan(\tilde{\alpha})) \cdot \vec{n}_R \Big), \\
\tilde{\varphi}_x &:= x - (x_R - d_1 \cdot \vec{n}_R).
\end{aligned}
$$

Figure 4.5: Modeling of the cone $\widetilde{\mathcal{K}}_1$ from Definition 4.1.6: a photon at the position x is "in the line of sight of the receiver FOV", i.e. $x \in \widetilde{\mathcal{K}}_1$. The situation showed here is a bit special since $\vec{n_R} \parallel \varphi_R$.

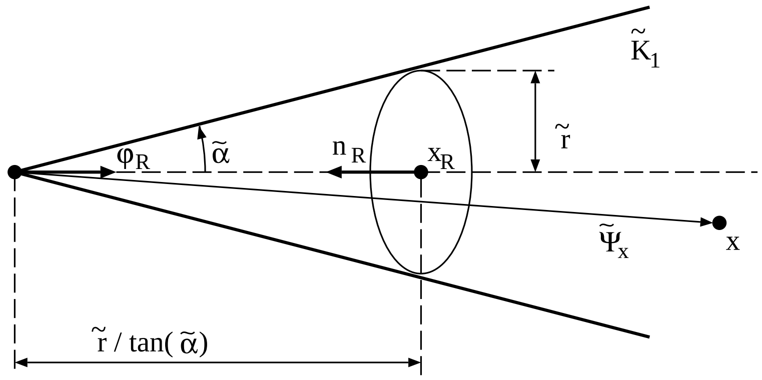

$\widetilde{\mathcal{K}}_1$ and $\widetilde{\mathcal{K}}_2$ are open sets in $\mathbb{R}^3$ and $\mathbb{R}^3 \times S^2$, respectively, and therefore, $\widetilde{\mathcal{K}}$ is an open set in $\mathbb{R}^3 \times S^2$. $\widetilde{\mathcal{K}}$ consists of the scattering positions $x \in \mathbb{R}^3$ and the directions before scattering $\varphi \in S^2$ with the following properties:

1. x is in the cone with the divergence $\tilde{\alpha}$, the direction of the cone axis φ_R, and the cone tip in $x_R + (\tilde{r}/\tan(\tilde{\alpha})) \cdot \vec{n}_R$ (see Figure 4.5).

2. φ is the direction of the photon before the scattering in x, with φ and $x - (x_R - d_1 \cdot \vec{n}_R)$ confining the angle $\widetilde{\beta}$.

We say, photons which are scattered at position x incident from direction φ, with $(x, \varphi) \in \widetilde{\mathcal{K}}$ are *in front of the receiver within the receiver field of view.*

We may interpretate this situation in the following way: A photon traveling away from the receiver will not contribute to the backscatter signal signifficantly at the next scattering position because of the strong forward peak of the phase functions If we perform splitting we split the photon into two (weighted) photons, one traveling into the forward and the other traveling backward direction. Therefore, we get with a "higher probability" a photon which contributes to the backsactter signal at the next scattering. Since only photons which are "within the receiver field of view" contribute with "high probability" we use this as an additional criterium wether to perform splitting or not. It is obvious that the estimation of the LIDAR backscatter signal remains unbiased.

In the definition of $\widetilde{\mathcal{K}}_2$ we choose the reference point to $x_R - d_1 \cdot \vec{n}_R$ instead of x_R. This is optimized for the situation of small extinction in front of the cloud at the distance d_1.

Figure 4.6: Modeling of $\widetilde{\mathcal{K}}_2$ from Definition 4.1.6: $(x, \varphi) \notin \widetilde{\mathcal{K}}_2$, i.e. the photon scattered at the position x arriving with the direction of propagation φ, "travels into the direction of the receiver".

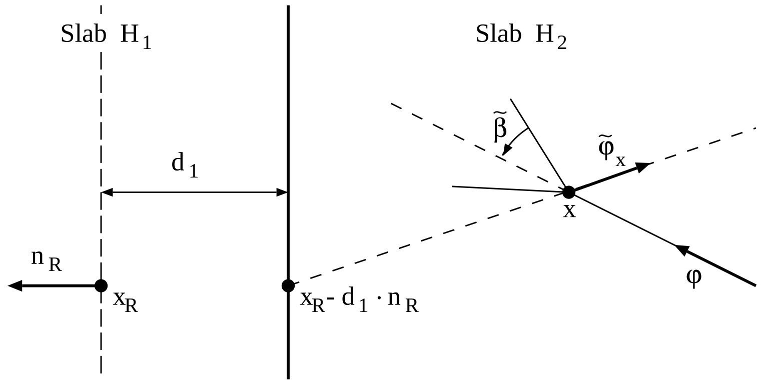

$\widetilde{\beta}$, $\tilde{\alpha}$, and $\tilde{r}$ are read in from the `pbs` input file (see Paragraph 4.2.2). (In the input file $\widetilde{\beta}$ must be given in degrees, $\tilde{\alpha}$ in radians.) With an additional logical parameter scattering splitting may be switched of.

Definition 4.1.7 (Monte Carlo parameters for exponential transform) Choose $\widetilde{C} \in [0, 1[$. Choosing $\widetilde{C} = 0$ switches exponential transform off.

$\widetilde{C}$ is read in from the `pbs` input file (see Paragraph 4.2.2).

Figure 4.7: Modeling of $\widetilde{\mathcal{K}}_2$ from Definition 4.1.6: $(x, \varphi) \in \widetilde{\mathcal{K}}_2$, i.e. the photon scattered at the position x arriving with the direction of propagation φ, "travels away from the receiver".

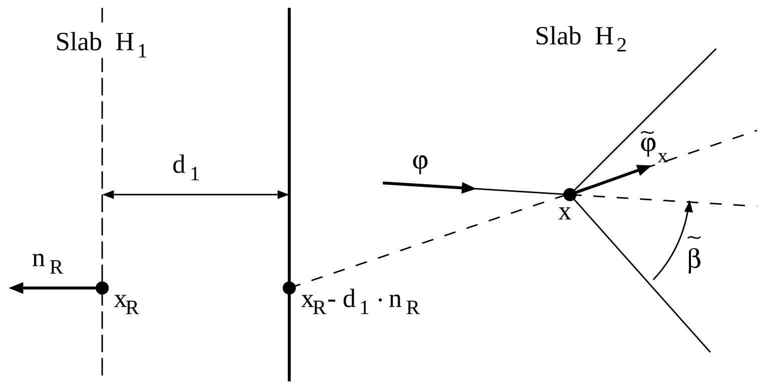

4.2 The handling of the program

In this section we describe the installation, the calling on a UNIX machine, the input and output files, the known bugs and possible enhancements.

4.2.1 The installation

The compilation of the program is easy on a UNIX machine. Copy all the files of Section 6.7 into one directory and then type `make`. We use the GNU C compiler `gcc`. This may be changed to any other ANSI C compiler in the `makefile`. Be careful with optimization! (As an example: `gcc` version 2.5.8 on a sun Sparc/10 compatible with `-O2` produces a program which gives wrong results!)

The program `pbs` was intentionally written as a command line program so that it may easily be used with batch processing. `pbs` is called in the following way:

`pbs input-file N step [w]` with

- `input-file` is the name of the input file described in Paragraph 4.2.2,
- `N` is the number of photon paths to be simulated,
- `step` is the stepsize (regarding the photon paths) after which a control output is written to `stdout`,
- `w` is an optional parameter. If used, `pbs` prints out the input parameters to `stdout` and waits for a confirmation from the user. Therfore, you should not use `w` for batch processing.

If you call `pbs` without any commandline parameters, `pbs` will print a short description of the calling sequence.

A typical calling sequence of `pbs` as a background process for a `csh` shell user looks the following way.

```
pbs input-file 100000 10000 >& tmp-file &
```

This means `pbs` will calculate 100000 photon paths, using the parameters given in the `input-file`. Every 10000 photon paths a control message is written to `stdout` which is redirected to `tmp-file`. All error messages go to `tmp-file`, too. At the end of the program `pbs` saves the results to the output file. The name of the output file must be given within the input file (see Paragraph 4.2.2).

4.2.2 The input file

All prameters have to be at the beginnig of the line followed by at least one empty space. Then arbitrary strings may follow, they are ignored by `pbs`.

The parameters discussed in Section 4.1 have to be given in the following order, special care has to be taken for the number of commentary lines.

- **8 commentary lines** (not evaluated),
- x–coordinate of the LIDAR transmitter x_T (in km),
- y–coordinate of the LIDAR transmitter x_T (in km),
- z–coordinate of the LIDAR transmitter x_T (in km),
- x–coordinate of the cone direction φ_T of the transmitter field of view FOV_T,
- y–coordinate of the cone direction φ_T of the transmitter field of view FOV_T,
- z–coordinate of the cone direction φ_T of the transmitter field of view FOV_T,
- x–coordinate of the transmitter reference vector ρ_T,
- y–coordinate of the transmitter reference vector ρ_T,
- z–coordinate of the transmitter reference vector ρ_T,
- $i_{||}$–component of the starting normed Stokes vector,
- $i_{\perp}$–component of the starting normed Stokes vector,
- u–component of the starting normed Stokes vector,
- v–component of the starting normed Stokes vector,
- divergence α_T of the transmitter field of view FOV_T (half angle, in rad),
- radius r_T of the effective transmitter plane A_T (in km),
- maximum pulse length s_T (in km),
- **commentary line** (not evaluated),
- x–coordinate of the cone direction φ_R of the receiver field of view FOV_R,
- y–coordinate of the cone direction φ_R of the receiver field of view FOV_R,
- z–coordinate of the cone direction φ_R of the receiver field of view FOV_R,

- x–coordinate of the receiver reference vector ρ_R,
- y–coordinate of the receiver reference vector ρ_R,
- z–coordinate of the receiver reference vector ρ_R,
- divergence α_R of th receiver field of view FOV_R (half angle, in rad),
- radius r_R of the effective receiver plane A_R (in km) or explicitely "*point*", if the photon flux for a point receiver (i.e. $r_R = 0$) shall be calculated,
- **commentary line** (not evaluated),
- minimum photon path length $c \cdot s_{\min}$ (in km),
- maximum photon path length $c \cdot s_{\max}$ (in km),
- 1 + number of measuring time intervals N_T,
- **commentary line** (not evaluated),
- number N_S of the homogeneous "slabs",
- distance d_1 (in km), see Figure 4.3
  ⋮
- distance d_{N_S-1} (in km) for $N_S > 1$, see Figure 4.3,
- **commentary line** (not evaluated),
- extinction σ_1 of "slab" $\mathcal{H}_1$ (in km^{-1}),
  ⋮
- extinction σ_{N_S} of "slab" $\mathcal{H}_{N_S}$ (in km^{-1}),
- **commentary line** (not evaluated),
- survival probability q_1 of a photon at a scattering in "slab" $\mathcal{H}_1$,
  ⋮
- survival probability q_1 of a photon at a scattering in "slab" $\mathcal{H}_{N_S}$,
- **commentary line** (not evaluated),
- number of support positions N_{ph_1} of the Mueller matrix of "slab" $\mathcal{H}_1$,
  ⋮
- number of support positions N_{ph_1} of the Mueller matrix of "slab" $\mathcal{H}_{N_S}$,

- **commentary line** (not evaluated),
- file name of the tabulated Mueller matrix of "slab" $\mathcal{H}_1$ (see Definition 4.1.5),
  $\vdots$
- file name of the tabulated Mueller matrix of "slab" $\mathcal{H}_{N_S}$,
- **commentary line** (not evaluated),
- parameter $\widetilde{C}$ for the exponential transform,
- flag wether scattering splitting is used or not ("1" is on, "0" is off),
- angle $\tilde{\gamma}$ (in *degrees*) of the "scattering splitting" hemisphere, see Figure 4.4,
- angle $\widetilde{\beta}$ (in *degrees*) of the "scattering splitting" region $\widetilde{\mathcal{K}}_2$, see Figures 4.6 and 4.7,
- divergence $\widetilde{\alpha}$ (in rad) of the "scattering splitting" region $\widetilde{\mathcal{K}}_1$, see Figure 4.5,
- radius $\tilde{r}$ of the ground plane of the "scattering splitting" region $\widetilde{\mathcal{K}}_1$ (in km), see Figure 4.5,
- **commentary lines** (not evaluated),
- name of the output file of `rbs`,
- number N_{out} of the n–times scattered portions of the normed (Θ–truncated), time dependent photon flux $\mathbb{E}_{\rho\times\widetilde{\mathbb{P}}^\tau}(\widetilde{\xi}_{\Theta,\mathcal{T}})$ with $n = 1, \ldots, N_{\text{out}}$, which shall be written to the output file,
- flag which determines wether the normed (Θ–truncated), time dependent photon flux (i.e. all orders of scattering) $\mathbb{E}_{\rho\times\widetilde{\mathbb{P}}^\tau}(\widetilde{\xi}_{\Theta,\mathcal{T}})$ shall be calculated or not, ("1" is on, "0" is off)
- **arbitrary amount of commentary lines** (not evaluated),

Now we give an example of a valid input file. Similar input files were used for the calculations described in section 5.2.

```
Version 18.02.95 (c) Masoud Noormohammadian and Martin Kerscher

Input data for the Monte Carlo program with :
  - the "backward" flux through the receiver in direction (0,0,-1)
  - geometry similar to MUSCLE comparison calculations
  - receiver FOV 0.5 mrad (i.e. 1 mrad full angle)

------Transmitter:--------------------------------------------------------------
0                                x-coord. of transmitter position        [km]
```

```
0               = receiver     y-coord.         "                        [km]
0                              z-coord.         "                        [km]
0                              x-coord. of transmitter FOV axis
0               --> 0 mrad     y-coord.         "          ( points away     )
1                              z-coord.         "          ( from transmitter)
1                              x-coord. of transmitter reference vector
0                              y-coord.    "  (HAS TO BE perpendicular to  )
0                              z-coord.    "  ( the transmitter FOV axis   )
1                              i1 component of the starting Stokes Vector
0                              i2 component     "
0                              u  component     "
0                              v  component     "
0.00005         = 0.05 mrad    divergence of source beam              [rad]
0                              radius of the transmitter               [km]
0.012           ~ 40 ns        pulse length                            [km]
------Receiver (located in (0,0,0)):---------------------------------------
0                              x-coord. of receiver FOV axis ( points away )
0               --> 0 mrad     y-coord.         "            ( from rec.   )
1                              z-coord.         "
1                              x-coord. of receiver reference vector
0                              y-coord.    "  (HAS TO BE perpendicular to  )
0                              z-coord.    "  ( the receiver FOV axis      )
0.005           = 0.5 mrad     semiaperture of the receiver           [rad]
point           point receiver radius of the receiver                  [km]
------Range:---------------------------------------------------------------
1.95            minimum value for range  (-> ptime * c)               [km]
2.55            maximum value for range                               [km]
151             time grid (range) resolution
------Geometry:------------------------------------------------------------
3               number of slabs (including halfspaces)
1               distance to plane betw. forw. halfspace and slab 1      [km]
1.3             distance to plane betw. slab 1 and backw. halfspace     [km]
------Extinction:----------------------------------------------------------
0               extinction coeff. of backward halfspace             [1/km]
15              extinction coeff. of slab 1                         [1/km]
0               extinction coeff. of forward halfspace              [1/km]
------Absorption:----------------------------------------------------------
1               survival probability of backward halfspace
1               survival probability of slab 1
1               survival probability of forward halfspace
------Indicatrix resolutions :---------------------------------------------
1801            resolution of the mueller matrix of "backward" halfspace
1801            resolution of the mueller matrix of slab 1
1801            resolution of the mueller matrix of "forward" halfspace
------Indicatrix file names :----------------------------------------------
c1.m            file name of the mueller matrix of "backward" halfspace
c1.m            file name of the mueller matrix of slab 1
c1.m            file name of the mueller matrix of "forward" halfspace
------Monte Carlo parameters: ---------------------------------------------
0.5             parameter ci of exponential transformation
1               flag, wether scat. split. is used (1 is on)
```

```
90                scattering splitting angle for forward hemisphere      [deg]
90                decision angle to fly away from the receiver           [deg]
0.0002            cone for scattering splitting                        [mrad]
0.000001          radius of cone for scattering splitting in (0,0,0)     [km]
------Output parameters:---------------------------------------------------------
c1.res            file name of output file
3                 number of output contributions
1                 calculation flag of total sum
=================================================================================
```

4.2.3 The output file

`pbs` generates the output file at the end of the calculation. At first the complete input file used in this calculation is written to the output file with a commentary sign # at the beginnig of the line. Then the commandline arguments, the used time, the average number of collisions and other quantities (related to the phase function) are written to the output file.

Now `pbs` is writing the results to the output file. The leftmost entry is the photon path length, then follows the total intensity of the whole signal (i.e. all scattering orders), the 4 components of the normed Stokes vector of the whole signal, the total intensity for single scattering, the 4 components of the normed Stokes vector for single scattering, the total intensity for double scattering, the 4 components of the normed Stokes vector for double scattering, and so on. This often results in a "long" line. In the next line there is always written one commentary sign # (to make the file more readable).

- $s_{\min,1} \quad \mathbb{E}_{\rho\times\widetilde{\mathbb{P}}^{\tau}}(\widetilde{\xi}_{\Theta,\mathcal{T}_1}) \quad \mathbb{E}_{\rho\times\widetilde{\mathbb{P}}^{\tau}}(\widetilde{\xi}_{\Theta,\mathcal{T}_1,1}) \quad \ldots \quad \mathbb{E}_{\rho\times\widetilde{\mathbb{P}}^{\tau}}(\widetilde{\xi}_{\Theta,\mathcal{T}_1,N_{\text{out}}})$
- #

  $\vdots$
- #
- $s_{\min,N_{\mathcal{T}}} \quad \mathbb{E}_{\rho\times\widetilde{\mathbb{P}}^{\tau}}(\widetilde{\xi}_{\Theta,\mathcal{T}_{N_{\mathcal{T}}}}) \quad \mathbb{E}_{\rho\times\widetilde{\mathbb{P}}^{\tau}}(\widetilde{\xi}_{\Theta,\mathcal{T}_{N_{\mathcal{T}}},1}) \quad \ldots \quad \mathbb{E}_{\rho\times\widetilde{\mathbb{P}}^{\tau}}(\widetilde{\xi}_{\Theta,\mathcal{T}_{N_{\mathcal{T}}},N_{\text{out}}})$

Now, the estimated errors (i.e. square roots of the empirical variances) are written to the output file:

- $\# \; s_{\min,1} \quad \sigma_{\Theta,\mathcal{T}_1} \quad \sigma_{\Theta,\mathcal{T}_1,1} \quad \cdots \quad \sigma_{\Theta,\mathcal{T}_1,N_{\mathrm{out}}}$
  $\vdots$
- $\# \; s_{\min,N_\mathcal{T}} \quad \sigma_{\Theta,\mathcal{T}_{N_\mathcal{T}}} \quad \sigma_{\Theta,\mathcal{T}_{N_\mathcal{T}},1} \quad \cdots \quad \sigma_{\Theta,\mathcal{T}_{N_\mathcal{T}},N_{\mathrm{out}}}$

The following listing shows the output file `c1.res` which `pbs` generated using the input file from paragraph 4.2.2 (the file is shortened).

```
# Version 18.02.95 (c) Masoud Noormohammadian and Martin Kerscher
#
# Input data for the Monte Carlo program with :
#   - the "backward" flux through the receiver in direction (0,0,-1)
#   - geometry similar to MUSCLE comparison calculations
#   - receiver FOV 0.5 mrad (i.e. 1 mrad full angle)
#
# ------Transmitter:------------------------------------------------------------
# 0                               x-coord. of transmitter position        [km]
# 0                  = receiver   y-coord.        "                       [km]
# 0                               z-coord.        "                       [km]
# 0                               x-coord. of transmitter FOV axis
# 0                  --> 0 mrad   y-coord.        "       ( points away      )
# 1                               z-coord.        "       ( from transmitter )
# 1                               x-coord. of transmitter reference vector
# 0                               y-coord.    "  (HAS TO BE perpendicular to  )
# 0                               z-coord.    "  ( the transmitter FOV axis   )
# 1                               i1 component of the starting Stokes Vector
# 0                               i2 component     "
# 0                               u  component     "
# 0                               v  component     "
# 0.00005            = 0.05 mrad  divergence of source beam              [rad]
# 0                               radius of the transmitter               [km]
# 0.012              ~ 40 ns      pulse length                            [km]
# ------Receiver (located in (0,0,0)):------------------------------------------
# 0                               x-coord. of receiver FOV axis ( points away )
# 0                  --> 0 mrad   y-coord.        "             ( from rec.   )
# 1                               z-coord.        "
# 1                               x-coord. of receiver reference vector
# 0                               y-coord.    "  (HAS TO BE perpendicular to  )
# 0                               z-coord.    "  ( the receiver FOV axis      )
# 0.005              = 0.5 mrad   semiaperture of the receiver           [rad]
# point              point receiver radius of the receiver                [km]
# ------Range:------------------------------------------------------------------
# 1.95               minimum value for range  (-> ptime * c)              [km]
# 2.55               maximum value for range                              [km]
# 151                time grid (range) resolution
# ------Geometry:---------------------------------------------------------------
# 3                  number of slabs (including halfspaces)
```

```
# 1                  distance to plane betw. forw. halfspace and slab 1      [km]
# 1.3                distance to plane betw. slab 1 and backw. halfspace     [km]
# ------Extinction:------------------------------------------------------------------
# 0                  extinction coeff. of backward halfspace               [1/km]
# 15                 extinction coeff. of slab 1                           [1/km]
# 0                  extinction coeff. of forward halfspace                [1/km]
# ------Absorption:------------------------------------------------------------------
# 1                  survival probability of backward halfspace
# 1                  survival probability of slab 1
# 1                  survival probability of forward halfspace
# ------Indicatrix resolutions :-----------------------------------------------------
# 1801               resolution of the mueller matrix of "backward" halfspace
# 1801               resolution of the mueller matrix of slab 1
# 1801               resolution of the mueller matrix of "forward" halfspace
# ------Indicatrix file names :------------------------------------------------------
# c1.m               file name of the mueller matrix of "backward" halfspace
# c1.m               file name of the mueller matrix of slab 1
# c1.m               file name of the mueller matrix of "forward" halfspace
# ------Monte Carlo parameters: -----------------------------------------------------
# 0.5                parameter ci of exponential transformation
# 1                  flag, wether scat. split. is used (1 is on)
# 90                 scattering splitting angle for forward hemisphere      [deg]
# 90                 decision angle to fly away from the receiver           [deg]
# 0.0002             cone for scattering splitting                         [mrad]
# 0.000001           radius of cone for scattering splitting in (0,0,0)      [km]
# ------Output parameters:-----------------------------------------------------------
# c1.res             fil ename of output file
# 3                  number of output contributions
# 1                  calculation flag of total sum
# ==================================================================================
# Output data of Monte Carlo program pbs:
#
# 241545            Needed time for calculation [sec]
#
# 90                the scattering splitting angle really used for slab 1
# 90                the scattering splitting angle really used for slab 2
# 90                the scattering splitting angle really used for slab 3
# 0.95174958        integral of forward hemisphere of slab 1
# 0.95174958        integral of forward hemisphere of slab 2
# 0.95174958        integral of forward hemisphere of slab 3
# 0.14475125        integral of backward hemisphere of slab 1
# 0.14475125        integral of backward hemisphere of slab 2
# 0.14475125        integral of backward hemisphere of slab 3
# 0.83516006        average cosine of slab 1
# 0.83516006        average cosine of slab 2
# 0.83516006        average cosine of slab 3
#
# 100000000         number of calculated photon histories
# 1000000           screen output step
#
# 0.004             length of time step interval
```

```
# 10000             nsize : max. number of different photon path families
#                   (increase nsize only if kmax > nsize)
# 36                kmax :  max. number of USED different photon families
# 4.5005736         average number of collisions
# ------------------------------------------------------------------------------
# Return Signals :
# distance total total Stokes vector 1th-order corr. Stokes vector 2nd-order
corr. Stokes vector 3th-order corr. Stokes vector
#
1.95 0 0 0 0 0 0 0 0 0 0 0 0 0 0 0 0 0 0 0 0 0 0
#
1.954 0 0 0 0 0 0 0 0 0 0 0 0 0 0 0 0 0 0 0 0 0 0
#
1.958 0 0 0 0 0 0 0 0 0 0 0 0 0 0 0 0 0 0 0 0 0 0
#
1.962 0 0 0 0 0 0 0 0 0 0 0 0 0 0 0 0 0 0 0 0 0 0
#
1.966 0 0 0 0 0 0 0 0 0 0 0 0 0 0 0 0 0 0 0 0 0 0
#
1.97 0 0 0 0 0 0 0 0 0 0 0 0 0 0 0 0 0 0 0 0 0 0
#
1.974 0 0 0 0 0 0 0 0 0 0 0 0 0 0 0 0 0 0 0 0 0 0
#
1.978 0 0 0 0 0 0 0 0 0 0 0 0 0 0 0 0 0 0 0 0 0 0
#
1.982 0 0 0 0 0 0 0 0 0 0 0 0 0 0 0 0 0 0 0 0 0 0
#
1.986 0 0 0 0 0 0 0 0 0 0 0 0 0 0 0 0 0 0 0 0 0 0
#
1.99 0 0 0 0 0 0 0 0 0 0 0 0 0 0 0 0 0 0 0 0 0 0
#
1.994 0 0 0 0 0 0 0 0 0 0 0 0 0 0 0 0 0 0 0 0 0 0
#
1.998 6.29406e-05 0.998674 0.00132645 -1.75045e-07 -5.96342e-06 6.26337e-05 1
-3.15618e-18 -5.50764e-16 3.74425e-17 3.06463e-07 0.72826 0.27174 -0.00089646
-0.00104495 4.94613e-10 0.576367 0.423633 0.533173 -0.111404
#
2.002 0.000497114 0.995551 0.00444854 -0.000502929 5.16407e-05 0.000489385 1
-2.98312e-18 -4.67573e-18 1.59138e-17 7.63703e-06 0.714325 0.285675 -0.0343327
0.00303671 9.18125e-08 0.676633 0.323367 0.132757 0.0270974
#
2.006 0.000976458 0.993373 0.00662725 0.00010187 -6.75395e-05 0.000949718 1
-2.98308e-18 3.1875e-16 6.97358e-17 2.60787e-05 0.761588 0.238412 0.00546049
-0.00200987 6.48414e-07 0.616266 0.383734 -0.0697772 -0.0214623
#
2.01 0.00137931 0.989276 0.0107239 -0.000241687 -4.15341e-05 0.00132053 1
-2.93532e-18 -1.24119e-16 2.3467e-17 5.64321e-05 0.751315 0.248685 -0.00497957
-0.00151986 2.25752e-06 0.676371 0.323629 -0.0316179 0.0140593
#
. . .
. . .
```

```
. . .
#
#
# relative error of return signals :
# distance total 1th-order 2nd-order 3th-order
#
# 1.95 0 0 0 0
# 1.954 0 0 0 0
# 1.958 0 0 0 0
# 1.962 0 0 0 0
# 1.966 0 0 0 0
# 1.97 0 0 0 0
# 1.974 0 0 0 0
# 1.978 0 0 0 0
# 1.982 0 0 0 0
# 1.986 0 0 0 0
# 1.99 0 0 0 0
# 1.994 0 0 0 0
# 1.998 0.243 0.232 14.7 57.2
# 2.002 0.0993 0.0821 3.64 19.9
# 2.006 0.0748 0.0582 1.75 10.4
# 2.01 0.0713 0.0489 1.24 7.87
. . .
. . .
. . .
#
# (c) 1992-94 Martin Kerscher, Masoud Noormohammadian
#
```

4.2.4 Hints, wishes and known bugs

The program `pbs` (and the programs `rbs` and `rbu` for unpolarized scattering, see Noormohammadian [37]) are now tested against several other aproaches and programs (see Bissonette et al. [2] and Noormohammadian [37]). We are quite sure that the program is working correctly, but we do not give any guarantee (see Paragraph 4.2.5).

As we pointed out in Pragraph 4.1.3 you have to know how variance reduction works within this program. Blind use of the Monte Carlo parameters will lead to misleading or even wrong results almost surley.

The definition of the receiver is a bit weired, and does meet intuition only for $\varphi_R \approx n_R$ (see Definition 4.1.1 and Figure 4.1).

`pbs` does not calculate the zeroth order signal. This is no problem for backscatter situations but with this restriction `pbs` is not applicable to transmission calculations.

The procedure for reading in the input file should be more comfortable, i.e. variable comments should be allowed.

Polarisation for non spherical and arbitrary orientated particles should be implemented.

It should be possible to store the complete quantities needed in a calculation in such a way that it is possible to start with these values a new calculation without loosing the time spent on the recent calculation.

4.2.5 License

The program was developed during the doctoral thesis of Masoud Noormohammadian and the diploma work of Martin Kerscher. We hope that this program will proof helpful in understanding the ongoing climate changes. The program is distributed under the GNU public license. Additionally the program, programs derived from it, and results achievd with it may not be used for miltary developments.

```
    GNU GENERAL PUBLIC LICENSE
       Version 2, June 1991

 Copyright (C) 1989, 1991 Free Software Foundation, Inc.
                          675 Mass Ave, Cambridge, MA 02139, USA
 Everyone is permitted to copy and distribute verbatim copies
 of this license document, but changing it is not allowed.

    Preamble

  The licenses for most software are designed to take away your
freedom to share and change it.  By contrast, the GNU General Public
License is intended to guarantee your freedom to share and change free
software--to make sure the software is free for all its users.  This
General Public License applies to most of the Free Software
Foundation's software and to any other program whose authors commit to
using it.  (Some other Free Software Foundation software is covered by
the GNU Library General Public License instead.)  You can apply it to
your programs, too.

  When we speak of free software, we are referring to freedom, not
price.  Our General Public Licenses are designed to make sure that you
have the freedom to distribute copies of free software (and charge for
this service if you wish), that you receive source code or can get it
if you want it, that you can change the software or use pieces of it
in new free programs; and that you know you can do these things.

  To protect your rights, we need to make restrictions that forbid
anyone to deny you these rights or to ask you to surrender the rights.
```

```
These restrictions translate to certain responsibilities for you if you
distribute copies of the software, or if you modify it.

  For example, if you distribute copies of such a program, whether
gratis or for a fee, you must give the recipients all the rights that
you have.  You must make sure that they, too, receive or can get the
source code.  And you must show them these terms so they know their
rights.

  We protect your rights with two steps: (1) copyright the software, and
(2) offer you this license which gives you legal permission to copy,
distribute and/or modify the software.

  Also, for each author's protection and ours, we want to make certain
that everyone understands that there is no warranty for this free
software.  If the software is modified by someone else and passed on, we
want its recipients to know that what they have is not the original, so
that any problems introduced by others will not reflect on the original
authors' reputations.

  Finally, any free program is threatened constantly by software
patents.  We wish to avoid the danger that redistributors of a free
program will individually obtain patent licenses, in effect making the
program proprietary.  To prevent this, we have made it clear that any
patent must be licensed for everyone's free use or not licensed at all.

  The precise terms and conditions for copying, distribution and
modification follow.


    GNU GENERAL PUBLIC LICENSE
   TERMS AND CONDITIONS FOR COPYING, DISTRIBUTION AND MODIFICATION

  0. This License applies to any program or other work which contains
a notice placed by the copyright holder saying it may be distributed
under the terms of this General Public License.  The "Program", below,
refers to any such program or work, and a "work based on the Program"
means either the Program or any derivative work under copyright law:
that is to say, a work containing the Program or a portion of it,
either verbatim or with modifications and/or translated into another
language.  (Hereinafter, translation is included without limitation in
the term "modification".)  Each licensee is addressed as "you".

Activities other than copying, distribution and modification are not
covered by this License; they are outside its scope.  The act of
running the Program is not restricted, and the output from the Program
is covered only if its contents constitute a work based on the
Program (independent of having been made by running the Program).
Whether that is true depends on what the Program does.

  1. You may copy and distribute verbatim copies of the Program's
```

with the Program (or with a work based on the Program) on a volume of a storage or distribution medium does not bring the other work under the scope of this License.

3. You may copy and distribute the Program (or a work based on it, under Section 2) in object code or executable form under the terms of Sections 1 and 2 above provided that you also do one of the following:

a) Accompany it with the complete corresponding machine-readable source code, which must be distributed under the terms of Sections 1 and 2 above on a medium customarily used for software interchange; or,

b) Accompany it with a written offer, valid for at least three years, to give any third party, for a charge no more than your cost of physically performing source distribution, a complete machine-readable copy of the corresponding source code, to be distributed under the terms of Sections 1 and 2 above on a medium customarily used for software interchange; or,

c) Accompany it with the information you received as to the offer to distribute corresponding source code. (This alternative is allowed only for noncommercial distribution and only if you received the program in object code or executable form with such an offer, in accord with Subsection b above.)

The source code for a work means the preferred form of the work for making modifications to it. For an executable work, complete source code means all the source code for all modules it contains, plus any associated interface definition files, plus the scripts used to control compilation and installation of the executable. However, as a special exception, the source code distributed need not include anything that is normally distributed (in either source or binary form) with the major components (compiler, kernel, and so on) of the operating system on which the executable runs, unless that component itself accompanies the executable.

If distribution of executable or object code is made by offering access to copy from a designated place, then offering equivalent access to copy the source code from the same place counts as distribution of the source code, even though third parties are not compelled to copy the source along with the object code.

4. You may not copy, modify, sublicense, or distribute the Program except as expressly provided under this License. Any attempt otherwise to copy, modify, sublicense or distribute the Program is void, and will automatically terminate your rights under this License. However, parties who have received copies, or rights, from you under this License will not have their licenses terminated so long as such parties remain in full compliance.

5. You are not required to accept this License, since you have not signed it. However, nothing else grants you permission to modify or distribute the Program or its derivative works. These actions are prohibited by law if you do not accept this License. Therefore, by modifying or distributing the Program (or any work based on the Program), you indicate your acceptance of this License to do so, and all its terms and conditions for copying, distributing or modifying the Program or works based on it.

6. Each time you redistribute the Program (or any work based on the Program), the recipient automatically receives a license from the original licensor to copy, distribute or modify the Program subject to these terms and conditions. You may not impose any further restrictions on the recipients' exercise of the rights granted herein. You are not responsible for enforcing compliance by third parties to this License.

7. If, as a consequence of a court judgment or allegation of patent infringement or for any other reason (not limited to patent issues), conditions are imposed on you (whether by court order, agreement or otherwise) that contradict the conditions of this License, they do not excuse you from the conditions of this License. If you cannot distribute so as to satisfy simultaneously your obligations under this License and any other pertinent obligations, then as a consequence you may not distribute the Program at all. For example, if a patent license would not permit royalty-free redistribution of the Program by all those who receive copies directly or indirectly through you, then the only way you could satisfy both it and this License would be to refrain entirely from distribution of the Program.

If any portion of this section is held invalid or unenforceable under any particular circumstance, the balance of the section is intended to apply and the section as a whole is intended to apply in other circumstances.

It is not the purpose of this section to induce you to infringe any patents or other property right claims or to contest validity of any such claims; this section has the sole purpose of protecting the integrity of the free software distribution system, which is implemented by public license practices. Many people have made generous contributions to the wide range of software distributed through that system in reliance on consistent application of that system; it is up to the author/donor to decide if he or she is willing to distribute software through any other system and a licensee cannot impose that choice.

This section is intended to make thoroughly clear what is believed to be a consequence of the rest of this License.

8. If the distribution and/or use of the Program is restricted in

certain countries either by patents or by copyrighted interfaces, the original copyright holder who places the Program under this License may add an explicit geographical distribution limitation excluding those countries, so that distribution is permitted only in or among countries not thus excluded. In such case, this License incorporates the limitation as if written in the body of this License.

9. The Free Software Foundation may publish revised and/or new versions of the General Public License from time to time. Such new versions will be similar in spirit to the present version, but may differ in detail to address new problems or concerns.

Each version is given a distinguishing version number. If the Program specifies a version number of this License which applies to it and "any later version", you have the option of following the terms and conditions either of that version or of any later version published by the Free Software Foundation. If the Program does not specify a version number of this License, you may choose any version ever published by the Free Software Foundation.

10. If you wish to incorporate parts of the Program into other free programs whose distribution conditions are different, write to the author to ask for permission. For software which is copyrighted by the Free Software Foundation, write to the Free Software Foundation; we sometimes make exceptions for this. Our decision will be guided by the two goals of preserving the free status of all derivatives of our free software and of promoting the sharing and reuse of software generally.

NO WARRANTY

11. BECAUSE THE PROGRAM IS LICENSED FREE OF CHARGE, THERE IS NO WARRANTY FOR THE PROGRAM, TO THE EXTENT PERMITTED BY APPLICABLE LAW. EXCEPT WHEN OTHERWISE STATED IN WRITING THE COPYRIGHT HOLDERS AND/OR OTHER PARTIES PROVIDE THE PROGRAM "AS IS" WITHOUT WARRANTY OF ANY KIND, EITHER EXPRESSED OR IMPLIED, INCLUDING, BUT NOT LIMITED TO, THE IMPLIED WARRANTIES OF MERCHANTABILITY AND FITNESS FOR A PARTICULAR PURPOSE. THE ENTIRE RISK AS TO THE QUALITY AND PERFORMANCE OF THE PROGRAM IS WITH YOU. SHOULD THE PROGRAM PROVE DEFECTIVE, YOU ASSUME THE COST OF ALL NECESSARY SERVICING, REPAIR OR CORRECTION.

12. IN NO EVENT UNLESS REQUIRED BY APPLICABLE LAW OR AGREED TO IN WRITING WILL ANY COPYRIGHT HOLDER, OR ANY OTHER PARTY WHO MAY MODIFY AND/OR REDISTRIBUTE THE PROGRAM AS PERMITTED ABOVE, BE LIABLE TO YOU FOR DAMAGES, INCLUDING ANY GENERAL, SPECIAL, INCIDENTAL OR CONSEQUENTIAL DAMAGES ARISING OUT OF THE USE OR INABILITY TO USE THE PROGRAM (INCLUDING BUT NOT LIMITED TO LOSS OF DATA OR DATA BEING RENDERED INACCURATE OR LOSSES SUSTAINED BY YOU OR THIRD PARTIES OR A FAILURE OF THE PROGRAM TO OPERATE WITH ANY OTHER PROGRAMS), EVEN IF SUCH HOLDER OR OTHER PARTY HAS BEEN ADVISED OF THE POSSIBILITY OF SUCH DAMAGES.

END OF TERMS AND CONDITIONS

Chapter 5

Some calculations

In this chapter we discuss results of Monte Carlo calculations made with the program `pbs` described in chapter 4.

5.1 DLR–Micro–LIDAR: measured and simulated return signals

We modeled a monostatic LIDAR directed perpendicularly to a C2–cloud (see Deirmendjian [12]) at a distance of $140\,m$ with a visibility of $80\,m$ (= extinction $37.5\,km^{-1}$) in the cloud. Figure 5.1 illustrates this situation.

Figure 5.1: The environmental situation.

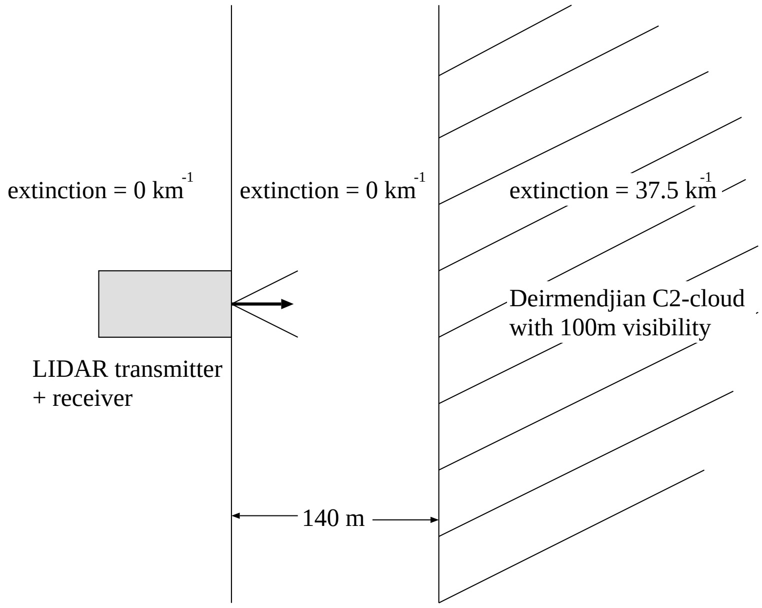

The transmitter field of view (FOV) is $1.75\,mrad$ (half angle of aperture), with beam radius $1\,mm$, pulse length $12\,ns$, wavelength $1.064\,\mu m$, and a linearly polarized beam. The receiver has a central FOV of $3\,mrad$ (half angle of aperture) and a ring–shaped exterior FOV of $3 - 9\,mrad$ (inner–outer half angle of aperture). This is a simple model for the DLR–Microlidar, see Krichbaumer et al. [28]. Results of variance reduction Monte Carlo simulations are shown in Figures 5.2, 5.3 and 5.4. For spherical particles, depolarization occurs only after multiple scattering. Therefore, the $I_\perp$ curve has its maximum at a longer photon path length than the $I_{||}$ curve, as we see in the Monte Carlo simulated signal for the central FOV (see Figure 5.2 and 5.3). In the exterior FOV we observe no difference in the position of the maxima, since there both signals result mainly from multiple

Figure 5.2: Monte Carlo simulated parallel polarized $I_{||}$ signals.

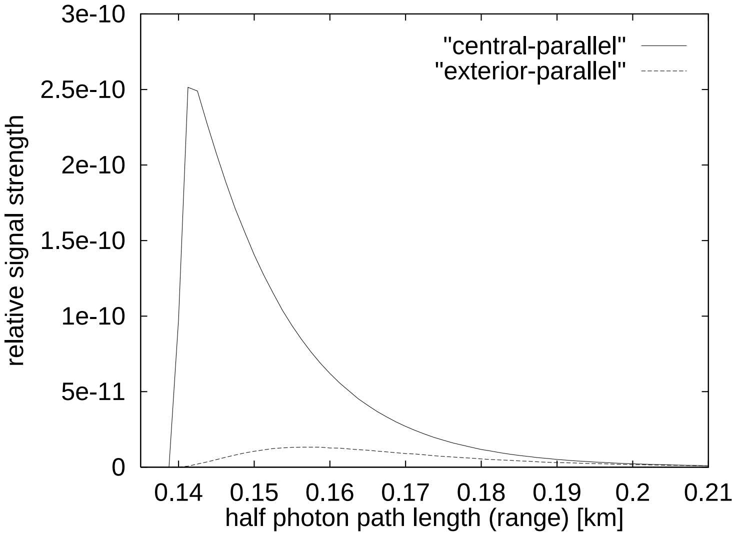

scattering (see Figure 5.3). The contribution of single scattering at the maximum of $I_{||}$ in the exterior FOV is less than the variance of this Monte Carlo simulation, the contribution of single scattering at the maximum of $I_{||}$ in the central FOV is about 96 %. Therefore, we observe the difference in the position of the maxima of $I_{||}$ for the central FOV and the exterior FOV (see Figure 5.2).

Figure 5.4 shows the slow increase of the linear depolarization ratio $I_\perp/(I_{||}+I_\perp)$ with the photon path length, which is typical for water clouds, see Figure 2 in Pal et al. [40]; note that their definition of the depolarization is different from the linear depolarization ratio used here.

In Figure 5.5 we show measurements with the four-channel DLR–Microlidar showing both multiple scattering and depolarization; for details see Krichbaumer [29]. The slower increase of the signal may be due to the fact that the beginning of the cloud is not sharp, in contrary to the Monte Carlo simulation. The differences of the positions of the maxima $I_{||}^{max}$ and $I_\perp^{max}$ for the simulated central and exterior FOV signals as in Figure 5.2 and 5.3 are in good agreement with the measured differences of Figure 5.5. The maxima $I_\perp^{max}$ for the simulated central and exterior FOV signals are nearly equal, which can be seen in the corresponding measured signals, too (see Figure 5.3 and 5.5). The ratios of $I_{||}^{max}$ to $I_\perp^{max}$ for the central FOV signal and for the exterior FOV simulated signal do not agree very well with the measured ratios. The stronger $I_\perp$ signals of the measurement are not astonishing since the measured cloud was a mixed–phase cloud where depolarization may already occur for single scattering only; see Krichbaumer [29].

Figure 5.3: Monte Carlo simulated perpendiculary polarized signals $I_{\perp}$ compared to the parallel polarized signal $I_{||}$ of the exterior FOV, for the same enviromental situation as in Figure 5.2

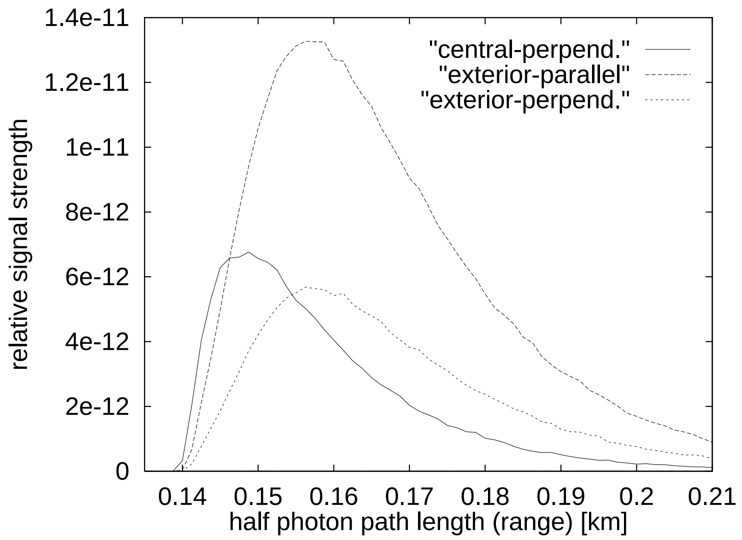

Figure 5.4: Simulated linear depolarization $I_{\perp}/(I_{||}+I_{\perp})$ of the central FOV signal, for the same enviromental situation as in Figure 5.2.

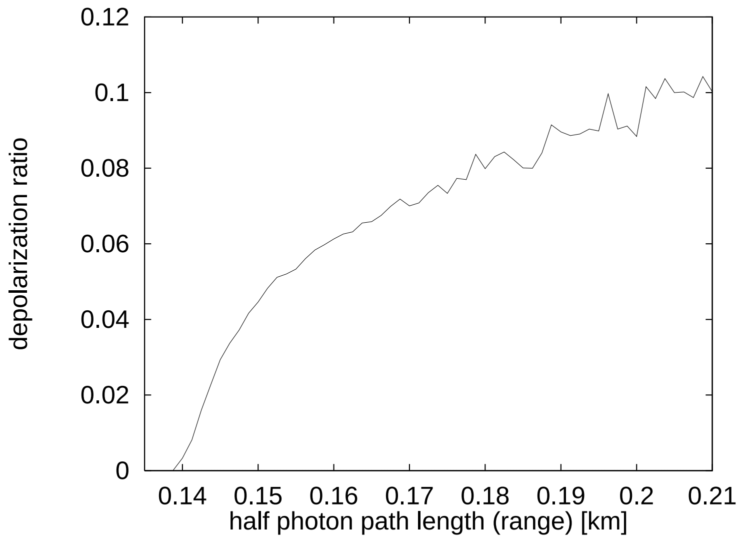

Figure 5.5: Measured four–channel signal of the DLR–Microlidar, see Krichbaumer [29].

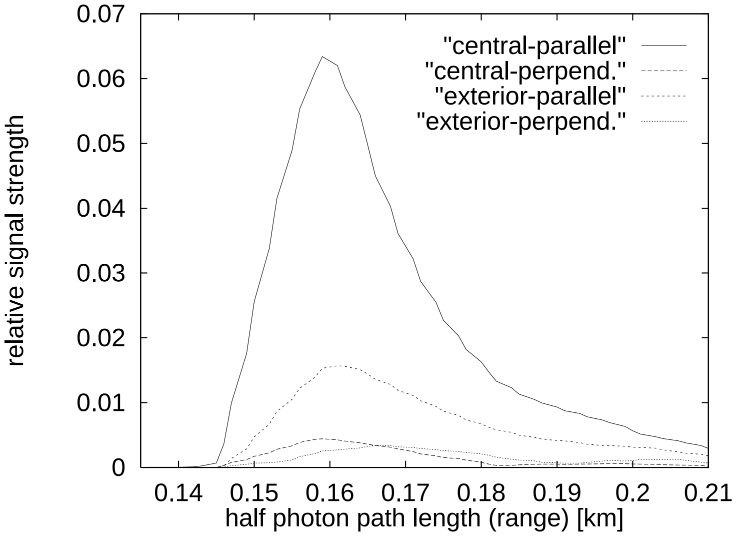

5.2 Sensitivity analysis for C1–type clouds

In this section we are interested wether it is possible to get informations about the size distribution (mainly the mode radius r_c, see Section 5.2.1) from the LIDAR signal. Therfore, we performed several Monte Carlo simulations with different size distributions (see Section 5.2.2). During this section we are not interested in the influence of the extinction which we fixed.

For each simulation we need as input the Mueller matrix of the particles describing the scattering properties in the cloud. A Mueller matrix for spherical particles of fixed radius is calculated from Mie theory (see Section 6.1.4). To get the Mueller matrix for a water cloud we integrate the Mueller matrix over the different radii using a specific size distribution (see Section 5.2.1 and Deirmendjian [12] §3).

In addition we need the extinction and the geometry for the simulations. We have chosen a point like transmitter emitting linearly polarized light with wavelength $1064\mu m$ and a conical transmitter field of view (FOV) of 0.05 mrad (half angle). The receiver is at the same position looking in the same direction with receiver FOV of 0.5 mrad (half angle). The cloud is located at a distance of 1km perpendiculary in front of the receiver with a thickness of 300m and a constant extinction of 15km^{-1} (see Figure 5.6). The refractive index of the water was chosen to be $1.326 + i \times 0.513 \times 10^{-5}$ (cf. Hale and Querry [16]). This geometry is similar to the geometry used for the MUSCLE calculations (cf. Bissonette et al. [2]).

Figure 5.6: The environmental situation.

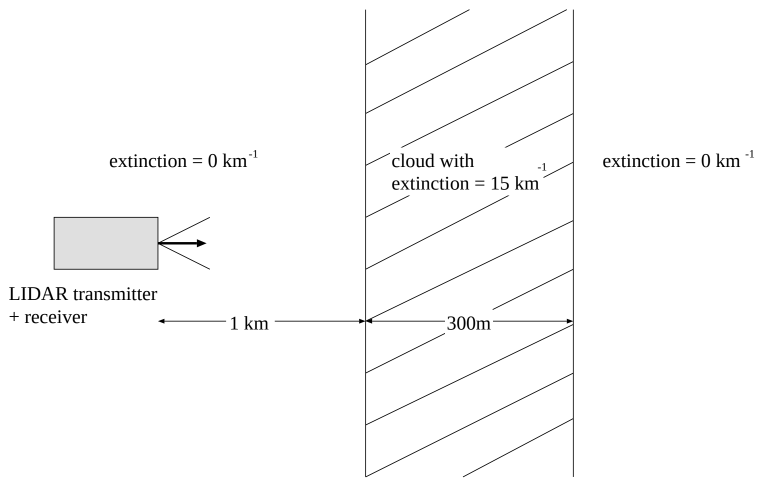

5.2.1 The size distribution

Deirmendjian uses a family of size distributions $n : \mathbb{R}_0^+ \to \mathbb{R}_0^+$ (more exactly, these are the densities of the distributions) which he called *modified gamma distributions* of the form

$$n(r) = ar^\alpha \exp(-br^\gamma)$$

depending on the parameters a, α, b, and γ with r the radius of the spherical particle (cf. Deirmendjian [12] §3.4). The parameter a is directly related to the particle density (i.e. mass density, cf. Deirmendjian [12] p76) and therefore to the extinction in the cloud. The parameters α and γ determine the shape (asymmetry and width) of the density n. The parameter b may be expressed in terms of the *mode radius* r_c where r_c is the mode of the size distribution.

$$b = \frac{\alpha}{\gamma r_c^\gamma}$$

We use r_c instead of b. Since a is directly related to the extinction which we want to leave fixed, there are only three parameters r_c, α, and γ which we may vary. Deirmendjian uses for the definition of the C1 cloud the following parameters $r_c = 4\mu$, $\alpha = 6$, and $\gamma = 1$ (cf. Deirmendjian [12] p78). We varied all three paramters in the following way. $r_c \in \{1\mu, 2\mu, 3\mu, 4\mu, 5\mu, 7\mu, 9\mu\}$, $\alpha \in \{6, 12, 18\}$ and $\gamma \in \{1, 5, 10\}$. Mainly we want show the dependence of the LIDAR return signals on the mode radius r_c. For the standard C1 cloud the densities show a strong overlap (see Figure 5.7). Therefore, we have choosen the parameters α and γ in order to "sharpen" the size distribution to increase the dependence on the mode radius. For $\alpha = 18$ and $\gamma = 10$ we see in Figure 5.15 that the densities show only a small overlap. These densities for big α and γ are highly arbitrary and probably do not represent any cloud in nature.

The following figures show the densities of the size distributions for the above mentioned parameters.

Figure 5.7: The densities for $\alpha = 6$ and $\gamma = 1$ (the Deirmendjian C1 cloud is the one labelled by $r4$).

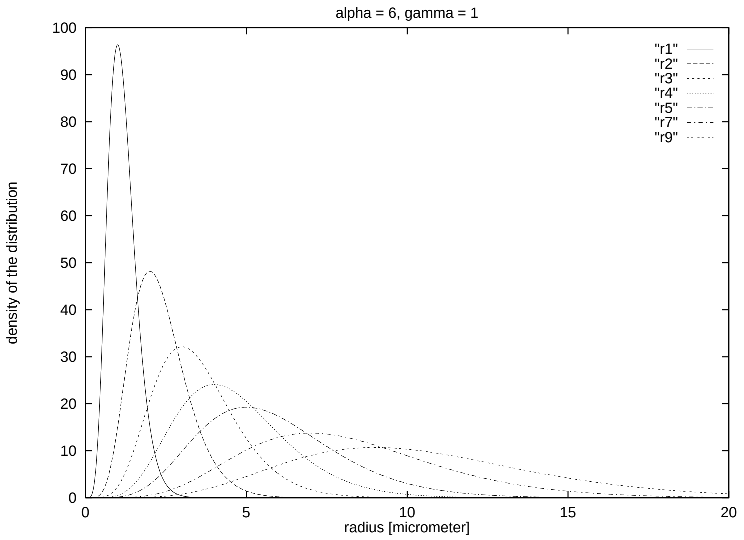

Figure 5.8: The densities for $\alpha = 12$ and $\gamma = 1$.

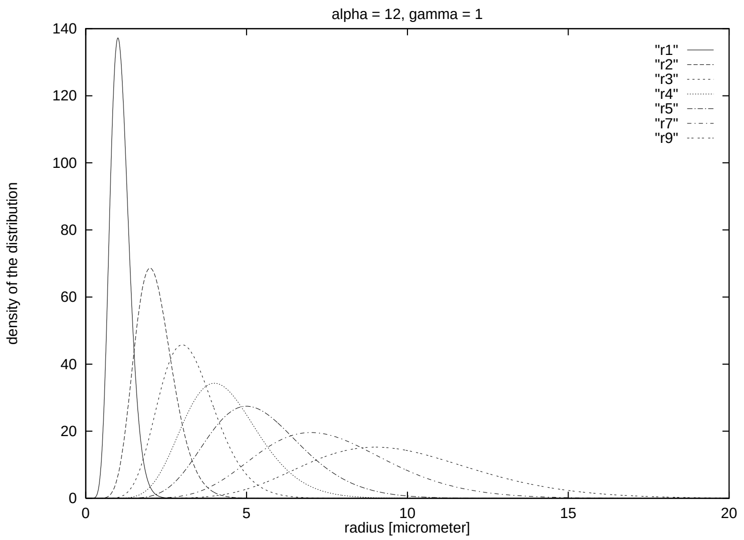

Figure 5.9: The densities for $\alpha = 18$ and $\gamma = 1$.

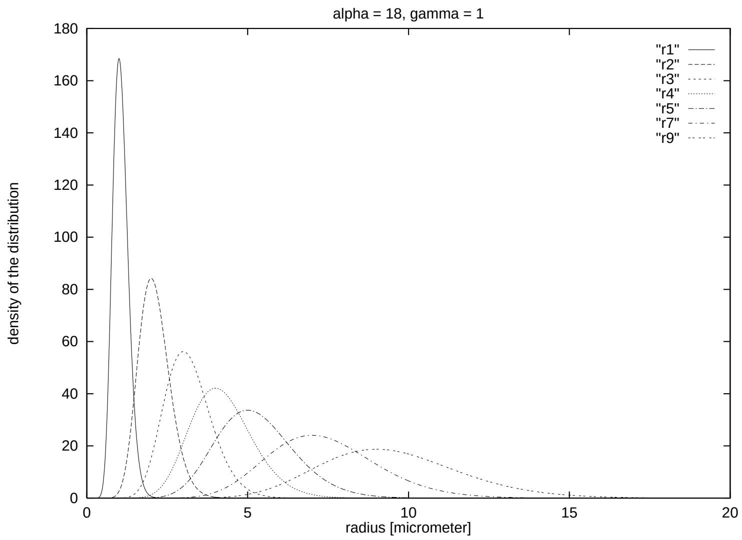

Figure 5.10: The densities for $\alpha = 6$ and $\gamma = 5$.

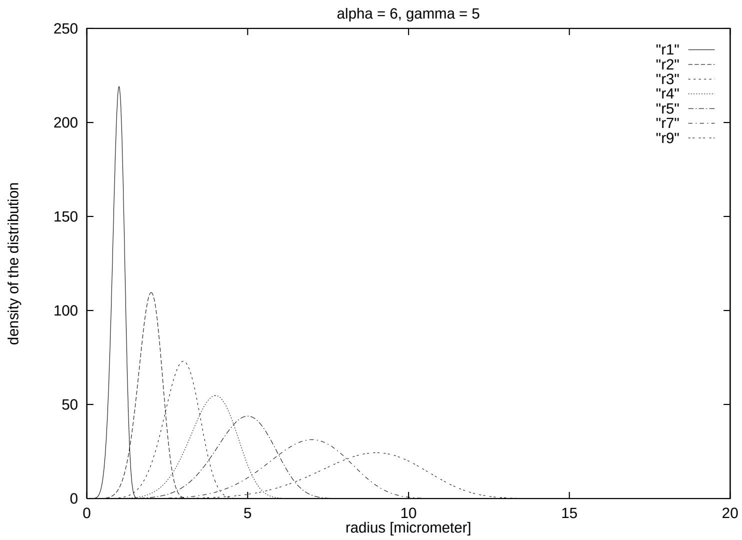

Figure 5.11: The densities for $\alpha = 12$ and $\gamma = 5$.

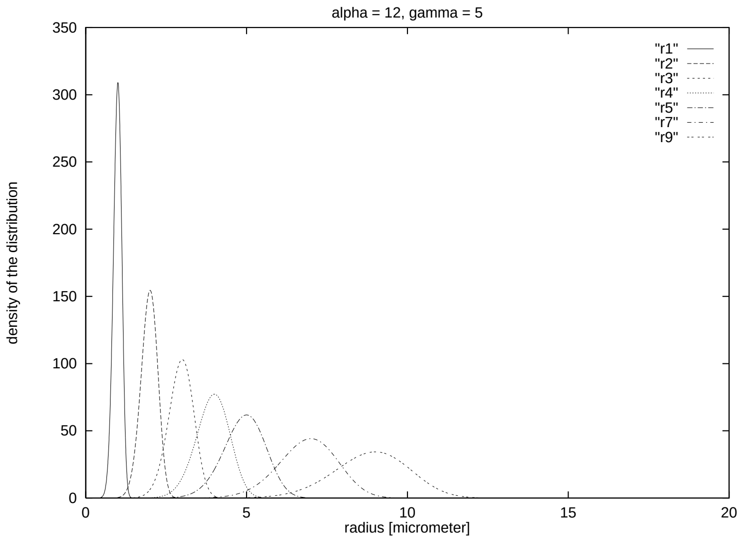

Figure 5.12: The densities for $\alpha = 18$ and $\gamma = 5$.

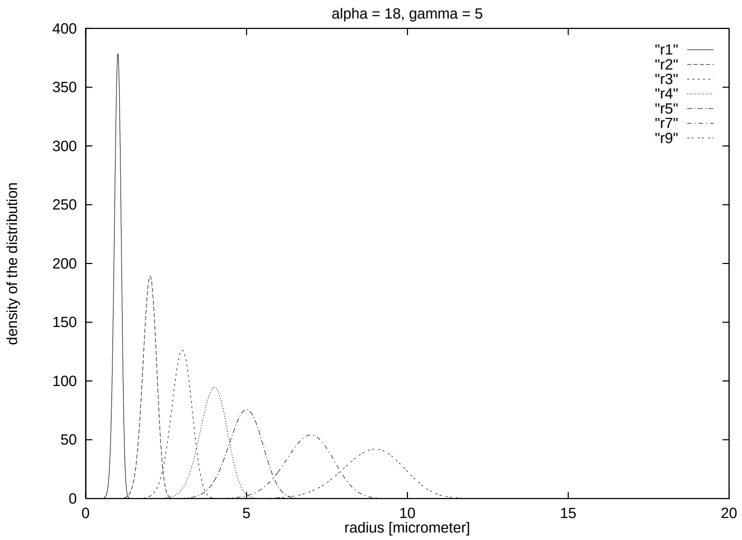

Figure 5.13: The densities for $\alpha = 6$ and $\gamma = 10$.

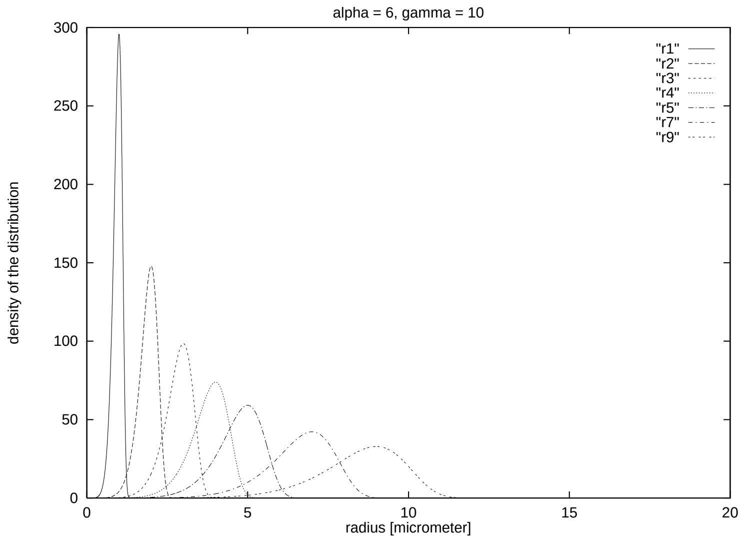

Figure 5.14: The densities for $\alpha = 12$ and $\gamma = 10$.

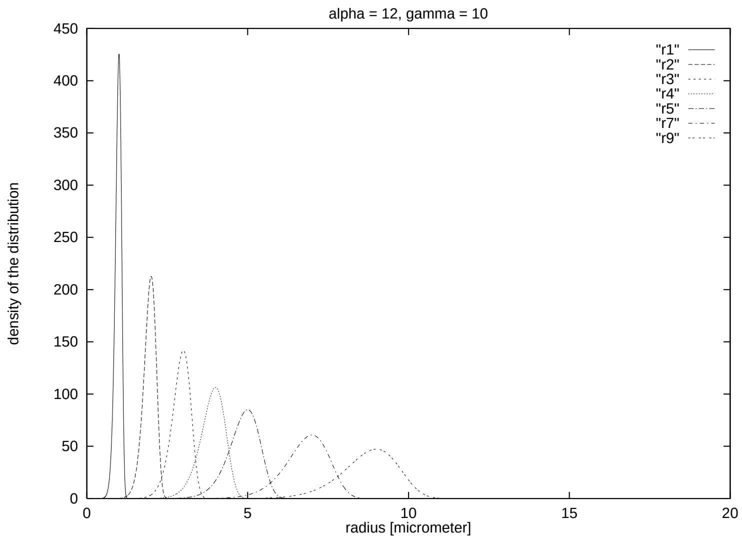

Figure 5.15: The densities for $\alpha = 18$ and $\gamma = 10$.

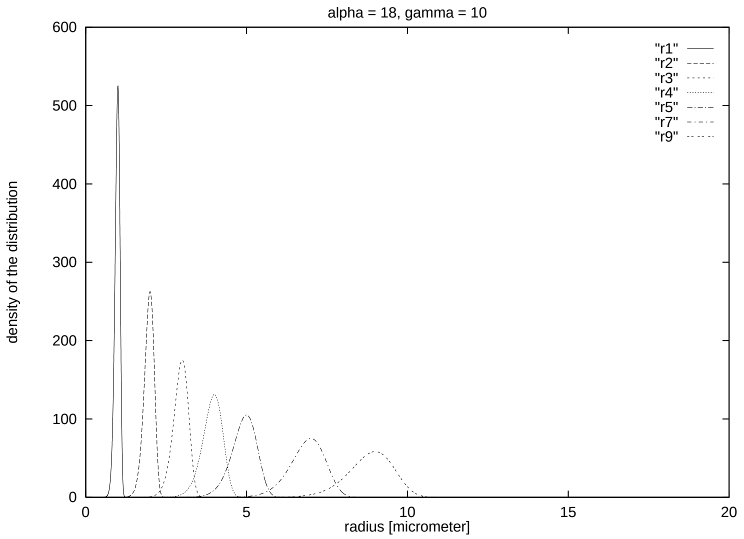

5.2.2 Results of Monte Carlo simulations

We used the size distributions of Section 5.2.1 to calculate the Mueller matrices according to 6.1.4. With these Mueller matrices we performed 27 Monte Carlo simulations of the polarized LIDAR backscatter signals with the geometry and extinction given above. Each simulation consumed about 70 hours of computing time on a Sparc 10.

Simulated $I = I_{||} + I_{\perp}$

In the following figures we present the received intensity $I = I_{||} + I_{\perp}$ of all scattering orders. For all parameters α and γ we see the exceptional behavior for $r_c = 1$. In the C1 case ($\alpha = 6$ and $\gamma = 1$, Figure 5.16) all other r_c show aproximately the same behavior. For larger α and γ the signals seperate for different r_c. This separation does not occure in a systematic way. (This might be a resonance effect with the wavelength $\lambda = 1.064\mu$)

Figure 5.16: The intensities I for $\alpha = 6$ and $\gamma = 1$ (the Deirmendjian C1 cloud is the one labelled by $r4$).

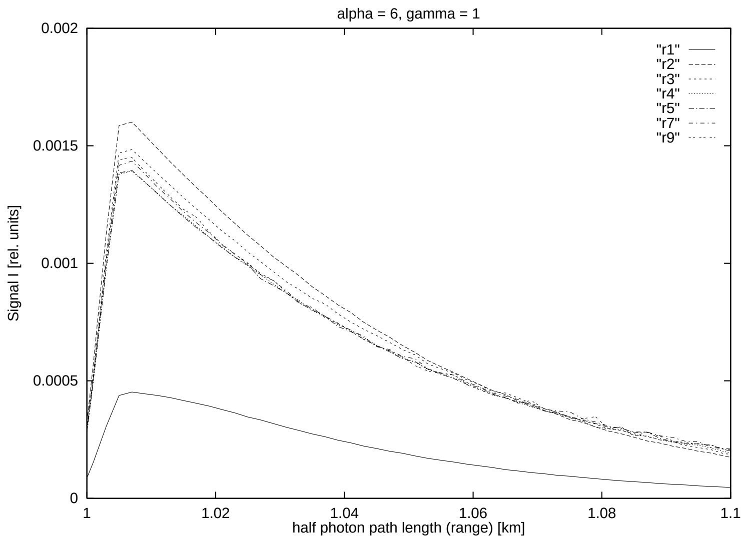

Figure 5.17: The intensities I for $\alpha = 12$ and $\gamma = 1$.

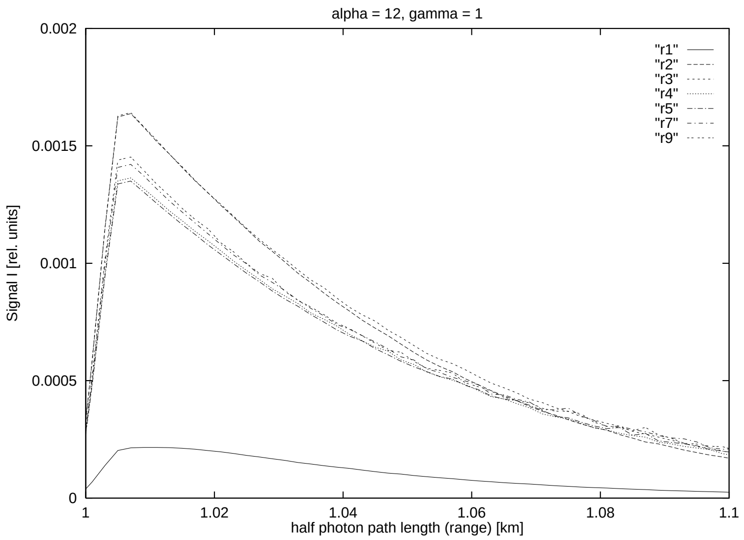

Figure 5.18: The intensities I for $\alpha = 18$ and $\gamma = 1$.

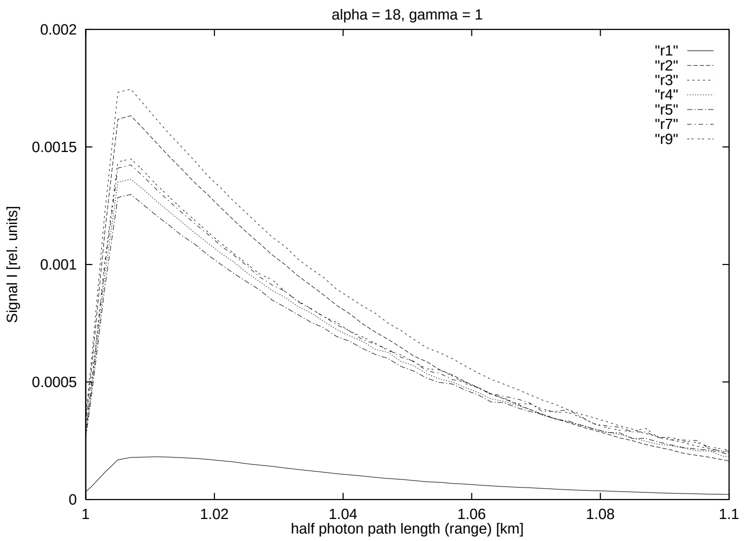

Figure 5.19: The intensities I for $\alpha = 6$ and $\gamma = 5$.

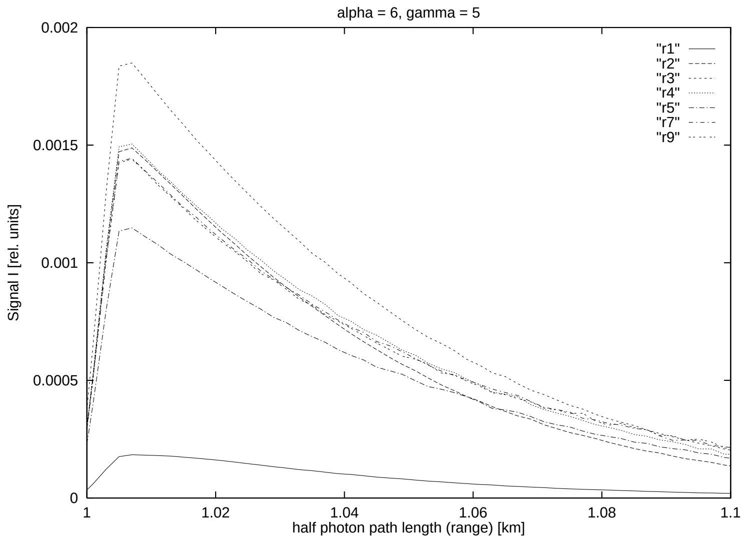

Figure 5.20: The intensities I for $\alpha = 12$ and $\gamma = 5$.

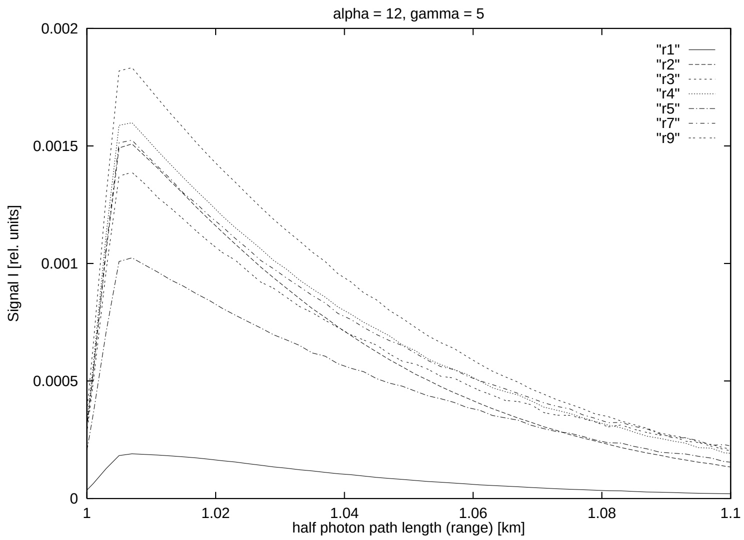

Figure 5.21: The intensities I for $\alpha = 18$ and $\gamma = 5$.

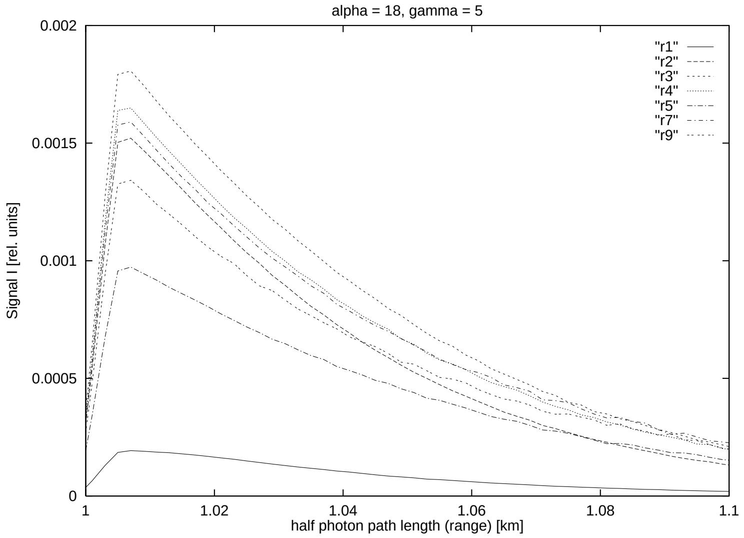

Figure 5.22: The intensities I for $\alpha = 6$ and $\gamma = 10$.

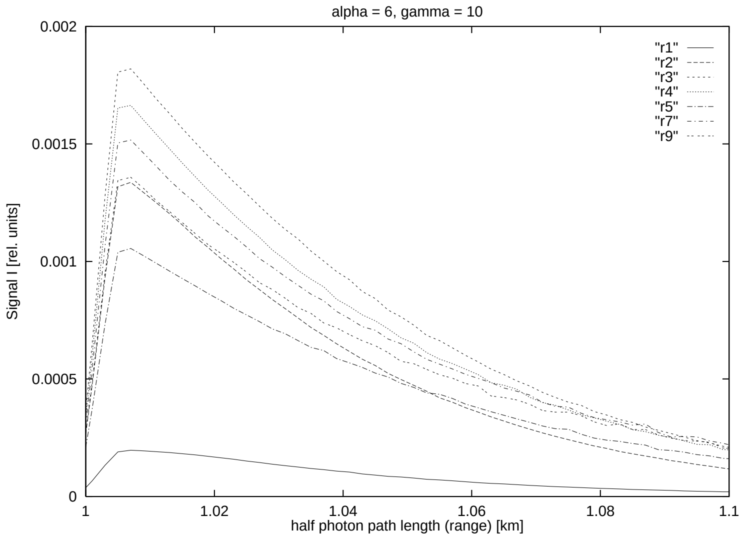

Figure 5.23: The intensities I for $\alpha = 12$ and $\gamma = 10$.

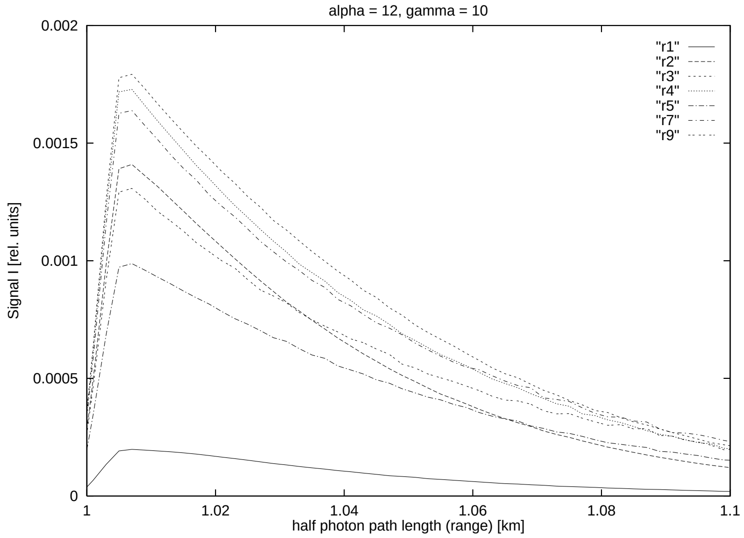

Figure 5.24: The intensities I for $\alpha = 18$ and $\gamma = 10$.

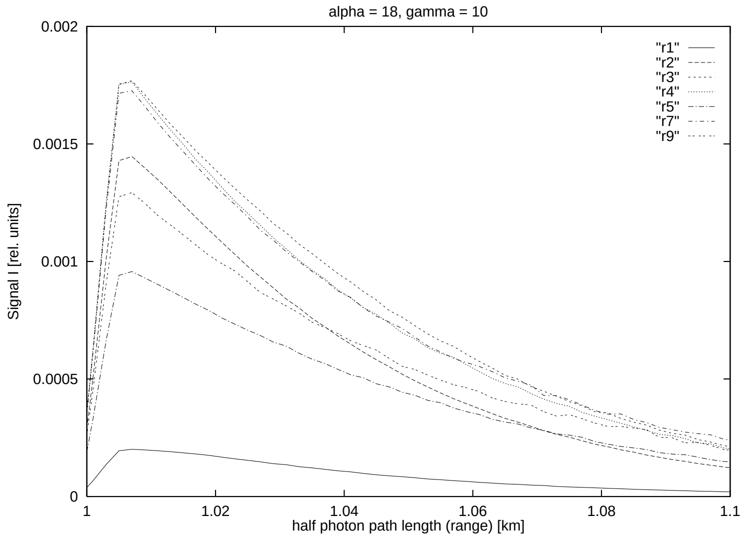

The ratio of the single scattered signal to the total signal

In this section we present the ratio of the single scattered portion of the signal versus the total backscattered signal (all scattering orders) of the signal. Again the ratio shows for $r_c = 1$ an exceptional behavior. For $r_c \in \{2, 3, 4, 5, 7, 9\}$ the ratios show the same behavior until penetration depth of 50m into the cloud, i.e. the percentage of single scattering reduces to 60%. For penetration depths greater than 50m the ratios show a small separation, especially $r_c = 2$ shows a lower portion of multiple scattering.

Figure 5.25: The relative signal strength of the single scattered portion of the signal versus the total backscattered signal for $\alpha = 6$ and $\gamma = 1$ (the Deirmendjian C1 cloud is the one labelled by $r4$).

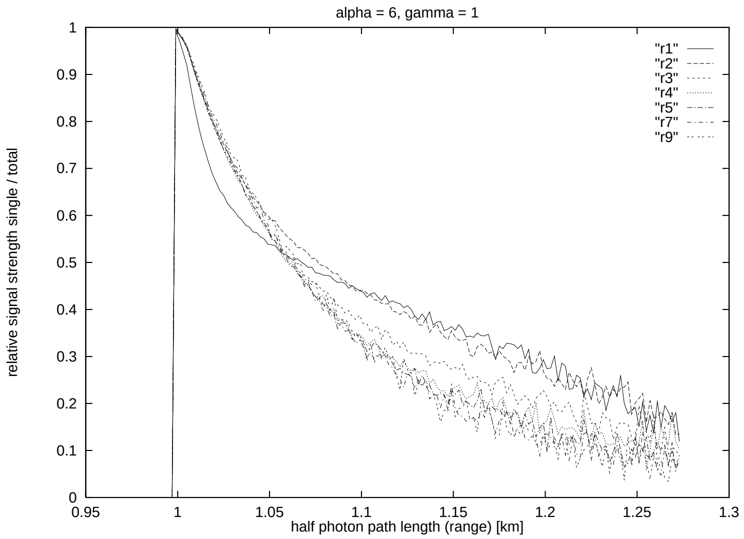

Figure 5.26: The relative signal strength of the single scattered portion of the signal versus the total backscattered signal for $\alpha = 12$ and $\gamma = 1$.

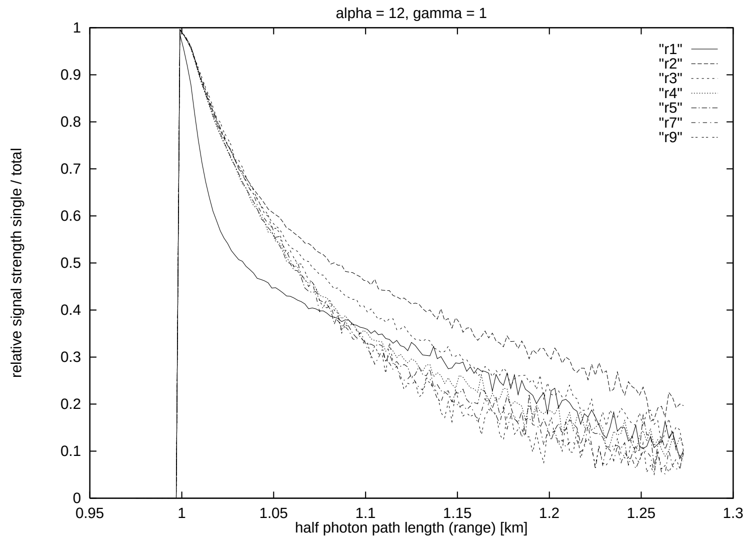

Figure 5.27: The relative signal strength of the single scattered portion of the signal versus the total backscattered signal for $\alpha = 18$ and $\gamma = 1$.

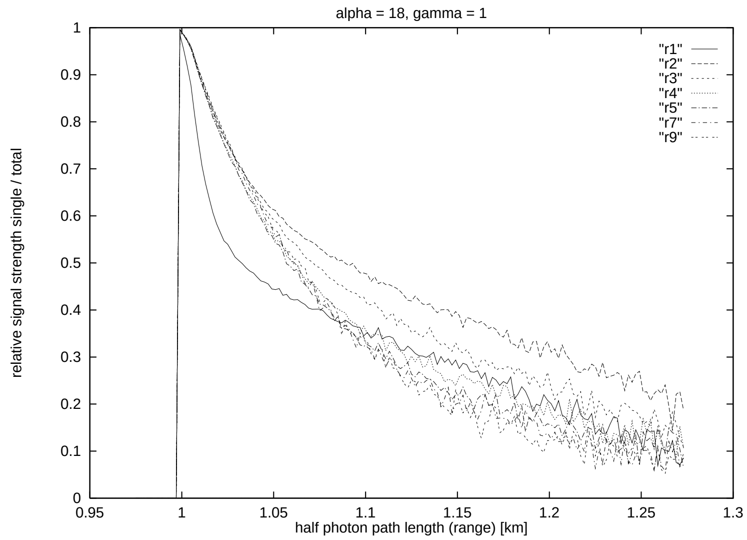

Figure 5.28: The relative signal strength of the single scattered portion of the signal versus the total backscattered signal for $\alpha = 6$ and $\gamma = 5$.

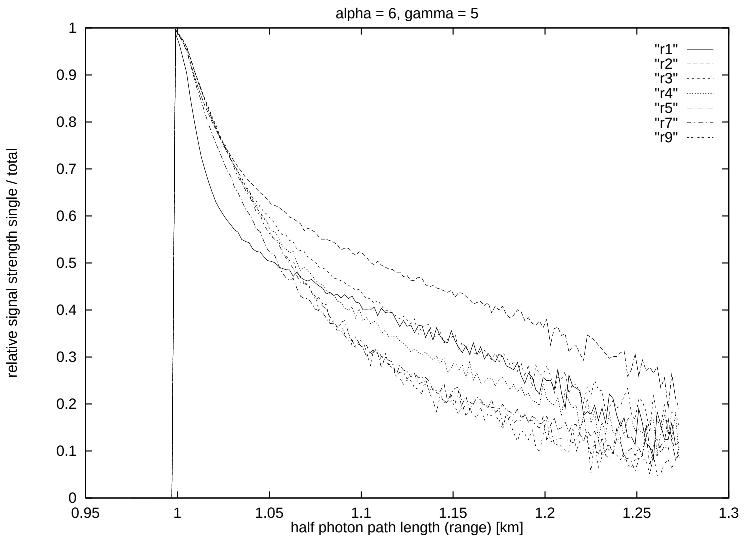

Figure 5.29: The relative signal strength of the single scattered portion of the signal versus the total backscattered signal for $\alpha = 12$ and $\gamma = 5$.

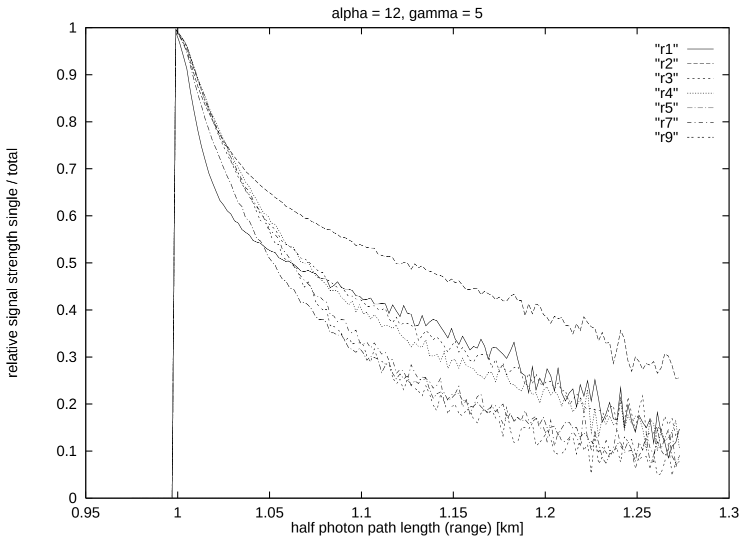

Figure 5.30: The relative signal strength of the single scattered portion of the signal versus the total backscattered signal for $\alpha = 18$ and $\gamma = 5$.

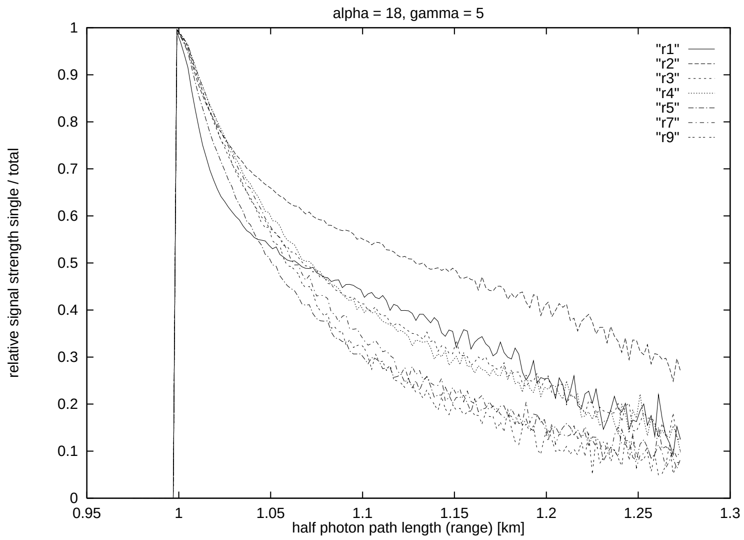

Figure 5.31: The relative signal strength of the single scattered portion of the signal versus the total backscattered signal for $\alpha = 6$ and $\gamma = 10$.

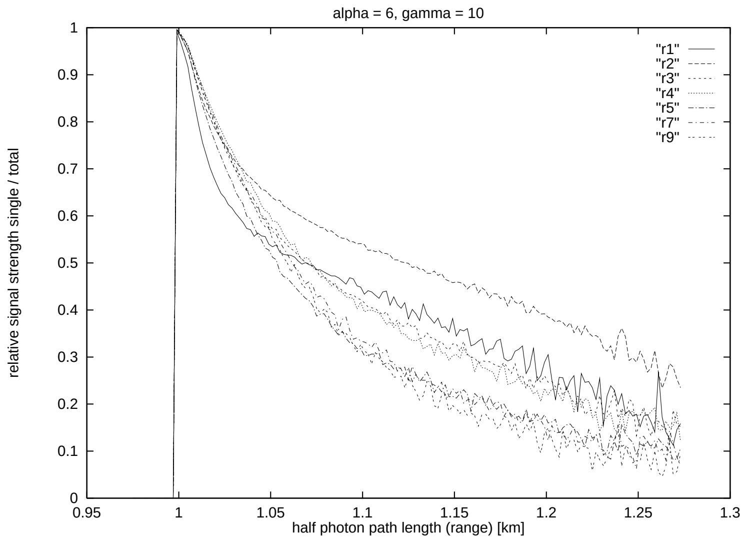

Figure 5.32: The relative signal strength of the single scattered portion of the signal versus the total backscattered signal for $\alpha = 12$ and $\gamma = 10$.

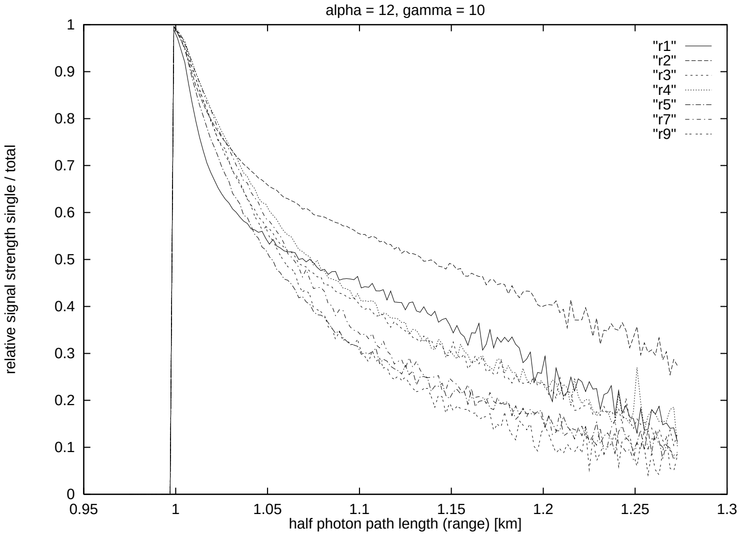

Figure 5.33: The relative signal strength of the single scattered portion of the signal versus the total backscattered signal for $\alpha = 18$ and $\gamma = 10$.

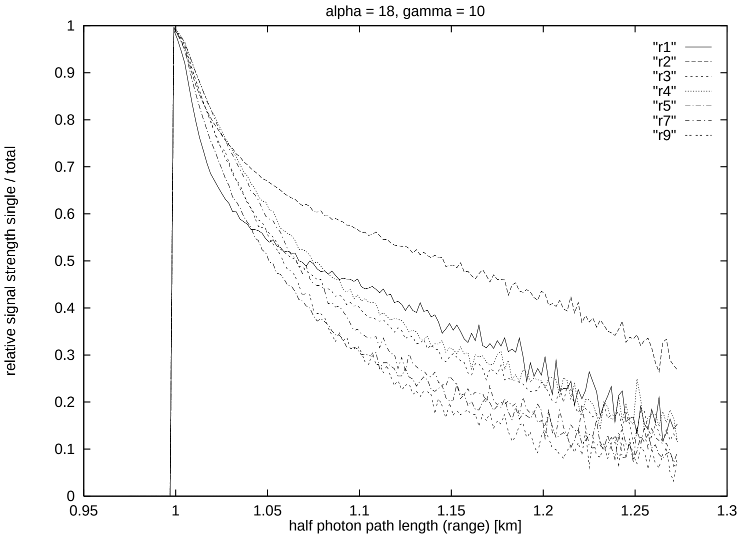

Simulated depolarisation

In the following figures we present the depolarisation ratio $I_\perp/I_{||}$ of the simulated signals. We see, except for mode radius $r_c = 1\mu$, no signifficant differences in the simulated signals. All show a slow rise, and reach a depolarisation ratio of $I_\perp/I_{||} = 0.1$ at a penetration depth of 40m.

Figure 5.34: The depolarisation ratios for $\alpha = 6$ and $\gamma = 1$ (the Deirmendjian C1 cloud is the one labelled by $r4$).

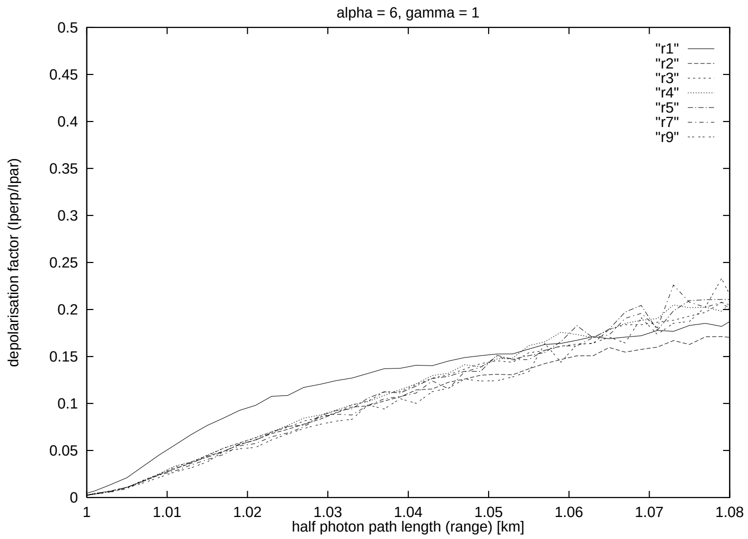

Figure 5.35: The depolarisation ratios for $\alpha = 12$ and $\gamma = 1$.

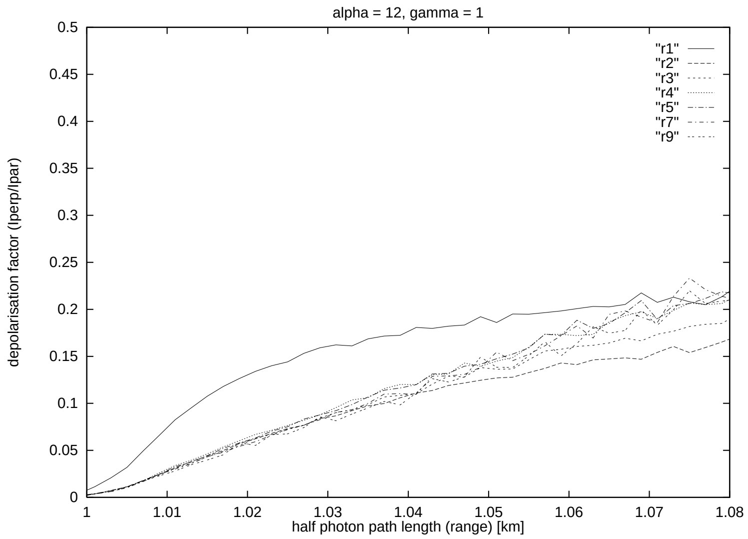

Figure 5.36: The depolarisation ratios for $\alpha = 18$ and $\gamma = 1$.

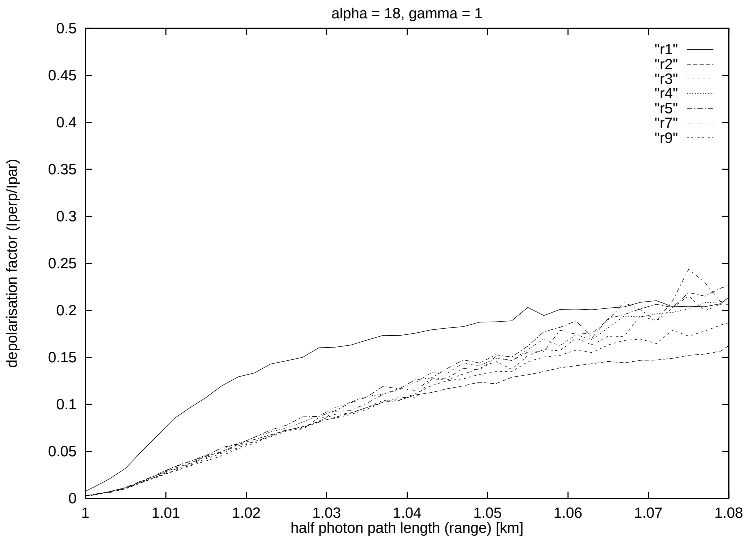

Figure 5.37: The depolarisation ratios for $\alpha = 6$ and $\gamma = 5$.

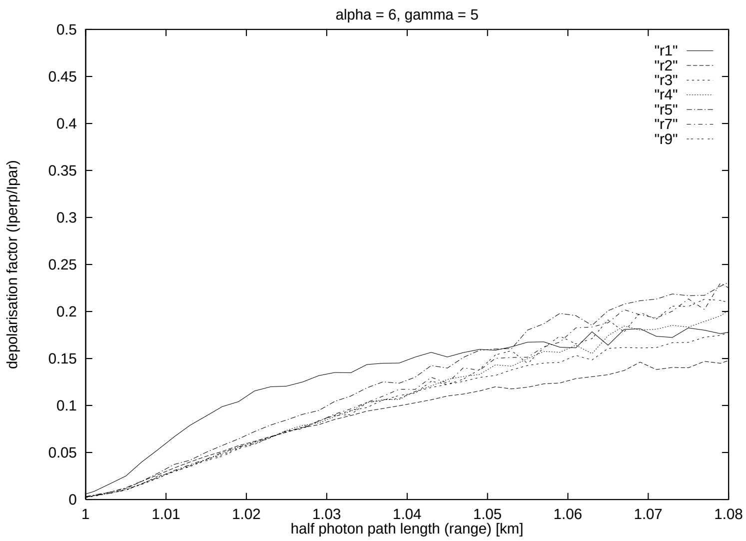

Figure 5.38: The depolarisation ratios for $\alpha = 12$ and $\gamma = 5$.

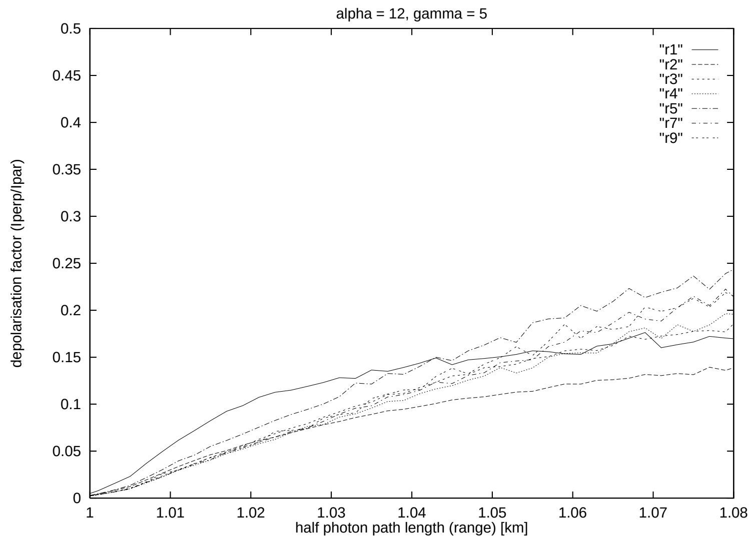

Figure 5.39: The depolarisation ratios for $\alpha = 18$ and $\gamma = 5$.

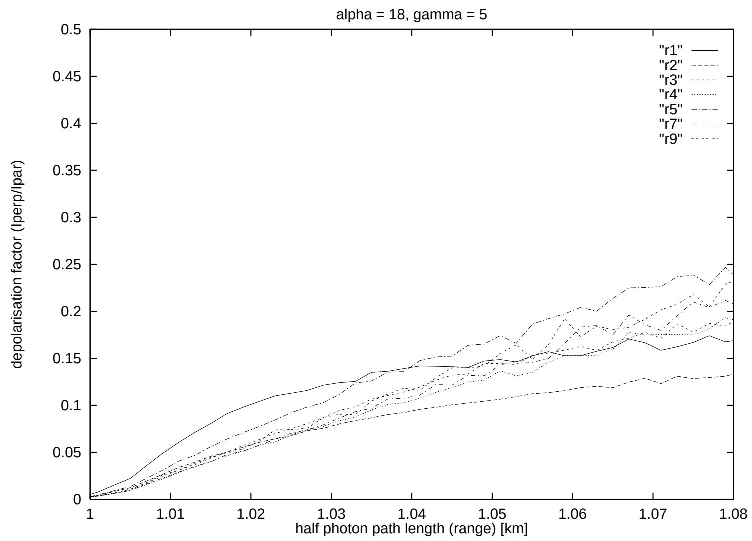

Figure 5.40: The depolarisation ratios for $\alpha = 6$ and $\gamma = 10$.

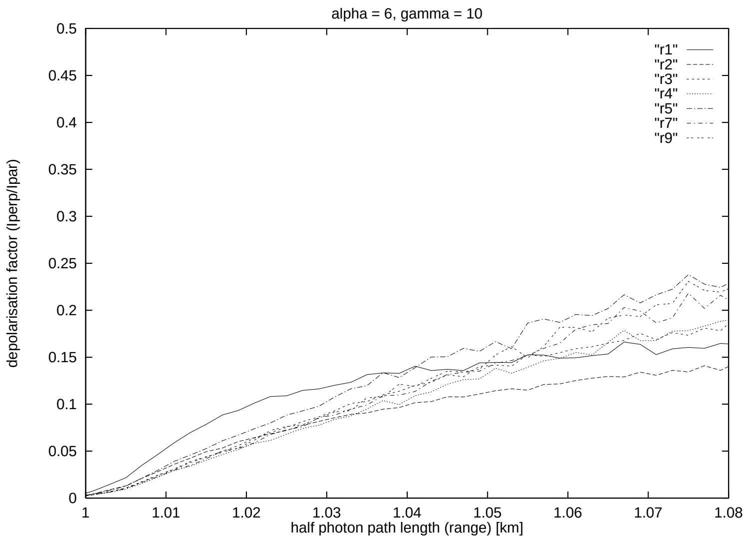

Figure 5.41: The depolarisation ratios for $\alpha = 12$ and $\gamma = 10$.

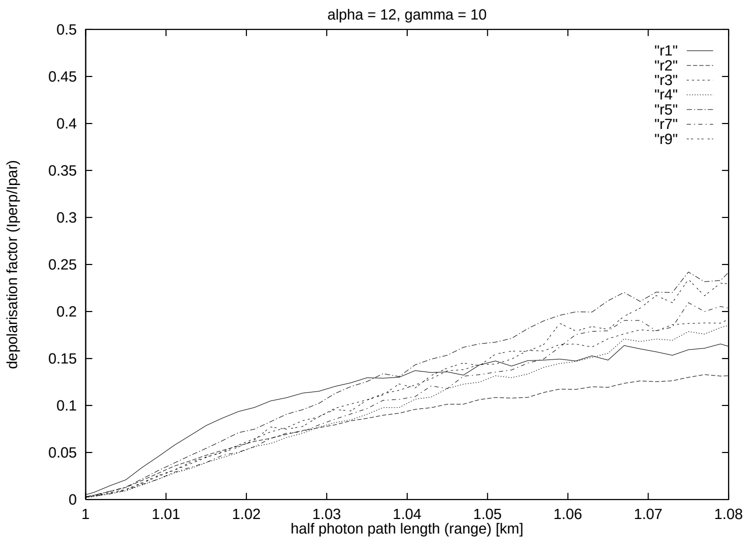

Figure 5.42: The depolarisation ratios for $\alpha = 18$ and $\gamma = 10$.

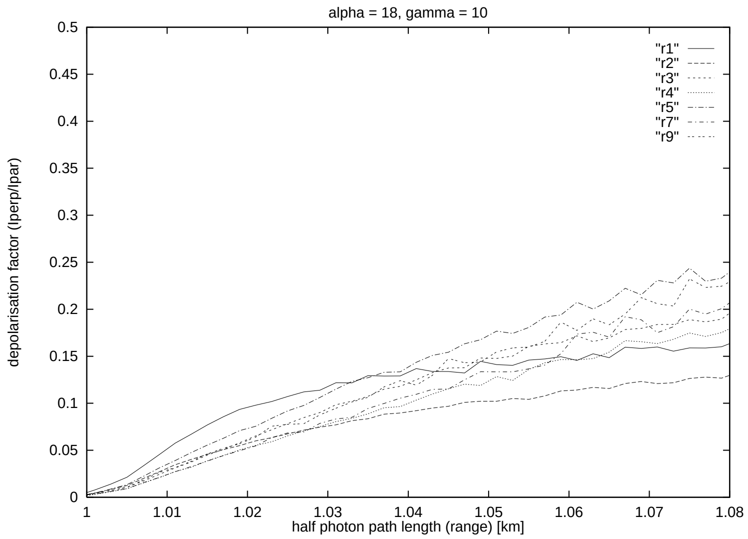

5.2.3 Conclusion

This sensitivity analysis suggests that it is not possible to determine parameters (i.e. mode radius) of the size distribution of a C1 type water cloud by a LIDAR having fixed FOV and fixed wavelength. Using polarization will be of no advantage. A way out of this dilemma might be the use of different wavelength and / or different FOVs. We did not test the influence of wavelength. The (small) separation of the ratios of the single scattered versus total signal (see Figures 5.25 – 5.33) for penetration depths greater than 50m suggests the use of different (especially sidelooking) FOVs for the determination of the above mentioned ratio.

This statement does not effect the use of a LIDAR with fixed wavelength and fixed FOV, especially using polarization information, in the detection wether the cloud consists of ice crystals or water droplets.

The exceptional behavior of mode radius of $r_c = 1\mu$ might be a resonance effect with the wavelength $\lambda = 1.064\mu$.

Chapter 6

Appendix

6.1 Single scattering of polarized light

In this paragraph we summarize some properties of Stokes vectors and show how they transform at a single scattering event with special attention to spherical particles. We derive the polarized phase function from the Mie solution and finally discuss the geometry of the scattering.

6.1.1 The Stokes vector formalism

In meteorological problems Stokes vectors are often used to describe polarized light. For a physical explanation and a detailed discussion see Bohren–Huffman [5], pp 46, and Born–Wolf [8], pp 554. The definition of Stokes vectors is not standardized. We use modified Stokes vectors according to Chandrasekhar [10] and Deirmendjian [12].

Definition 6.1.1 (Stokes vector) Since a LIDAR uses a laser as its light source, we are interested in the Stokes vector of a monochromatic plane wave which is usually described by a time dependent complex valued vector field $E : \mathbb{R}^3 \times \mathbb{R} \to \mathbb{C}^3$ with the direction of propagation $\varphi \in S^2$ and the local and rectangular coordinate system with orthogonal vectors $e_{||} := \rho \in S^2$ with $\rho \perp \varphi$ and $e_\perp := \rho \times \varphi \in S^2$ and the origin at x (see Figure 6.1). As mentioned in the table of symbols, $\times$ is the cross product in $\mathbb{R}^3$, ω the circular frequency and i the imaginary unit. x denotes a position in $\mathbb{R}^3$ (i.e. the position of a scattering particle). We define:

$$E(x,t) \quad := \quad E_0(x)\exp(-i\omega t)$$

Where $E_0(x) := E_{||}(x)e_{||}(x) + E_\perp(x)e_\perp(x)$ is given with the complex fields $E_{||}, E_\perp : \mathbb{R}^3 \to \mathbb{C}$ with respect to the local coordinate vectors $e_{||}, e_\perp : \mathbb{R}^3 \to S^2$. We are able to seperate the time harmonic component. Therfore, we only look at the time independent part $E_0(x)$. For given $e_{||}(x) = \rho$ and $e_\perp(x) \times e_{||}(x) = \varphi$ the vectors $e_\perp(x), e_{||}(x)$ and $e_\perp(x) \times e_{||}(x)$ define a locally orthogonal coordinate system for all $x \in \mathbb{R}^3$. The plane given by φ and ρ is called the reference plane, ρ is called the reference vector (see Figure 6.1).

Figure 6.1: The local coordinate system for the definition of the Stokes vector of a field E with the direction of propagation φ and the reference vector ρ. In the picture the real part of the fields $E_{||}$ and $E_{\perp}$ at position x is shown.

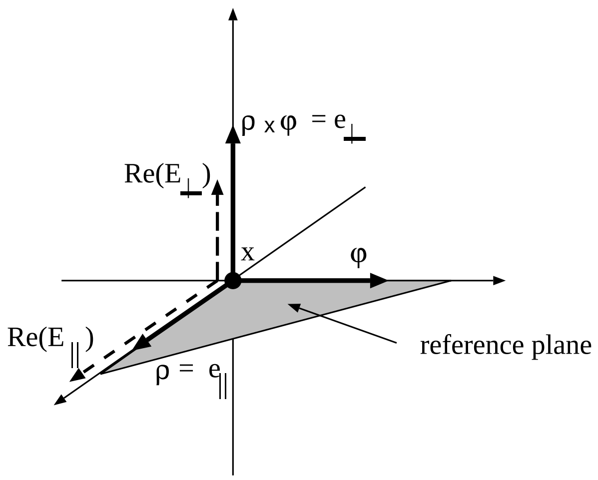

Now, we are able to define the Stokes vector $ST(x)$ at position x as a column vector. * is denoting the complex conjugation.

$$
\begin{aligned}
ST(x) &:= \Big(I_{||}(x), I_{\perp}(x), U(x), V(x)\Big)^T \quad \text{with} \\
I_{||}(x) &:= E_{||}(x)E^*_{||}(x) \\
I_{\perp}(x) &:= E_{\perp}(x)E^*_{\perp}(x) \\
U(x) &:= E_{||}(x)E^*_{\perp}(x) + E_{\perp}(x)E^*_{||}(x) \\
V(x) &:= i\,(E_{||}(x)E^*_{\perp}(x) - E_{\perp}(x)E^*_{||}(x)).
\end{aligned}
$$

The intensity $I(x) := I_{||}(x) + I_{\perp}(x)$ is the sum of the parallelly polarized intensity $I_{||}$ and the perpendicularly polarized intensity $I_{\perp}$ of the light beam.

Another equivalent and widely used definition of the Stokes vector is (cf. Bohren–Huffman [5], van de Hulst [19], and Born–Wolf [8]:

$$\Big(I(x), Q(x), U(x), V(x)\Big)^T \quad \text{with}$$
$$I(x) := I_{||}(x) + I_{\perp}(x) \quad \text{and} \quad Q(x) := I_{||}(x) - I_{\perp}(x).$$

Definition and Remark 6.1.2 (Normed Stokes vector) The normed Stokes vector is defined in the following way:

$$st(x) \;:=\; \begin{cases} \left(i_{||}(x), i_{\perp}(x), u(x), v(x)\right)^T & \text{for } I(x) \neq 0, \\ (0,0,0,0) & \text{for } I(x) = 0, \end{cases}$$

with

$$i_{||}(x) := \tfrac{I_{||}(x)}{I(x)}, \quad i_{\perp}(x) := \tfrac{I_{\perp}(x)}{I(x)}, \quad u(x) := \tfrac{U(x)}{I(x)}, \quad v(x) := \tfrac{V(x)}{I(x)}.$$

For $I(x) \neq 0$ the equality $i_{||}(x) + i_{\perp}(x) = 1$ holds.

Now we are able to define the set of normed Stokes vectors:

$$\begin{aligned} Pol \;:=\; & \{(i_{||}, i_{\perp}, u, v) \in \mathbb{R}^4 \;:\; i_{||}, i_{\perp} \in [0,1],\; u, v \in [-1,1], \\ & i_{||} + i_{\perp} = 1,\; 4\, i_{||} i_{\perp} = u^2 + v^2\} \cup \{(0,0,0,0)\} \end{aligned}$$

The last condition in the definition of *Pol* follows from the property of Stokes vectors for monochromatic light (cf. Bohren–Huffman [5], p 51):

$$(I_{||} + I_{\perp})^2 = (I_{||} - I_{\perp})^2 + U^2 + V^2$$

Evidently, each $st \in Pol$ is a normed Stokes vector.

Definition and Remark 6.1.3 (Rotation of a Stokes vector) $st \in Pol$ is defined with respect to the reference plane (ρ, φ). We are rotating the reference

Figure 6.2: Rotation of the reference plane

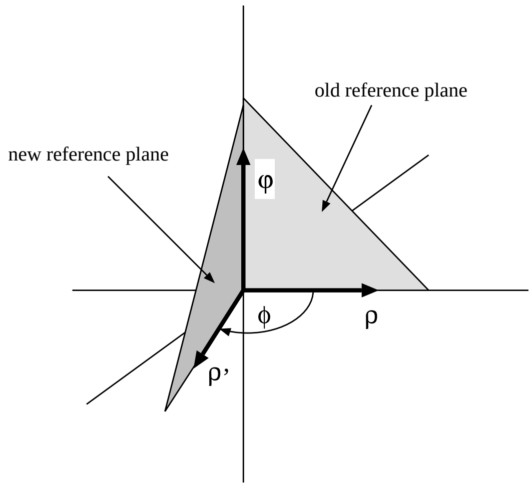

plane (ρ, φ) lefthandedly around φ (anticlockwisely looking into the direction of

φ) with the angle $\phi \in [0, 2\pi]$. The new Stokes vector with the new reference plane (ρ', φ) with $\rho' \in S^2$ and $\rho' \perp \varphi$ is calculated from the initial Stokes vector with following linear transformation (see Chandrasekhar [10], p 35). For the definition of ϕ and ρ' see Figure 6.2 or Definition 6.1.13.

$$
\begin{aligned}
st_{rot} &:= \mathcal{L}(\phi) \cdot st \quad \text{with} \\
\mathcal{L}(\phi) &:= \begin{pmatrix} \cos^2(\phi) & \sin^2(\phi) & \frac{1}{2}\sin(2\phi) & 0 \\ \sin^2(\phi) & \cos^2(\phi) & -\frac{1}{2}\sin(2\phi) & 0 \\ -\sin(2\phi) & \sin(2\phi) & \cos(2\phi) & 0 \\ 0 & 0 & 0 & 1 \end{pmatrix}
\end{aligned}
$$

We see that $\mathcal{L}(\phi) = \mathcal{L}(\phi + \pi)$ holds. This means that a rotation around 180 degrees has no influence on the rotation matrix and the Sokes vectors. Therefore, we only have to determine the angle between the reference planes modulo π. The orientation has to be preserved. Furthermore $st_{rot} \in Pol$ is still holding, the norming $i_{||,rot} + i_{\perp,rot} = 1$ of the Stokes vector is preserved which is obvious since the underlying electromagnetic field is expressed in another local coordinate system and no physical process changing the intensity I takes place.

The mapping $\mathcal{L} : [0, 2\pi] \times Pol \to Pol$ is $\mathfrak{B}([0, 2\pi] \times Pol)$–$\mathfrak{B}(Pol)$ measurable and bounded.

Definition and Remark 6.1.4 (Scattering of a Stokes vector) The scattering of polarized light is described by a linear transformation $\mathcal{M}(x, \theta, \phi)$ of the Stokes vector at position $x \in \mathbb{R}^3$ with the angles $\theta \in [0, \pi]$ and $\phi \in [0, 2\pi]$ (see van de Hulst [19], Chapter 5). Often $\mathcal{M}$ is called *Mueller matrix*.

$$
\begin{aligned}
ST' &:= \mathcal{M}(x, \theta, \phi) \cdot st_{rot} \quad \text{with} \\
\mathcal{M}(x, \theta, \phi) &:= \begin{pmatrix} m_{11}(x,\theta,\phi) & m_{12}(x,\theta,\phi) & m_{13}(x,\theta,\phi) & m_{14}(x,\theta,\phi) \\ m_{21}(x,\theta,\phi) & m_{22}(x,\theta,\phi) & m_{23}(x,\theta,\phi) & m_{24}(x,\theta,\phi) \\ m_{31}(x,\theta,\phi) & m_{32}(x,\theta,\phi) & m_{33}(x,\theta,\phi) & m_{34}(x,\theta,\phi) \\ m_{41}(x,\theta,\phi) & m_{42}(x,\theta,\phi) & m_{43}(x,\theta,\phi) & m_{44}(x,\theta,\phi) \end{pmatrix}
\end{aligned}
$$

The angle θ is the elevation angle, i.e. the angle between direction before and after the scattering. ϕ is the azimuthal angle, i.e. the angle between the reference plane before and after the scattering (see Figure 6.3 or Definition 6.1.13). The Stokes vector ST' is still given with respect to the same reference plane as $st_{rot} \in Pol$.

The scattering now reads:

$$ST' := \mathcal{M}(x, \theta, \phi) \cdot \mathcal{L}(\phi) \cdot st.$$

In general, ST' is not normed any longer.

Figure 6.3: The geometry for polarized scattering with the incident direction φ and the reference vector ρ before scattering and the new direction φ' and the new reference vector ρ' after the scattering.

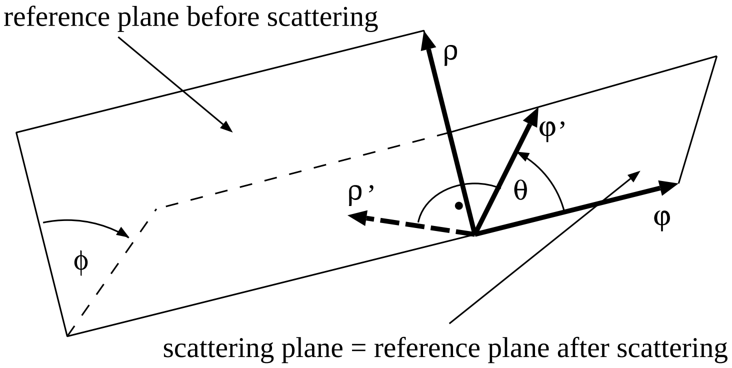

Definition and Remark 6.1.5 (Norming after the scattering) To iterate the single scattering process as in the stochastic model we have to normalize ST'. Then we get the normalized scattered Stokes vector st':

$$st' \;:=\; \mathcal{N}(x,\theta,\phi,st)\cdot ST' = \mathcal{N}(x,\theta,\phi,st)\cdot \mathcal{M}(x,\theta)\cdot \mathcal{L}(\phi)\cdot st$$

with $\mathcal{N} : \mathrm{I\!R}^3 \times [0,\pi] \times [0,2\pi] \times Pol \to \mathrm{I\!R}_0^+$ and

$$\mathcal{N}(x,\theta,\phi,st) \;:=\; \begin{cases} \dfrac{1}{I'(x,\theta,\phi,st)} & \text{for } I'(x,\theta,\phi,st) \neq 0, \\ 0 & \text{for } I'(x,\theta,\phi,st) = 0. \end{cases}$$

$I'(x,\theta,\phi,st)$ is the intensity of the scattered Stokes vector. The multiplication of the Stokes vector with a scalar has to be performed for each component. This multiplication with the inverse intensity does make physical sense, since *all* components of the Stokes vector are intensities or differencies of intensities (see Bohren–Huffman [5], p 46). Obviously, st' is in *Pol*.

The complete scattering as performed in the stochastic model now reads:

$$st' \;:=\; \mathcal{N}(x,\theta,\phi,st)\cdot \mathcal{M}(x,\theta,\phi)\cdot \mathcal{L}(\phi)\cdot st.$$

6.1.2 Scattering at spherical particles

In this paragraph we discuss scattering of a Stokes vector assuming the scattering particles are spherical (sometimes called Mie particles cf. Bohren [6]). With the results of this Paragraph we derive in Paragraph 6.1.3 a polarized phase function. This procedure is an outline of the derivation of a polarized phase functions for arbitrary Mueller matrices, too.

Definition and Remark 6.1.6 (Scattering at a spherical particle) The shape of $\mathcal{M}$ and the numerical values of the matrix elements may be derived from Mie theory (see Remark 6.1.12). The Mueller matrix reduces to the following form:

$$\mathcal{M}(x,\theta) \;:=\; \begin{pmatrix} m_{11}(x,\theta) & 0 & 0 & 0 \\ 0 & m_{22}(x,\theta) & 0 & 0 \\ 0 & 0 & m_{33}(x,\theta) & -m_{43}(x,\theta) \\ 0 & 0 & m_{43}(x,\theta) & m_{33}(x,\theta) \end{pmatrix}$$

$\mathcal{M}(x,\theta)$ is independent of ϕ and stisfies the following norming condition (see Deirmendjian [12], p 73):

$$\int_0^{2\pi}\int_0^{\pi} \frac{1}{2}(m_{11}(x,\theta)+m_{22}(x,\theta))\ \sin(\theta)\ d\theta\ d\phi \;=\; 4\pi,$$

and therefore

$$\int_0^{\pi} \frac{1}{2}(m_{11}(x,\theta)+m_{22}(x,\theta))\ \sin(\theta)\ d\theta = 2.$$

Now, we can write down the scattering of a Stokes vector according to Definition 6.1.4:

$$\begin{aligned} ST' \;&:=\; \mathcal{M}(x,\theta)\cdot\mathcal{L}(\phi)\cdot st \\ &= \begin{pmatrix} m_{11}(x,\theta)\cos^2(\phi) & m_{11}(x,\theta)\sin^2(\phi) & \frac{1}{2}m_{11}(x,\theta)\sin(2\phi) & 0 \\ m_{22}(x,\theta)\sin^2(\phi) & m_{22}(x,\theta)\cos^2(\phi) & -\frac{1}{2}m_{22}(x,\theta)\sin(2\phi) & 0 \\ -m_{33}(x,\theta)\sin(2\phi) & m_{33}(x,\theta)\sin(2\phi) & m_{33}(x,\theta)\cos(2\phi) & m_{43}(x,\theta) \\ m_{43}(x,\theta)\sin(2\phi) & -m_{43}(x,\theta)\sin(2\phi) & -m_{43}(x,\theta)\cos(2\phi) & m_{33}(x,\theta) \end{pmatrix}\cdot st \end{aligned}$$

Remark 6.1.7 (Intensity after the scattering) According to Definition 6.1.1 the intensity after the scattering is given by

$$I'(x,\theta,\phi,st) \;=\; (I'_{\|}+I'_{\perp})(x,\theta,\phi,st),$$

where $I'_{\|}$ and $I'_{\perp}$ are the components of the scattered Stokes vector $ST' = (I'_{\|}, I'_{\perp}, U', V')^T = \mathcal{M}(x,\theta)\cdot\mathcal{L}(\phi)\cdot st$ (see 6.1.6). For given x,φ,ρ,φ', incident normed Stokes vector $st=(i_{\|},i_{\perp},u,v)^T$, and for $\theta=\theta(\varphi,\varphi')$, $\phi=\phi(\varphi,\rho,\varphi')$ according to definition 6.1.13 (see also Figure 6.3) we get:

$$\begin{aligned} &I'(x,\theta,\phi,st) = \\ &= \; i_{\|}\,m_{11}(x,\theta)\cos^2(\phi) + i_{\perp}\,m_{11}(x,\theta)\sin^2(\phi) + u\,\tfrac{1}{2}\,m_{11}(x,\theta)\sin(2\phi)\ + \\ &\quad\ +i_{\|}\,m_{22}(x,\theta)\sin^2(\phi) + i_{\perp}\,m_{22}(x,\theta)\cos^2(\phi) - u\,\tfrac{1}{2}\,m_{22}(x,\theta)\sin(2\phi) \end{aligned}$$

$$= \mathcal{m}_{11}(x,\theta)\Big(i_{||}\cos^2(\phi) + i_\perp \sin^2(\phi)\Big) + \mathcal{m}_{22}(x,\theta)\Big(i_{||}\sin^2(\phi) + i_\perp \cos^2(\phi)\Big) + \\ +\Big(\mathcal{m}_{11}(x,\theta) - \mathcal{m}_{22}(x,\theta)\Big)u\,\tfrac{1}{2}\,\sin(2\phi).$$

Norming of the incoming Stokes vector, $i_{||} + i_\perp = 1$, we get:

$$I'(x,\theta,\phi,st) =$$

$$= \mathcal{m}_{11}(x,\theta)[\ \sin^2(\phi) + i_{||}(\cos^2(\phi) - \sin^2(\phi))\ ] + \mathcal{m}_{22}(x,\theta)[\ \cos^2(\phi) + \\ + i_{||}(\sin^2(\phi) - \cos^2(\phi))\ ] + (\mathcal{m}_{11}(x,\theta) - \mathcal{m}_{22}(x,\theta))u\tfrac{1}{2}\sin(2\phi).$$

With $\cos(2\phi) = \cos^2(\phi) - \sin^2(\phi)$ we get:

$$I'(x,\theta,\phi,st) =$$

$$= \mathcal{m}_{11}(x,\theta)(\ \sin^2(\phi) + i_{||}\cos(2\phi)\ ) + \mathcal{m}_{22}(x,\theta)(\ \cos^2(\phi) - i_{||}\cos(2\phi)\ ) + \\ +(\mathcal{m}_{11}(x,\theta) - \mathcal{m}_{22}(x,\theta))u\,\tfrac{1}{2}\sin(2\phi),$$

and with $\cos^2(\phi) = \frac{1}{2}(1 + \cos(2\phi))$ and $\sin^2(\phi) = \frac{1}{2}(1 - \cos(2\phi))$ we get:

$$I'(x,\theta,\phi,st) =$$

$$\begin{aligned} &= \mathcal{m}_{11}(x,\theta)(\ \tfrac{1}{2} - \tfrac{1}{2}\cos(2\phi) + i_{||}\cos(2\phi)\ ) + \\ &\quad + \mathcal{m}_{22}(x,\theta)(\ \tfrac{1}{2} + \tfrac{1}{2}\cos(2\phi) - i_{||}\cos(2\phi)\ ) + \\ &\quad + (\mathcal{m}_{11}(x,\theta) - \mathcal{m}_{22}(x,\theta))u\tfrac{1}{2}\sin(2\phi) \\ &= \tfrac{1}{2}(\mathcal{m}_{11}(x,\theta) + \mathcal{m}_{22}(x,\theta)) - \tfrac{1}{2}(\mathcal{m}_{11}(x,\theta) - \mathcal{m}_{22}(x,\theta))\cos(2\phi) + \\ &\quad + (\mathcal{m}_{11}(x,\theta) - \mathcal{m}_{22}(x,\theta))i_{||}\cos(2\phi) + (\mathcal{m}_{11}(x,\theta) - \mathcal{m}_{22}(x,\theta))u\tfrac{1}{2}\sin(2\phi) \\ &= \tfrac{1}{2}(\mathcal{m}_{11}(x,\theta) + \mathcal{m}_{22}(x,\theta)) + \tfrac{1}{2}(\mathcal{m}_{11}(x,\theta) - \mathcal{m}_{22}(x,\theta))\ \Big(\ (2i_{||} - 1)\cos(2\phi) + u\sin(2\phi)\ \Big). \end{aligned}$$

From the norming condition of the Mueller matrix $\mathcal{M}$ (see Remark 6.1.6) we finally get:

$$\int_0^{2\pi}\!\!\int_0^{\pi} I'(x,\theta,\phi,st)\ \sin(\theta)\,d\theta\,d\phi =$$

$$\begin{aligned} &= \int_0^{2\pi}\!\!\int_0^{\pi} \tfrac{1}{2}(\mathcal{m}_{11}(x,\theta) + \mathcal{m}_{22}(x,\theta))\ \sin(\theta)\,d\theta\,d\phi + \\ &\quad + \int_0^{2\pi}\!\!\int_0^{\pi} \Big(\tfrac{1}{2}(\mathcal{m}_{11}(x,\theta) - \mathcal{m}_{22}(x,\theta))\,((2i_{||} - 1)\cos(2\phi) + u\sin(2\phi))\ \Big)\ \sin(\theta)\,d\theta\,d\phi \\ &= 4\pi. \end{aligned}$$

6.1.3 The polarized phase function for spherical particles

With the intensity after the scattering (see Remark 6.1.7) we define the polarized phase function for spherical particles and discuss some of its properties.

Definition and Remark 6.1.8 (Polarized phase function)
For iterating the scattering we need the phase function for the determination of the scattering distribution (see Remark 2.3.4).

The phase function is calculated in the far field from the intensity after the scattering at the point $x \in \mathbb{R}^3$ (cf. Krichbaumer [27] p 197). We define the polarized phase function:

$$\begin{aligned} ph_{pol} &: \mathbb{R}^3 \times [0,\pi] \times [0,2\pi] \times Pol \to \mathbb{R}_0^+ \quad \text{with} \\ ph_{pol}(x,\theta,\phi,st) &:= \frac{1}{4\pi} I'(x,\theta,\phi,st) = \\ &= \frac{1}{4\pi} \Big[\tfrac{1}{2}(m_{11}(x,\theta) + m_{22}(x,\theta)) + \\ &\quad + \tfrac{1}{2}(m_{11}(x,\theta) - m_{22}(x,\theta)) \Big((2i_{\|} - 1)\cos(2\phi) + u\sin(2\phi) \Big) \Big] \end{aligned}$$

The phase function ph_{pol} is $\mathfrak{B}(\mathbb{R}^3 \times [0,\pi] \times [0,2\pi] \times Pol) - \mathfrak{B}(\mathbb{R}_0^+)$ measurable and bounded since m_{11} and m_{22} are $\mathfrak{B}(\mathbb{R}^3 \times [0,\pi])$–$\mathfrak{B}(\mathbb{R}_0^+)$ measurable and bounded (see Remark 6.1.12).

The proof of the following Lemma is left to the reader (use Definition 6.1.3 and Remark 6.1.6).

Lemma 6.1.9 If the following conditions are satisfied (i.e. for spherical particles, see Remark 6.1.12)

1. $m_{11}, m_{22}, m_{33}, m_{43}$ are $\mathfrak{B}(\mathbb{R}^3 \times [0,\pi])$–$\mathfrak{B}(\mathbb{R})$ measurable and bounded,
2. for $x \in \mathbb{R}^3$ and $\theta \in [0,\pi]$, $m_{11}(x,\theta) \geq 0$ and $m_{22}(x,\theta) \geq 0$,

then $\mathcal{N} \cdot \mathcal{M} \cdot \mathcal{L}$ is $\mathfrak{B}(\mathbb{R}^3 \times [0,\pi] \times [0,2\pi] \times Pol)$–$\mathfrak{B}(Pol)$ measurable.

Definition and Remark 6.1.10 (Factorization of ph_{pol}) With the marginal density ph_1 and the conditional density ph_2 we are able to factorize ph_{pol} in the following way:

$$ph_{pol}(x,\theta,\phi,st) = ph_1(x,\theta) \cdot ph_2(x,\phi,st \mid \theta),$$

with

$$ph_1(x,\theta) \;:=\; \int_0^{2\pi} ph_{pol}(x,\theta,\phi,st)\,d\phi = \frac{1}{4}\Big(m_{11}(x,\theta) + m_{22}(x,\theta)\Big),$$

and

$$ph_2(x,\phi,st \mid \theta) \;:=\; \begin{cases} \dfrac{ph_{pol}(x,\theta,\phi,st)}{ph_1(\theta)} & \text{for } ph_1(x,\theta) \neq 0, \\ 0 & \text{for } ph_1(x,\theta) = 0. \end{cases}$$

Especially for $ph_1(x,\theta) \neq 0$ we get

$$ph_2(\phi, st \mid \theta) = \\ = \frac{1}{2\pi} + \frac{1}{2\pi}\,\frac{m_{11}(x,\theta) - m_{22}(x,\theta)}{m_{11}(x,\theta) + m_{22}(x,\theta)}\Big(\,(2i_{\|} - 1)\cos(2\phi) + u\sin(2\phi)\,\Big).$$

For unpolarized scattering we use the well–known unpolarized phase function $ph_{unpol}(x,\theta) = ph_1(x,\theta)/(2\pi)$ which is independent of ϕ. We see that the deviation of ph_{pol} from ph_{unpol} is proportional to $(m_{11}(\theta) - m_{22}(\theta))\,/\,(m_{11}(\theta) + m_{22}(\theta))$. Figure 6.4 shows that this deviation is significant.

Figure 6.4: $(m_{11}(x,\theta) - m_{22}(x,\theta))\,/\,(m_{11}(x,\theta) + m_{22}(x,\theta))$ of a C1–cloud.

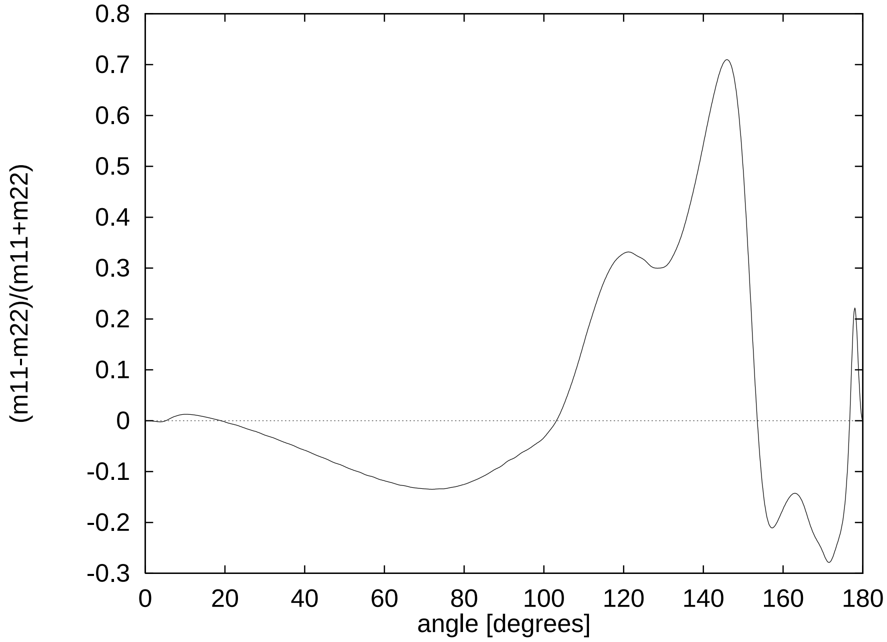

Remark 6.1.11 (Estimation of the maximum of ph_2) Let be $x \in \mathbb{R}^3$, $st \in Pol$, and $\theta \in [0,\pi]$. For the simulation algorithm, especially for the scattering splitting, we need the maximum $\max_{\phi\in[0,2\pi]}\Big(ph_2(x,\phi,st \mid \theta)\Big)$ of ph_2.

According to Remark 6.1.12 we get $m_{11}(x,\theta) \geq 0$, $m_{22}(x,\theta) \geq 0$ and therfore

$$-1 \leq \frac{m_{11}(x,\theta) - m_{22}(x,\theta)}{m_{11}(x,\theta) + m_{22}(x,\theta)} \leq 1.$$

Furthermore with the definition of the normed Stokes vector (see Definition 6.1.2) we get

$$0 \leq i_{||} \leq 1 \quad \text{and} \quad -1 \leq u \leq 1.$$

Now we are able to give an estimate of a bound from above for ph_2 for arbitrary x, st and θ.

$$\begin{aligned} ph_2(x,\phi,st \mid \theta) &= \frac{1}{2\pi} + \frac{1}{2\pi}\,\frac{m_{11}(x,\theta) - m_{22}(x,\theta)}{m_{11}(x,\theta) + m_{22}(x,\theta)}\Big(\,(2i_{||}-1)\cos(2\phi) + u\sin(2\phi)\,\Big) \\ &\leq \frac{1}{2\pi} + \frac{1}{2\pi}\left|\frac{m_{11}(x,\theta) - m_{22}(x,\theta)}{m_{11}(x,\theta) + m_{22}(x,\theta)}\right|\Big(\,|2i_{||}-1|\,|\cos(2\phi)| + |u|\,|\sin(2\phi)|\,\Big) \\ &\leq \frac{3}{2\pi}\,. \end{aligned}$$

Hence we get:

$$\max_{\phi\in[0,2\pi]}\Big(ph_2(x,\phi,st \mid \theta)\Big) \;\leq\; \frac{3}{2\pi}.$$

6.1.4 A short digression on Mie theory

Mie theory gives the exact solution for the scattering of a plane wave at a spherical dielectricum (see Mie [34]). A more recent discussion is given in Liou [31]. The solution is given as a series expansion in spherical harmonics with coefficients given in terms of spherical Bessel functions.

The Mueller matrix $\mathcal{M}$ is derived from the far field solution. A derivation is given in Deirmendjian [12], p 69. The extension to polydispersions is given in Deirmendjian [12], pp 72, too.

Remark 6.1.12 (Properties of the Mueller matrix) We summarize some properties of the Mueller matrix for spherical particles.

- The structure

$$\mathcal{M}(x,\theta) \;:=\; \begin{pmatrix} m_{11}(x,\theta) & 0 & 0 & 0 \\ 0 & m_{22}(x,\theta) & 0 & 0 \\ 0 & 0 & m_{33}(x,\theta) & -m_{43}(x,\theta) \\ 0 & 0 & m_{43}(x,\theta) & m_{33}(x,\theta) \end{pmatrix},$$

- and the properties

$$m_{11}, m_{22} \in \mathbb{R}_0^+,$$
$$m_{33}, m_{43} \in \mathbb{R},$$

  and

$$m_{11}(x,\theta) - m_{22}(x,\theta) = 0 \quad \text{for } x \in \mathbb{R}^3 \text{ and } \theta \in \{0,\pi\}$$

  may be derived from Mie theory (see Deirmendjian [12] p 68).

- The $\mathfrak{B}(\mathbb{R}^3 \times [0,\pi])$–$\mathfrak{B}(\mathbb{R}_0^+)$ measurability and the $\mathfrak{B}(\mathbb{R}^3 \times [0,\pi])$–$\mathfrak{B}(\mathbb{R})$ measurability of the m_{ij}, respectively, is clear from physical reasons.

- For the reason of energy conservation the m_{ij} are bounded.

These properties should as well apply to nonspherical particles i.e. ice crystals even though with another shape of the Mueller matrix $\mathcal{M}$.

The numerically stable evaluation of the Mie series expansion is not trivial (see Deirmendjian [12], pp 14). For our calculations we relied on the Fortran code of W. J. Wiscombe [47] (and references within). The code is available via the internet by anonymous ftp from `climate.gsfc.nasa.gov` in the directory `pub/wiscombe/Mie_Code`. This code was rewritten for `DOUBLE PRECISION`. The extension for a polydisperse system was implemented according to Deirmendjian [12].

6.1.5 The geometry of scattering

During the simulation of the stochastic process we have to determine the new reference plane after the scattering. Therefore, we calculate the new reference vector $\rho' \in S^2$ with $\rho' \perp \varphi'$ from the given incoming direction of propagation φ, the incoming reference vector ρ with $\rho \perp \varphi$, and the new direction of propagation φ'.

In the following we will denote both the functions and the variables (angles) with θ and ϕ.

Definition 6.1.13 (Angles) We define:

$$\begin{aligned} \theta : S^2 \times S^2 &\to [0,\pi] \quad \text{with} \\ \theta(\varphi,\varphi') &:= \arccos\Big(\langle\varphi,\varphi'\rangle\Big). \end{aligned}$$

$\theta(\cdot)$ gives us the angle between the incoming direction of propagation φ and the direction of propagation after the scattering φ' (see Figure 6.3).

Now, we define:

$$\phi : S^2 \times S^2 \times S^2 \quad \to \quad [0, 2\pi[\quad \text{with}$$

$$\phi(\varphi, \rho, \varphi') \quad := \quad \begin{cases} \arccos\left(\langle \varphi \times \rho, \frac{\varphi \times \varphi'}{\|\varphi \times \varphi'\|} \rangle\right) & \text{for } \langle \varphi, \varphi' \rangle \neq 0,\ \varphi \perp \rho \\ & \text{and } \|\rho - \frac{\varphi \times \varphi'}{\|\varphi \times \varphi'\|}\| < \sqrt{2}, \\ \pi + \arccos\left(\langle \varphi \times \rho, \frac{\varphi \times \varphi'}{\|\varphi \times \varphi'\|} \rangle\right) & \text{for } \langle \varphi, \varphi' \rangle \neq 0,\ \varphi \perp \rho \\ & \text{and } \|\rho - \frac{\varphi \times \varphi'}{\|\varphi \times \varphi'\|}\| \geq \sqrt{2}, \\ 0 & \text{otherwise.} \end{cases}$$

$\phi(\cdot)$ gives us the angle between the reference plane before the scattering derived from φ and ρ and the scattering plane (= reference plane after the scattering) derived from φ and φ', or ρ' and φ', respectively (see Figure 6.3).

Definition and Remark 6.1.14 (Rotation in $\mathbb{R}^3$) A rotation $O_{\vec{u}}(\beta)$ of a vector $\vec{v} \in \mathbb{R}^3$ righthandedly around the rotation axis $\vec{u} \in S^2$ is defined the following way:

$$O_{\vec{u}}(\beta) \cdot \vec{v} \quad := \quad \vec{v} \cos\beta \; - \; \vec{u} \times \vec{v} \sin\beta \; + \; (1 - \cos\beta) \langle \vec{u}, \vec{v} \rangle \, \vec{u}$$

Each element of the $SO(3)$ may be represented that way (for a proof see Scheck [44] p 76.)

Definition and Remark 6.1.15 (Rotation of φ and ρ) To make things clearer, we look at the sequence of rotations needed for the transformation of φ and ρ into φ' and ρ' for given θ and ϕ (see Figure 6.3).

- At first we rotate the direction of propagation φ and the reference vector ρ with angle θ around the rotation axis $\varphi \times \rho$ (see Figure 6.5):

$$\tilde{\varphi} \quad := \quad O_{\varphi \times \rho}(\theta) \cdot \varphi \quad \text{and}$$
$$\tilde{\rho} \quad := \quad O_{\varphi \times \rho}(\theta) \cdot \rho.$$

- Then we rotate $\tilde{\varphi}$ and $\tilde{\rho}$ with angle $-\phi$ around the direction of propagation φ (see Figure 6.6):

$$\varphi' \quad := \quad O_{\varphi}(-\phi) \cdot \tilde{\varphi} \quad \text{and}$$
$$\rho' \quad := \quad O_{\varphi}(-\phi) \cdot \tilde{\rho}.$$

Figure 6.5: The rotation of the vectors φ and ρ with θ around $\varphi \times \rho$.

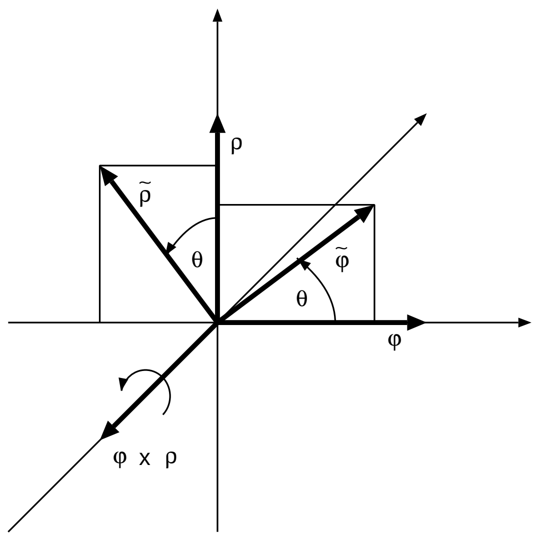

Figure 6.6: The rotation of the vectors $\tilde{\varphi}$ and $\tilde{\rho}$ with ϕ around φ

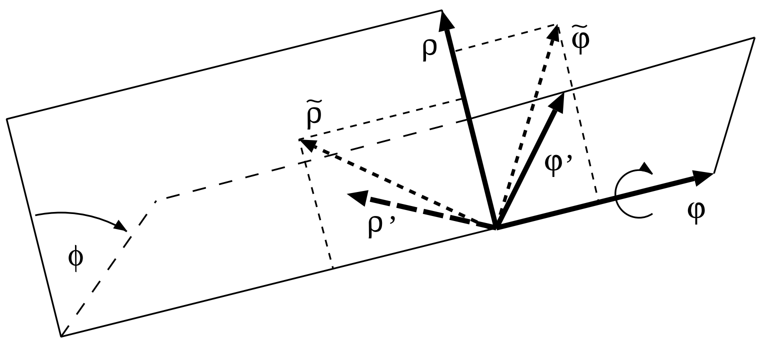

Now, we are able to define two rotations in $\mathbb{R}^3$:

$$\begin{aligned}
Rot'_1, Rot'_2 \quad &: \quad S^2 \times S^2 \times [0,\pi] \times [0, 2\pi] \to SO(3) \quad \text{with} \\
Rot'_1(\varphi, \rho, \theta, \phi) \quad &:= \quad O_{\varphi\times\rho}(\theta) \cdot O_{\varphi}(-\phi) \\
Rot'_2(\varphi, \rho, \theta, \phi) \quad &:= \quad O_{\varphi\times\rho}(\theta) \cdot O_{\varphi}(-\phi).
\end{aligned}$$

According to the construction we get (see Figure 6.3):

$$\begin{aligned}
\varphi' \quad &= \quad Rot'_1(\varphi, \rho, \theta, \phi) \cdot \varphi \quad \text{and} \\
\rho' \quad &= \quad Rot'_2(\varphi, \rho, \theta, \phi) \cdot \rho.
\end{aligned}$$

With the mappings $\theta(\cdot)$ and $\phi(\cdot)$ (see Definition 6.1.13) we define the following rotation in $\mathbb{R}^3$:

$$\begin{aligned} Rot_2 \quad &: \quad S^2 \times S^2 \times S^2 \to SO(3) \quad \text{with} \\ Rot_2(\varphi, \rho, \varphi') \quad &:= \quad Rot_2'(\varphi, \rho, \theta(\varphi, \varphi'), \phi(\varphi, \rho, \varphi')). \end{aligned}$$

According to the construction Rot_1' and Rot_2' are $\mathfrak{B}(S^2 \times S^2 \times [0, \pi] \times [0, 2\pi] \times S^2)$–$\mathfrak{B}(S^2)$ measurable. With the definition of $\theta(\cdot)$ and $\phi(\cdot)$ the mapping Rot_2 is $\mathfrak{B}(S^2 \times S^2 \times S^2 \times S^2)$–$\mathfrak{B}(S^2)$ measurable.

6.4 Proofs of Section 2.2

Proof of Lemma 2.2.2:

Proof:

To 1: The assertion follows at once since FOV_R is an open set in S^2 and $\mathcal{C}_x = f(x,\cdot)^{-1}([0,r_R[)$ for all $x \in \mathcal{H}^+ \cup \mathcal{H}^-$ where

$$f : \mathcal{H}^+ \cup \mathcal{H}^- \times S_R^2 \to \mathbb{R}_0^+ \quad \text{with} \quad f(x,\varphi) := \left\| x + \frac{-\langle x, \vec{n}_R\rangle}{\langle \varphi, \vec{n}_R\rangle}\varphi \right\|$$

is continuous.

To 2: We use the mapping f from above and define

$$g : \mathbb{R}^3 \times S^2 \times \mathbb{R}_0^+ \to \mathbb{R} \quad \text{with} \quad g(x,\varphi,t) := \langle x + ct\varphi, \vec{n}_R\rangle.$$

The set $\mathcal{R}$ may be represented the following way:

$$\mathcal{R} \;=\; \bigcup_{(x,\varphi)\in\mathcal{R}'} \{(x,\varphi)\} \times g(x,\varphi,\cdot)^{-1}(\mathbb{R}^+)$$

where (cf. item 1)

$$\begin{aligned}
\mathcal{R}' &:= \{(x,\varphi) \in \mathbb{R}^3 \times S^2 : x \in \mathcal{H}^- \text{ and } \varphi \in \mathcal{C}_x \cap FOV_R\} \\
&= \bigcup_{x\in\mathcal{H}^-} \{x\} \times \Big(f(x,\cdot)^{-1}([0,r_R[) \cap FOV_R\Big) \\
&= \Big(\bigcup_{x\in\mathcal{H}^-} \{x\} \times f(x,\cdot)^{-1}([0,r_R[)\Big) \;\cap\; pr_\varphi^{-1}(FOV_R)
\end{aligned}$$

and $pr_\varphi : \mathbb{R}^3 \times S^2 \to S^2$ is the canonical projection on the second coordinate. Since f and g are continuous and since FOV_R is an open set, from Lemma 6.2.1 we get that $\mathcal{R}'$ and $\mathcal{R}$ are open sets.

To 3: This follows from 2 and Remark 2.1.3, since we get for $n \in \mathbb{N}_0$:

$$\begin{aligned}
\{N = n\} &= (X_{(n)}, \Phi_n, T_{n+1})^{-1}(\mathcal{R}) \quad \cap \\
&\quad \bigcap_{i=0}^{n-1} (X_{(i)}, \Phi_i, T_{i+1})^{-1}\Big((\mathbb{R}^3 \times S^2 \times \mathbb{R}_0^+) \setminus \mathcal{R}\Big) \quad \in \quad \mathfrak{P}_{2n+1}, \\
\{N = \infty\} &= \Omega \setminus \bigcup_{i\in\mathbb{N}_0} \{N = i\} \quad \in \quad \sigma\Big(\bigcup_{i\in\mathbb{N}_0} \mathfrak{P}_{2i+1}\Big).
\end{aligned}$$

To 4: This is a consequence of 3 and Remark 2.1.3. ■

6.5 Proofs of Section 2.3

Proof of lemma 2.3.3:

Proof:

To 1: See Oppel et al. [38], p 22 and p 40.

To 2: Follows from Remark 2.3.1.

To 3: Holds, since for all $(x,\varphi) \in \mathbb{R}^3 \times S^2$

$$e'_{x,\varphi} : \left(\mathbb{R}_0^+, \mathfrak{B}(\mathbb{R}_0^+)\right) \to [0,1], \quad \text{with} \quad t \mapsto \exp\left(-\int_0^t c\,\sigma(x + cs\varphi)\,ds\right)$$

is a well defined, nonnegative and Borel measurable mapping.

To 4: Follows from the generalized Theorem of Fubini (cf. Ash [1], Theorem 2.6.4 (a)), since $e'_{x,\varphi}$ is nonnegative for all $(x,\varphi) \in \mathbb{R}^3 \times S^2$ and the Lebesgue measure does not depend on x or φ (i.e. the condition of the uniform σ–finiteness of this version of the theorem of Fubini is fullfiled).

To 5: It is sufficient to show the assertion for $(x,\varphi) \in \mathbb{R}^3 \times S^2$: $E'_\sigma(x,\varphi;\,\cdot\,)$ is a measure because of Gänßler–Stute [15], Corollary 1.6.15. Since the Lebesgue measure is σ–finite and $e'_{x,\varphi}$ is bounded, $E'_\sigma(x,\varphi;\,\cdot\,)$ is σ–finite. ∎

6.6 Proofs of Section 2.4

Proof of Theorem 2.4.7:

Proof:

To 1: Follows immediately from the definition of f, $f_{\mathcal{T}}$ and the definition of $\not{f}$, $\not{f}_\Theta, \ldots$ and $g, g_\Theta, \ldots$ and from the statement 1 of Lemma 2.3.3.

To 2–4: They follow in an analogous way as 5.

To 5: Let $n \in \mathbb{N}_0$. From Theorem 2.2.6 and with the definitions of E_k and P_k, $k \in \mathbb{N}$ and with $x_{(i)} := x_0 + \sum_{j=1}^{i} ct_j\varphi_{j-1}$ for $i \in \mathbb{N}$ we get:

$$
\begin{aligned}
&\mathbb{E}^\tau(\xi_{\Theta,\mathcal{T},n}) = \\
&= \int\limits_{\mathbb{R}^3\times S^2\times Pol\times S^2\times\mathbb{R}_0^+} \int\limits_{\mathbb{R}_0^+} \int\limits_{S^2\times Pol\times S^2} \cdots \int\limits_{S^2\times Pol\times S^2} \int\limits_{\mathbb{R}_0^+} \\
&\quad \not{f}_{\Theta,\mathcal{T}}\Big(x_{(n)}, \varphi_n, st_n, \rho_n, \sum_{i=0}^{n} t_i\Big) \quad 1_{\mathcal{R}}(x_{(n)}, \varphi_n, t_{n+1}) \quad \Big(\prod_{i=0}^{n-1} 1_{\overline{\mathcal{R}}}(x_{(i)}, \varphi_i, t_{i+1})\Big) \\
&\quad E_\sigma(x_{(n)}, \varphi_n; dt_{n+1}) \quad P_p(x_{(n)}, \varphi_{n-1}, st_{n-1}, \rho_{n-1}; d(\varphi_n, st_n, \rho_n)) \quad \ldots \\
&\quad \ldots \quad P_p(x_{(1)}, \varphi_0, st_0, \rho_0; d(\varphi_1, st_1, \rho_1)) \quad E_\sigma(x_0, \varphi_0; dt_1) \quad \tau(d(x_0, \varphi_0, st_0, \rho_0, t_0))
\end{aligned}
$$

and from the definition of $\mathcal{P}_s^*$ (see Definition 2.4.1) we get:

$$
\begin{aligned}
&= \int\limits_{\mathbb{R}^3\times S^2\times Pol\times S^2\times\mathbb{R}_0^+} \int\limits_{\mathbb{R}^3\times S^2\times Pol\times S^2} \cdots \int\limits_{\mathbb{R}^3\times S^2\times Pol\times S^2} \int\limits_{\mathbb{R}_0^+} \\
&\quad \not{f}_{\Theta,\mathcal{T}}\Big(x_n, \varphi_n, st_n, \rho_n, t_0 + \sum_{i=1}^{n} \frac{\|x_i - x_{i-1}\|}{c}\Big) \quad 1_{\mathcal{R}}(x_n, \varphi_n, t_{n+1}) \\
&\quad \Big(\prod_{i=1}^{n} 1_{\overline{\mathcal{R}}}(x_{i-1}, \varphi_{i-1}, \frac{\|x_i - x_{i-1}\|}{c})\Big) \quad E_\sigma(x_n, \varphi_n; dt_{n+1}) \\
&\quad \mathcal{P}_s^*(x_{n-1}, \varphi_{n-1}, st_{n-1}, \rho_{n-1}; d(x_n, \varphi_n, st_n, \rho_n)) \quad \ldots \\
&\quad \ldots \quad \mathcal{P}_s^*(x_0, \varphi_0 st_0, \rho_0; d(x_1, \varphi_1, st_1, \rho_1)) \quad \tau\Big(d(x_0, \varphi_0, st_0, \rho_0, t_0)\Big).
\end{aligned}
$$

With statement 4 of Lemma 2.4.5 and with the definition of $f_{\mathcal{T}}$ and $g_{\Theta,\mathcal{T}}$ we get:

$$
\begin{aligned}
&= \int\limits_{\mathbb{R}^3\times S^2\times Pol\times S^2\times\mathbb{R}} \Big((K_{s,\mathcal{T}}^*)^n g_{\Theta,\mathcal{T}}\Big)(x, \varphi, st, \rho, t) \quad f_{\mathcal{T}}(x, \varphi, st, \rho, t) \\
&\quad \lambda_3 \times \lambda \times \lambda_{Pol} \times \lambda \times \lambda_1\Big(d(x, \varphi, st, \rho, t)\Big)
\end{aligned}
$$

$$= \left\langle f_{\mathcal{T}} \,,\, (K^*_{s,\mathcal{T}})^n \, g_{\Theta,\mathcal{T}} \right\rangle_{\mathcal{T}}$$

$$= \left\langle (K_{s,\mathcal{T}})^n \, f_{\mathcal{T}} \,,\, g_{\Theta,\mathcal{T}} \right\rangle_{\mathcal{T}}.$$

The claim for $\mathbb{E}^{\tau}(\xi_{\Theta,\mathcal{T}})$ follows from Theorem 2.2.6. ■

Proof of Theorem 2.4.10:

Proof:

To 1: Follows from the definition of f and $f_{\mathcal{T}}$ or from the definition of $\not{f}, \not{f}_{\Theta}, \ldots$ and $g, g_{\Theta}, \ldots$

To 2: Follows in an analogous way as statement 3.

To 3: Let $n \in \mathbb{N}_0$. From Theorem 2.2.6 and with the definitions of E_k and P_k, $k \in \mathbb{N}$, and $\not{f}_{\mathcal{T}}$ (see Definition 2.2.3) with $x_{(i)} := x_0 + \sum_{j=1}^{i} ct_j\varphi_{j-1}$ for $i \in \mathbb{N}$ we get:

$$\begin{aligned}
\mathbb{E}^{\tau}(\xi_{\mathcal{T},n}) \;=\; & \int\limits_{\mathbb{R}^3\times S^2\times Pol\times S^2\times\mathbb{R}_0^+} \; \int\limits_{\mathbb{R}_0^+} \; \int\limits_{S_1^2\times Pol\times S^2} \cdots \int\limits_{S_n^2\times Pol\times S^2} \; \int\limits_{\mathbb{R}_0^+} \\
& \langle\varphi_n, \vec{n}_R\rangle \; 1_{\mathcal{T}}\left[\left(\sum_{i=0}^{n} t_i\right) + \frac{-\langle x_{(n)}, \vec{n}_R\rangle}{c\cdot\langle\varphi_n, \vec{n}_R\rangle}\right] \not{L}(\Gamma(\varphi_n, \rho_n))\cdot st_n \\
& 1_{\mathcal{R}}(x_{(n)}, \varphi_n, t_{n+1}) \quad \left(\prod_{i=0}^{n-1} 1_{\overline{\mathcal{R}}}(x_{(i)}, \varphi_i, t_{i+1})\right) \\
& E_{\sigma}(x_{(n)}, \varphi_n; dt_{n+1}) \quad P_p(x_{(n)}, \varphi_{n-1}, st_{n-1}, \rho_{n-1}; d(\varphi_n, st_n, \rho_n)) \quad \ldots \\
& \ldots \quad P_p(x_{(1)}, \varphi_0, st_0, \rho_0; d(\varphi_1, st_1, \rho_1)) \quad E_1(x_0, \varphi_0, t_0; dt_1) \\
& \tau(d(x_0, \varphi_0, st_0, \rho_0, t_0)).
\end{aligned}$$

with $S_1^2 := \ldots := S_{n-1}^2 := S^2$ and $S_n^2 := \{\varphi \in S^2 : \langle\varphi, \vec{n}_R\rangle \neq 0\}$. Because of the definition of P_p and the assumptions made regarding p and τ we are able to use Lemma 2.4.9. Hence, we get:

$$\begin{aligned}
= \; & \int\limits_{\mathbb{R}^3\times S^2\times Pol\times S^2\times\mathbb{R}_0^+} \; \int\limits_{\mathbb{R}_0^+} \; \int\limits_{S_1^2\times Pol\times S^2} \cdots \int\limits_{S_n^2\times Pol\times S^2} \; \int\limits_{\mathbb{R}_0^+} \\
& \langle\varphi_n, \vec{n}_R\rangle \quad 1_{\mathcal{T}}\left[\left(\sum_{i=0}^{n+1} t_i\right) + \frac{-\langle x_{(n+1)}, \vec{n}_R\rangle}{c\cdot\langle\varphi_n, \vec{n}_R\rangle}\right] \not{L}(\Gamma(\varphi_n, \rho_n))\cdot st_n \\
& 1_{\mathcal{H}^+}(x_{(n+1)}) \quad 1_{FOV_R}(\varphi_n) \quad 1_{\mathcal{C}_{x_{(n+1)}}}(-\varphi_n) \\
& E_{\sigma}(x_{(n)}, \varphi_n; dt_{n+1}) \quad P_p(x_{(n)}, \varphi_{n-1}, st_{n-1}, \rho_{n-1}; d(\varphi_n, st_n, \rho_n)) \quad \ldots
\end{aligned}$$

$$\ldots \quad P_p(x_{(1)}, \varphi_0, st_0, \rho_0; d(\varphi_1, st_1, \rho_1)) \quad E_1(x_0, \varphi_0, t_0; dt_1)$$
$$\tau(d(x_0, \varphi_0, st_0, \rho_0, t_0)).$$

and with the definition of $\not{f}_{\mathcal{T}}$ (see Definition 2.2.3):

$$= \int\limits_{\mathbb{R}^3\times S^2\times Pol\times S^2\times\mathbb{R}_0^+} \int\limits_{\mathbb{R}_0^+} \int\limits_{S^2\times Pol\times S^2} \cdots \int\limits_{S^2\times Pol\times S^2} \int\limits_{\mathbb{R}_0^+}$$
$$\not{f}_{\mathcal{T}}\Big(x_{(n+1)}, \varphi_n, st_n, \rho_n, \sum_{i=0}^{n+1} t_i\Big) \quad 1_{\mathcal{H}^+}(x_{(n+1)}) \quad 1_{FOV_R}(\varphi_n) \quad 1_{\mathcal{C}_{x_{(n+1)}}}(-\varphi_n)$$
$$E_\sigma(x_{(n)}, \varphi_n; dt_{n+1}) \quad P_p(x_{(n)}, \varphi_{n-1}, st_{n-1}, \rho_{n-1}; d(\varphi_n, st_n, \rho_n)) \quad \ldots$$
$$\ldots \quad P_p(x_{(1)}, \varphi_0, st_0, \rho_0; d(\varphi_1, st_1, \rho_1)) \quad E_1(x_0, \varphi_0, t_0; dt_1)$$
$$\tau(d(x_0, \varphi_0, st_0, \rho_0, t_0)).$$

With the definition of $g_{\mathcal{T}}$ in this theorem we get:

$$= \int\limits_{\mathbb{R}^3\times S^2\times Pol\times S^2\times\mathbb{R}_0^+\times\mathbb{R}_0^+} \int\limits_{S^2\times Pol\times S^2} \cdots \int\limits_{S^2\times Pol\times S^2} \int\limits_{\mathbb{R}_0^+}$$
$$g_{\mathcal{T}}\Big(x_{(n+1)}, \varphi_n, st_n, \rho_n, \sum_{i=0}^{n+1} t_i\Big) \quad E_\sigma(x_{(n)}, \varphi_n; dt_{n+1})$$
$$P_p(x_{(n)}, \varphi_{n-1}, st_{n-1}, \rho_{n-1}; d(\varphi_n, st_n, \rho_n)) \quad \ldots \quad P_p(x_{(1)}, \varphi_0, st_0, \rho_0; d(\varphi_1, st_1, \rho_1))$$
$$(\tau \times E_1)\Big(d(x_0, \varphi_0, st_0, \rho_0, t_0, t_1)\Big),$$

and with the definition of $\mathcal{P}_c^*$ (see Definition 2.4.1):

$$= \int\limits_{\mathbb{R}^3\times S^2\times Pol\times S^2\times\mathbb{R}_0^+\times\mathbb{R}_0^+} \int\limits_{\mathbb{R}^3\times S^2\times Pol\times S^2} \cdots \int\limits_{\mathbb{R}^3\times S^2\times Pol\times S^2}$$
$$g_{\mathcal{T}}\Big(x_{n+1}, \varphi_n, st_n, \rho_n, t_0 + t_1 + \sum_{i=1}^{n} \frac{\|x_{i+1} - x_i\|}{c}\Big)$$
$$\mathcal{P}_c^*(x_n, \varphi_{n-1}, st_{n-1}, \rho_{n-1}; d(x_{n+1}, \varphi_n, st_n, \rho_n)) \quad \ldots \quad \mathcal{P}_c^*(x_1, \varphi_0, st_0, \rho_0; d(x_2, \varphi_1, st_1, \rho_1))$$
$$(\tau \times E_1)\Big(d(x_0, \varphi_0, st_0, \rho_0, t_0, t_1)\Big),$$

where we used $x_1 := x_{(1)} := x_0 + ct_1\varphi_0$. From statement 4 of Lemma 2.4.5 and the integral transformation theorem we get:

$$= \int\limits_{\mathbb{R}^3\times S^2\times Pol\times S^2\times\mathbb{R}_0^+} \Big((K_{c,\mathcal{T}}^*)^n g_{\mathcal{T}}\Big)(x, \varphi, st, \rho, t)$$

$$(\tau \times E_1) \circ \Big(X_{(1)}, \Phi_0, ST_0, R_0, T_0 + T_1\Big)^{-1}\Big(d(x, \varphi, st, \rho, t)\Big)$$

$$\overset{\text{def. } \mathbf{f}_{\mathcal{T}}}{=} \quad \Big\langle f_{\mathcal{T}} \, , \, (K^*_{c,\mathcal{T}})^n \, g_{\mathcal{T}} \Big\rangle_{\mathcal{T}}$$

$$= \quad \Big\langle (K_{c,\mathcal{T}})^n \, f_{\mathcal{T}} \, , \, g_{\mathcal{T}} \Big\rangle_{\mathcal{T}}.$$

The claim for $\mathbb{E}^{\tau}(\xi_{\mathcal{T}})$ follows immediately from Theorem 2.2.6. ■

Table of symbols

Number sets and topological spaces:

Let:

$\mathbb{N}$	be the set of the natural numbers (without 0),
$\mathbb{N}_0$	be the set of natural numbers including 0,
$\mathbb{N}_{0,\infty}$	$:= \mathbb{N}_0 \cup \{\infty\}$,
$\mathbb{R}$	the field of the real numbers,
$\mathbb{R}^+$	the set of real numbers > 0,
$\mathbb{R}_0^+$	the set of real numbers ≥ 0,
$\mathbb{R}_\infty$	$:= \mathbb{R} \cup \{\infty\} \cup \{-\infty\}$,
$\mathbb{R}_{0,\infty}^+$	$:= \mathbb{R}_0^+ \cup \{\infty\}$,
$\mathbb{R}_\infty^n$	$:= \mathbb{R}^n \cup \{\vec{\infty}_n\}$ for $n \in \mathbb{N} \setminus \{1\}$,
S^2	$:= \{x \in \mathbb{R}^3 : \|x\| = 1\}$ and
S_∞^2	$:= S^2 \cup \{\overset{\mathrm{d}}{\infty}\}$.

$\mathbb{N}$, $\mathbb{N}_0$ and $\mathbb{N}_{0,\infty}$ are equiped with the discrete topology.
On $\mathbb{R}$ we have the standard Euclidian topology, on $\mathbb{R}_\infty$ its Alexandrov compactification, and on $\mathbb{R}^n$ the product topology. We always look at $\mathbb{R}^n$ as a vector space with the Euclidian scalar product $\langle \cdot, \cdot \rangle$ and the Euclidian norm $\| \cdot \|$.
S_∞^2 is the topological sum of S^2 and $\{\overset{\mathrm{d}}{\infty}\}$. On $\mathbb{R}_\infty^n$ for $n \geq 2$ we have the one point compactification (cf. Bourbaki [7]) of $\mathbb{R}^n$ (take care, $\overset{\mathrm{d}}{\infty}$ and $\vec{\infty} := \vec{\infty}_3$ differ, in general we get $\overset{\mathrm{d}}{\infty} \neq \vec{\infty}$!).
For the sets $\mathbb{R}^+$, $\mathbb{R}_0^+$, $\mathbb{R}_{0,\infty}^+$ and S^2 we use the associated trace?? topology of $\mathbb{R}$, $\mathbb{R}_\infty$ and $\mathbb{R}^3$.

Measure and probability theoretical symbols:

Let be $I \neq \emptyset$ and A any set, $(X, \mathfrak{X})$, $(Y, \mathfrak{Y})$ and $(X_i, \mathfrak{X}_i)$ for $i \in I$ measurable spaces and $\mathcal{X}$ a topology on X, then we denote by:

$\mathfrak{P}(A)$	the power set of A (i.e. the set of all subsets of A,
$\mathfrak{B}(X)$	the sigma algebra of Borel subsets of $(X, \mathfrak{X})$,
$\mathfrak{A} \otimes \mathfrak{B}$	the product–σ–algebra of the σ–algebras $\mathfrak{A}$ and $\mathfrak{B}$,
$\sigma(\mathcal{A})$	σ–Algebra generated by $\mathcal{A}$ for $\mathcal{A} \subset \mathfrak{P}(A)$,
$\sigma(\{f_i : i \in I\})$	the initial σ–algebra of the measurable mapping $f_i : X \to (X_i, \mathfrak{X}_i)$,
$\mathfrak{M}(X, Y)$	the set of Markov kernels (transition probabilities) from $(X, \mathfrak{X})$ to $(Y, \mathfrak{Y})$,
λ	$: \mathfrak{B}(S^2) \to [0,1]$ the normed surface measure on S^2,
λ_n	$: \mathfrak{B}(\mathbb{R}^n) \to [0,1]$ the Lebesgue measure on $\mathbb{R}^n$,
λ_{Pol}	$: \mathfrak{B}(Pol) \to [0,1]$ the restriction of the Lebesgue measure on $\mathbb{R}^4$ on Pol (for the definition of Pol see 6.1.2),
$\mu \times \nu$	the product measure of the two σ finite measures μ and ν,
δ_x	$: \mathfrak{X} \to [0,1]$ the Dirac measure in $x \in X$,
1_A	$: X \to \{0,1\}$ The indicator function of A for $A \subset X \neq \emptyset$,
$\mathbb{E}(X)$	the expected value and
$\mathrm{Var}(X)$	the variance of a random varaible $X : \Omega \to \mathbb{R}$ over the probability space $(\Omega, \mathfrak{K}, \mathbb{P})$.

Function spaces:

Let E be a normed space and E' the continuous dual space of E, i.e the space of the continuous (real valued) linear functionals on E, then with the bilinear form $(f, g) := g(f)$ for $f \in E$ and $g \in E'$, (E, E') is a dual pair.

For normed vector spaces E and F and a linear bounded operator T from E to F we design by T^* the adjoint operator of T.

Furthermore, for a measure space $(X, \mathfrak{X}, \mu)$ we use (cf. Hewitt–Stromberg [18] p 173 and p 347):

$L^1(X, \mathfrak{X}, \mu)$	the vector spaces of (equivalence classes) of the μ–integrable funktions on X,

$L^\infty(X,\mathfrak{X},\mu)$	the vector spacess of (equivalence classes) of the μ–essentially bounded $\mathfrak{X}$ measurable functions on X,
L^1	$:= L^1\Big(\mathbb{R}^3 \times S^2 \times Pol \times S^2,\ \mathfrak{B}(\mathbb{R}^3 \times S^2 \times Pol \times S^2),\ \lambda_3 \times \lambda \times \lambda_{Pol} \times \lambda\Big)$,
L^∞	$:= L^\infty\Big(\mathbb{R}^3 \times S^2 \times Pol \times S^2,\ \mathfrak{B}(\mathbb{R}^3 \times S^2 \times Pol \times S^2),\ \lambda_3 \times \lambda \times \lambda_{Pol} \times \lambda\Big)$,
L^1_T	$:= L^1\Big(\mathbb{R}^3 \times S^2 \times Pol \times S^2 \times \mathbb{R},\ \mathfrak{B}(\mathbb{R}^3 \times S^2 \times Pol \times S^2 \times \mathbb{R}),\ \lambda_3 \times \lambda \times \lambda_{Pol} \times \lambda \times \lambda_1\Big)$,
L^∞_T	$:= L^\infty\Big(\mathbb{R}^3 \times S^2 \times Pol \times S^2 \times \mathbb{R},\ \mathfrak{B}(\mathbb{R}^3 \times S^2 \times Pol \times S^2 \times \mathbb{R}),\ \lambda_3 \times \lambda \times \times \lambda_{Pol} \times \lambda\lambda_1\Big)$.

Equiped with the usual norm $L^1(X,\mathfrak{X},\mu)$ and $L^\infty(X,\mathfrak{X},\mu)$ are normed spaces.

For every decomposable measure space $(X,\mathfrak{X},\mu)$ the mapping

$$\mathcal{L} \;:\; L^\infty(X,\mathfrak{X},\mu) \to L^1(X,\mathfrak{X},\mu)', \quad \text{with} \quad g \mapsto \mathcal{L}(g) := \langle\!\langle \cdot\,,\, g \rangle\!\rangle$$

is an isomorphism from $L^\infty(X,\mathfrak{X},\mu)$ to $L^1(X,\mathfrak{X},\mu)'$ (cf. Hewitt–Stromberg [18] Theorem 20.20, S.353) if the mapping

$$\langle\!\langle \cdot\,,\, g \rangle\!\rangle \;:\; L^1(X,\mathfrak{X},\mu) \to \mathbb{R}, \quad \text{with} \quad f \mapsto \langle\!\langle f, g \rangle\!\rangle \;:=\; \int\limits_X f \cdot g \; d\mu$$

is a bounded linear functional on $L^1(X,\mathfrak{X},\mu)$ for each $g \in L^\infty(X,\mathfrak{X},\mu)$ (cf. Hewitt–Stromberg [18] Theorem 20.16, S.349). Therefore, with the bilinear form

$$(f,g) \;=\; (\mathcal{L}(g))(f) \;=\; \langle\!\langle f, g \rangle\!\rangle \quad \text{for } f \in L^1(X,\mathfrak{X},\mu) \text{ and } g \in L^\infty(X,\mathfrak{X},\mu)$$

$(L^1(X,\mathfrak{X},\mu), L^\infty(X,\mathfrak{X},\mu))$ are a dual pair (cf. additionally Fremlin, [14] 52E and 63). If confusions are excluded we use the symbol $\langle \cdot\,,\,\cdot \rangle$ for the bilinear form concerning the dual pair (L^1, L^∞) and $\langle \cdot\,,\,\cdot \rangle_T$ concerning the dual pair (L^1_T, L^∞_T).

Bibliography

[1] R.B. Ash: Measure, Integration and Functional Analysis. Academic Press: New York 1972.

[2] Luc R. Bissonette, P. Bruscaglioni, A. Ismaelli, G. Zaccanti, A. Cohen, Y. Benayahu, M. Kleinman, S. Eggert, C. Flesia, P. Schwendimann, U. G. Oppel, A.V. Starkov, M. Noormohammadian, D.M. Winker, E.P. Zege, I.L. Katsev and I.N. Polonsky: Lidar Multiple Scattering from Clouds. To appear in: Applied Physics B.

[3] Avishai Ben-David, Benjamin M. Herman, John A. Reagan: Inverse problem and the pseudoempirical orthogonal function method of solution. 1: theory. Applied Optics, Vol. 27, No. 7, March April 1988.

[4] Avishai Ben-David, Benjamin M. Herman, John A. Reagan: Inverse problem and the pseudoempirical orthogonal function method of solution. 2: use. Applied Optics, Vol. 27, No. 7, March April 1988.

[5] C. Bohren, D. Huffman: Absorption and Scattering of Light by Small Particles. Wiley and Sons: 1983.

[6] Craig F. Bohren: On the Absurdity and Inadvisability of Calling Particles Mie Scatterers. Optics & Photonic News, February 1992.

[7] N. Bourbaki: General Topology, Part 1. Addison Wesley: Reading 1966.

[8] Max Born, Emil Wolf: Principles of Optics. Pergamon Press Oxford, 1980, Reprinted Sixth (corrected) Edition, 1987.

[9] Edward A. Bucher: Computer Simulation of Light Pulse Propagation for Communication Through Thick Clouds. Applied Optics 12, 10, October 1973.

[10] S. Chandrasekhar: Radiative Transfer. Dover, New York, 1960.

[11] R.T.H. Collis, P.B. Russel: Lidar Measurement of Particles and Gases by Elastic Backscattering and Differential Absorbtion. In: E.D. Hinkley: Laser Monitoring of the Atmosphere. Springer: New York 1976.

[12] D. Deirmendjian: Electromagnetic Scattering on Spherical Polydispersions. Elsevier: New York 1969.

[13] B.T.N. Evans: Sensitivity of the Lidar Ratio to Changes in the Particle Size Distribution and Refractive Index. DRFVR–4479/89, 1989.

[14] D.H. Fremlin: Topological Riesz Spaces and Measure Theory. Cambridge University Press: London 1974.

[15] P. Gänßler, W. Stute: Wahrscheinlichkeitstheorie. Springer: Berlin 1977.

[16] George M. Hale and Marvin R. Querry: Optical Constants of Water in the 200–nm to 200μm Wavelength Region. Applied Optics, Vol. 12, No. 3, March 1973.

[17] Benjamin M. Herman, Samuel R. Browning, John A. Reagan: Determination of Aerosol Size Distributions from Lidar Measurments. Journal of the Atmospheric Sciences, Vol. 28, July 1971.

[18] E. Hewitt, K. Stromberg: Real and Abstract Analysis – A modern treatment of the theory of functions of a real variable. Springer: Berlin 1965.

[19] H.C van de Hulst: Light Scattering by Small Particles. Wiley, New York, reprinted by Dover: New York 1981.

[20] Kalos: .

[21] B.A. Kargin, K.B. Rakimgulov: A weighting Monte Carlo method for modelling the optical radiation field in thr ocean–athmosphere system. Russ. J. Numer. Anal. Math. Modelling, Vol. 7, No. 3, 1992.

[22] Brian W. Kernighan and Dennis M. Ritchie: The C Programming Language. Second Edition. Prentice Hall, New Jersey, 1988.

[23] M. Kerscher, W. Krichbaumer, M. Noormohammadian, U.G. Oppel: Polarized Multiply Scattered LIDAR Signals. Submitted for publication to Optical Reviews.

[24] James D. Klett: Stable analytical inversion solution for processing lidar returns, Applied Optics, Vol. 20, No. 2, January 1981.

[25] James D. Klett: Lidar inversion with variable backscatter/extinction ratios, Applied Optics, Vol. 24, No. 11, June 1985.

[26] W. Krichbaumer, H. Herrmann, J. Streicher, Werner: Results of the Lidar Measurements during the Campaign CLEOPATRA. Proceedings of the 6^{th} International Workshop on Multiple Scattering Lidar Experiments: Neuchatel (CH), January 1993.

[27] W. Krichbaumer: Polarization and the Stochastic Model. Proceedings of the 3^{rd} International Workshop on Multiple Scattering Lidar Experiments:Oberpfaffenhofen, Fed. Rep. of Germany, October 24-26, 1989.

[28] W. Krichbaumer, H. Herrmann, E. Nagel, R. Häring, J. Streicher, Ch. Werner, A. Mehnert, Th. Halldorssohn, S. Heinemann, P. Peuser, N.P. Schmitt: A diode–pumped ND:YAG Lidar for airborne cloud measurements. Optics & Laser Technology 25, 1993.

[29] W. Krichbaumer: Multiple Scattering and Depolarisation: Classification of Ice and Water Clouds and PSCs. in: Laser in Remote Sensing, Proceedings of the 11th International Congress LASER 93. Springer: Berlin, 1994.

[30] K.E. Kunkel, J.A. Weinman: Monte Carlo analysis of multiple scattered lidar returns. Journal of the Athmospheric Sciences, Vol. 33, 1978.

[31] Kuo–Nan Liou: A Complementary Theory of Light Scattering by Homogeneous Spheres. Applied Mathematics and Computation 3, 1977.

[32] Kuo–Nan Liou, Richard M. Schotland: Multiple Backscattering and Depolarization from Water Clouds for a Pulsed Lidar System. Journal of the Athmospheric Sciences vol. 28, July 1971.

[33] G.I. Marchuk, G.A. Mikhailov, M.A. Nazaraliev, R.A. Darbinjan, B.A. Kargin, and B.S. Elepov: The Monte Carlo Methods in Atmospheric Optics. Springer: Berlin 1980.

[34] G. Mie: Ann. Phys. 25, 1908.

[35] H. Müller, R. Wendling, H. Quenzel: Final Report of the: "Study on the information content of ground based LIDAR–measurements". Euratom–Contracts No. 649–76–12–SISP C, 791–77–10–SISP D, 974–78–11–SISP D. July 1980.

[36] J. Neveu: Mathematische Grundlagen der Wahrscheinlichkeitstheorie. Oldenburg: München 1969.

[37] Masoud Noormohammadian: Varianzreduzierende Monte–Carlo Methoden zur Berechnung mehrfach gestreuter LIDAR Rücksignale. Dissertation LMU–München, 1995.

[38] U.G. Oppel, A. Findling, W. Krichbaumer, S. Krieglmeier, and M. Noormohammadian: A Stochastic Model for the Calculation of Multiply Scattered LIDAR Returns. DLR-FB 89–36, Köln 1989.

[39] U.G. Oppel, A.V. Starkov, M. Noormohammadian: A Stochastic Model and Monte Carlo Sampling of LIDAR Returns. To appear in Proceedings of the Sixth International Workshop on Multiple Scattering Lidar Exeriments (MUSCLE 6), Neuchatel, Switzerland, January 26–28, 1993.

[40] S.R. Pal, A.I. Carswell: Multiple scattering in atmospheric clouds: lidar observations. Applied Optics, Vol. 15, No. 8, August 1976.

[41] K.R. Parthasarathy: Probability Measures on Metric Spaces. Academic Press: New York, London 1967.

[42] G.H.Ruppersberg, M.Kerscher, W.Krichbaumer, M.Noormohammadian, U.G.Oppel, W.Renger: The Influence of Multiple Scattering from Ice Clouds and a new ultra-highspeed Inversion Algorithm for Lidar Signals. in preparation.

[43] J.S. Ryan, A.I. Carswell: Laser beam broadening and depolarization in dense fog. Journal of the Optical Society of America, Vol. 68, 1978.

[44] Florian Scheck: Mechanik. Springer–Verlag Berlin, 1988.

[45] S.T. Shipley: The measurement of rainfall by lidar. PhD Thesis, Univ. of Wisconsin, 1980.

[46] W. Vizee,J. Oblanas, R.T.H. Collis: Evaluation of the Lidar Technique of Determining Slant Range Visibility for Aircraft Landing Operations. SRI Reprt AFCRL–TR–0708, 1973.

[47] W. J. Wiscombe: Improved Mie scattering algorithms. Applied Optics, Vol. 19, No. 9, May 1980.